LUND UNIVERSITY

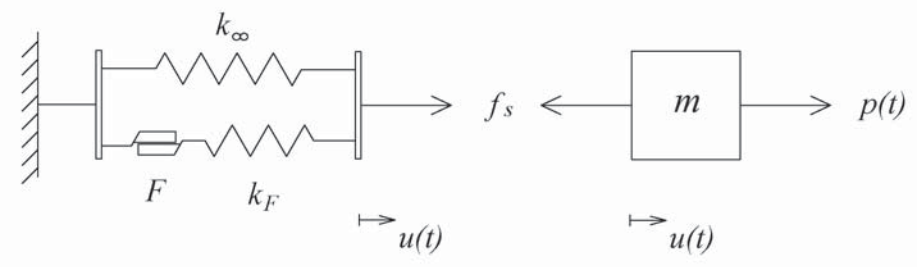


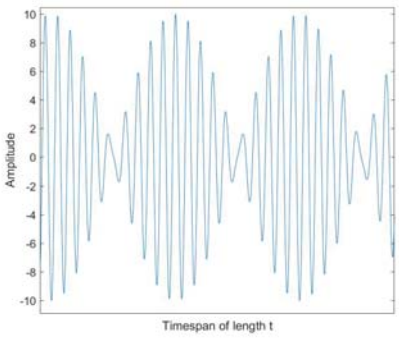


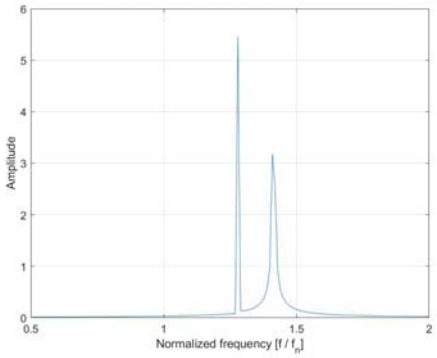


# SOME DEVIATIONS FROM LINEAR DYNAMICS DUE TO MORE ACCURATE DAMPING MODELS

JAKOB SJÖSTRAND

Structural Mechanics

*Master's Dissertation*

DEPARTMENT OF CONSTRUCTION SCIENCES
DIVISION OF STRUCTURAL MECHANICS

ISRN LUTVDG/TVSM--17/5228--SE (1-113) | ISSN 0281-6679
MASTER'S DISSERTATION

# SOME DEVIATIONS FROM LINEAR DYNAMICS DUE TO MORE ACCURATE DAMPING MODELS

JAKOB SJÖSTRAND

Supervisor: Professor **PER-ERIK AUSTRELL**, Division of Structural Mechanics, LTH.
Examiner: Professor **KENT PERSSON**, Division of Structural Mechanics, LTH.


Printed by V-husets tryckeri LTH, Lund, Sweden, November 2017 *(Pl)*.

**For information, address:**
Division of Structural Mechanics,
Faculty of Engineering LTH, Lund University, Box 118, SE-221 00 Lund, Sweden.
Homepage: www.byggmek.lth.se

# Abstract

Damping is present in all dynamic systems. In one way or another energy is being dissipated in the system. To capture this aspect of reality in a computational model is a difficult task. A common simplification is to assume that the damping is of a linear viscous nature. This assumption provides an equation of motion (linear dynamics) which is easy to handle mathematically. However, the simplicity of linear dynamics can in turn result in a poor representation of the physical reality. Perhaps the material is not viscous, perhaps friction is present either inside the material or at the boundaries? Different material models can take different damping phenomena into account, and it could be wise to work with a model or a combination of models that represent the physical properties of the material in the best way possible.

This thesis starts with an introduction to linear dynamics of *single degree of freedom* systems, where the structure is modeled as a spring and viscous damper in parallel. Free vibration response, steady-state response and the response to sinus-shaped pulses are discussed.

In the next chapter linear visco-elastic and non-linear frictional material models are discussed. An introduction to linear visco-elasticity is followed by a comparison between the *Kelvin-Voigt model* and the *Standard linear solid model*, which are the two most basic linear visco-elastic models, describing solid materials.

This section is followed by a comparison between the two most basic frictional models. These are 1) a model based on Coulomb friction and 2) a more refined friction model referred to as the SFS model.

In the following chapter a comparative study of the dynamic behavior of the *Kelvin-Voigt model* and the *Standard linear solid model* (SLS) is conducted. The models are given a structural formulation and a mass is attached. The main idea is to study if the behavior of the SLS model could be represented by a Kelvin model. Free vibration response, steady state response and response to sine-shaped pulses are investigated.

In the last chapter the steady state response of the frictional SFS model is studied. This model has bilinear hysteresis. The idea is to show the number of physical phenomenas that goes missing if a system is described as purely linear visco-elastic. Finally a short introduction to a model which combines both visco-elasticity and friction behavior is given. This model is referred to as the *5-parameter model*.



**Keywords:** Bilinear hysteresis, Standard linear solid, SLS, Linear Dynamics, Non-linear Dynamics

# Preface

This concludes my five years of studies at the Faculty of Engineering, Lund University. The thesis was initiated by Prof. Per Erik Austrell at the Division of Structural Mechanics and this is also where this work was carried out. I would like to thank Per Erik for all the invaluable input during the process and for pointing me in the right direction at times of confusion.

Moreover I would like to thank family, friends and fellow students for their support during the years.

Jakob Sjöstrand

Lund, June 2017

# Abbrevations

| | |
|---|---|
| FEM | Finite Element Method |
| FFT | Fast Fourier Transform |
| SLS | Standard Linear Solid |
| SFS | Simple Friction Solid |
| SDOF | Single degree of freedom |
| $R_d$ | Displacement response factor |
| $\omega$ | Angular frequency |
| $f$ | Frequency |
| $\omega t_r$ | Normalized frequency |
| $\varepsilon$ | Strain |
| $\dot{\varepsilon}$ | Strain-rate |
| $u$ | Displacement |
| $\dot{u}$ | Displacement velocity |
| $\zeta$ | Damping ratio |
| $t_r$ | Relaxation time |
| $\delta$ | Phase angle |
| $\phi$ | Phase shift |
| $t_d$ | Pulse duration time |
| $E_{dyn}$ | Dynamic modulus |

# Contents

# Chapter 1

# Introduction

Damping is present in all dynamic systems. In one way or another energy is being dissipated in the system. To capture this aspect of reality in a computational model is a difficult task. A common simplification is to assume that the damping is of a particular linear viscous nature. This assumption provides an equation of motion (linear dynamics) which is easy to handle mathematically. However, the simplicity of linear dynamics can in turn result in a poor representation of the physical reality. Perhaps the material is not viscous, perhaps friction is present either inside the material or at the boundaries? Different material models can take different damping phenomena into account, and it could be wise to work with a model or a combination of models that represent the physical properties of the material in the best way possible.

The main idea of the thesis is to show how more realistic viscoelastic material models and the inclusion of frictional effects will give rise to various nonlinear dynamic phenomena. The thesis will present and discuss a number of existing material models and different physical aspects connected to them. For example, rate dependence/independence, amplitude dependence/ independence, linearity/non-linearity.

Some examples of material models that will be investigated in a dynamic context are the *Kelvin-Voigt model*, the *standard linear solid model* (SLS) and an enhanced friction-model, here referred to as the *simple friction model* (SFS). Where analytical solutions does not exist or are hard to obtain, numerical timestepping procedures, using the central difference method, will be applied in order to evaluate the different dynamic systems.

The aim is primarily to see if the standard material model, the *Kelvin-Voigt model*, used in linear dynamics is able to capture the dynamic behavior of actual visco-elastic systems. In order to verify the results the more physically realistic *Standard linear solid model* will be used as a reference. Numerical experiments using *MATLAB* will be carried out in order to compare the models.

The following topics will be investigated:

- The free vibration response of the systems.
- The *steady state* response to a harmonic load.

- The response to pulse excitation.

Moreover the dynamic steady state response of the non-linear amplitude dependent friction model, termed the *SFS model*, will be investigated in order to show the variety of dynamic phenomenas that can be missed if an inherently non-linear system is described by a linear computational model.

The following pictures shows the mentioned dynamic systems.

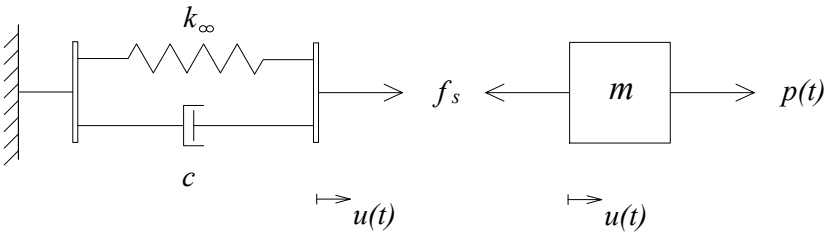


**Figure 1.1:** *Freebody diagram of the Kelvin-Voigt model*

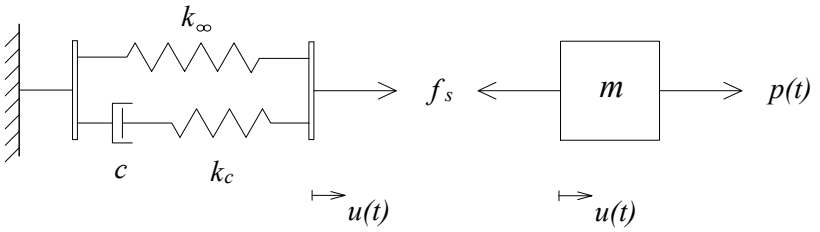


**Figure 1.2:** *Freebody diagram of the Standard linear solid model*

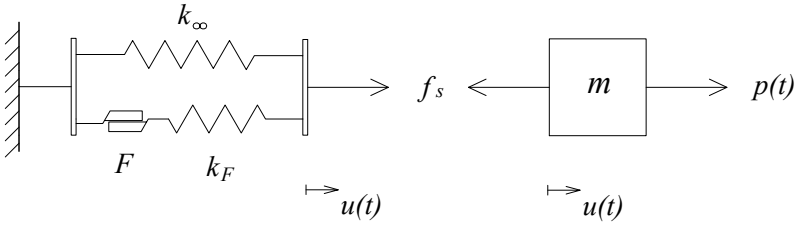


**Figure 1.3:** *Freebody diagram of the non-linear SFS model*

# Chapter 2

# Introduction to linear dynamics

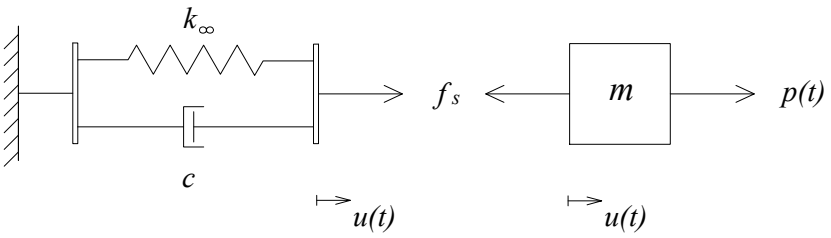


**Figure 2.1:** *Freebody diagram of the Kelvin-Voigt model*

Figure 2.1 shows a commonly used and particularly simple setup of a dynamic system, where the spring and the viscous damper symbolizes a certain material. As the mass $m$ is displaced to the right, this could be due to a time variant force $p(t)$ or an initial displacement $u(0) = u_0$, the material reacts with a restoring force $f_s$ to the left. The material wants to *restore* the system to its equilibrium and it is often assumed that this force is a function of the the displacement and the rate of this displacement, $f_s(u, \dot{u})$. From Newtons 2:nd law we get

$$(\rightarrow) \qquad p(t) - f_S(u, \dot{u}) = m\ddot{u} \tag{2.1}$$

The easiest way to describe the restoring force $f_s$ is through the model with a spring and a damper in parallel, displayed in Figure 2.1. The force in the spring is proportional to the displacement $f_{spring} = k_\infty u$ and the force in the viscous damper is proportional to the displacement rate $f_{damper} = c\dot{u}$. Since they are coupled in parallel the restoring force $f_s$ will be the sum of these two forces and after rearranging Eq.(2.1) one end up with

$$m\ddot{u} + c\dot{u} + k_\infty u = p(t) \tag{2.2}$$

This equation is called the equation of motion. The aim here is to find the displacement as a function of time $u(t)$.

Generally three situations are of interest to study.

1) The response of the system when it is let go from rest, with an initial displacement $u(0) = u_0$ and $p(t) = 0$

$$m\ddot{u} + c\dot{u} + k_\infty u = 0, \qquad u(0) = u_0,\ \dot{u}(0) = 0 \tag{2.3}$$

This is one form of a *free vibration response* used here.

2) The response of the system to a harmonic load $p(t) = p_0 \sin(\omega t)$

$$m\ddot{u} + c\dot{u} + k_\infty u = p_0 \sin(\omega t), \qquad u(0) = 0,\ \dot{u}(0) = 0 \tag{2.4}$$

where $\omega$ is the angular frequency of the load. After a while a damped system like this reaches *steady state* conditions which makes special solution techniques possible.

3) The response to a pulse load. In this thesis the focus lies on half-sine pulses characterized by their pulse duration times $t_d$. With at rest initial conditions, $u(0) = 0$, $\dot{u}(0) = 0$, the equation of motion becomes.

$$m\ddot{u} + c\dot{u} + k_\infty u = p(t), \qquad p(t) = \begin{cases} p_0 \sin(\pi t/t_d) & t \leq t_d \\ 0 & t > t_d; \end{cases} \tag{2.5}$$

## 2.1 Free vibration response

When trying to determine the free vibration response it is common to introduce a reformulation of the damping parameter $c$. The alternative formulation of $c$ is $c = 2m\zeta\omega_n$ where $\omega_n$ is the natural angular frequency of the system defined as $\omega_n = \sqrt{k/m}$. The property $\zeta$ is called the damping ratio.

$c$ is a measure of how much energy is being dissipated in one vibration cycle, while $\zeta$ also depends on the mass and the stiffness of the system.

The value of $\zeta$ characterize the system. If $\zeta > 1$ the system is called *overdamped*, if $\zeta = 1$ the system is called *critically damped* and if $\zeta < 1$ the system is called *underdamped*. Figure 2.2 shows this three characteristics respectively. Most structures have a damping ratio of $\zeta < 20\%$. Damping ratios higher than 20 % will be outside the scope of this thesis.

For more information on free vibrations the reader is referred to *Dynamics of structures* [1].

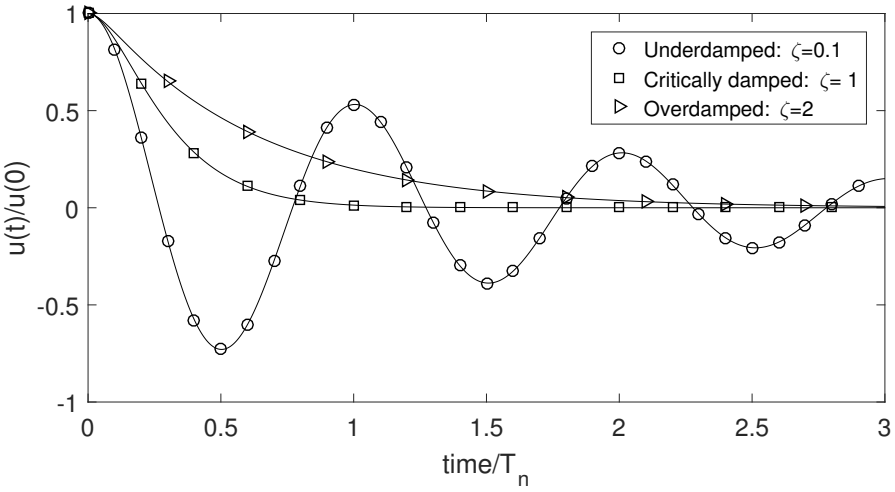


**Figure 2.2:** *The free vibration response of an overdamped, critically damped and underdamped system respectively.*

Figure 2.3 shows the influence of the damping ratio on the free vibration response. All damping ratios are under 20 %. The response of the systems are normalized with respect to their natural period time $T_n = 2\pi/\omega_n$

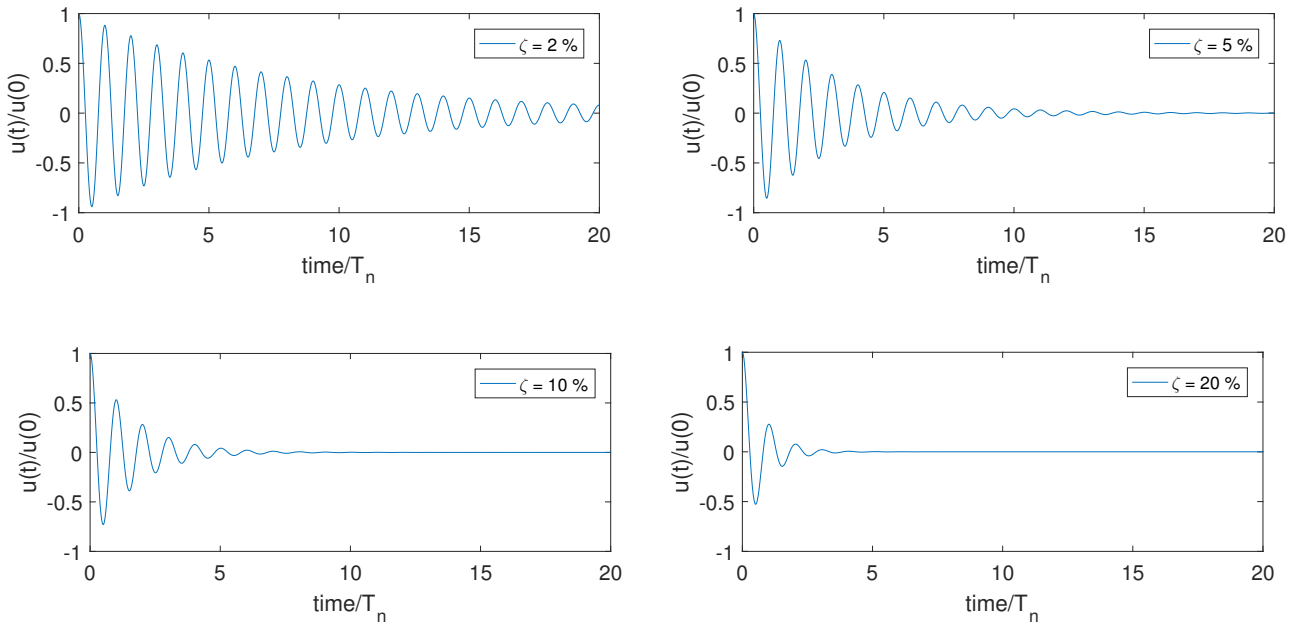


**Figure 2.3:** *The free vibration response for different values of the damping ratio $\zeta$. The damping at $\zeta = 20\%$ is considerable.*

## 2.2 Steady state response to harmonic excitation

For a damped linear dynamic system the response to a harmonic load $p(t) = p_0 \sin(\omega t)$ will after some time be a function with the same fundamental frequency $\omega$ and a phase-shift $\phi$.

The phase shift describes the *phase lag* between the movement of the mass and the load $p(t)$. This function is written $u(t) = u_0 \sin(\omega t - \phi)$. All possible combinations of linear springs and viscous dampers will generate a linear dynamic system and the simplest way to create a linear model of a solid material is through the Kelvin model, Figure 2.1.

[2]

For a linear system a complex function $H^* = H^*(\omega)$ exists that can relate the static displacement $u_s$ of the system to the maximum displacement caused by the time-variant force $u_0$. This relation will be different for different frequencies, i.e $H^*$ is a function of frequency. For a load with amplitude $p_0$ the static displacement is determined by the stiffness $k$ of the system $u_s = p_0/k$. The magnitude of the complex function $H^*(\omega)$ will give the relation between the quasi-static and the dynamic displacement $u_0$

$$u_0 = |H^*(\omega)|u_s \tag{2.6}$$

$|H^*(\omega)|$ is called the deformation response factor of the system, $R_d$. For the Kelvin model the deformation response factor, expressed in terms of the damping ratio $\zeta$, becomes

$$R_d = |H^*(\omega)| = \frac{u_0}{p_0/k} = \frac{1}{\sqrt{\left(1 - \left(\frac{\omega}{\omega_n}\right)^2\right)^2 + \left(2\zeta\frac{\omega}{\omega_n}\right)^2}} \tag{2.7}$$

The formulation in Equation (2.7) is obtained by rewriting the following expression for the displacement amplitude.

$$u_0 = \frac{p_0}{|-\omega^2 m + k_\infty + i\omega c|} \tag{2.8}$$

where $k^* = k_\infty + i\omega c$ is the complex stiffness of the system. Figure 2.4 shows $R_d$ as a function of the normalized frequency $\omega/\omega_n$, for different different values of the damping ratio $\zeta$. When the forcing frequency is the same as the natural frequency of the system, resonance occur. This happens around $\omega/\omega_n = 1$. The *displacement resonant frequency* for a Kelvin system is partly determined by the damping through $\omega_n\sqrt{1 - 2\zeta^2}$.

The phase-shift $\phi$ is obtained by taking the argument of the complex function $H^*(\omega)$. Figure (2.5) shows $\phi = -\arg(H^*(\omega))$ plotted for different values of the damping ratio.

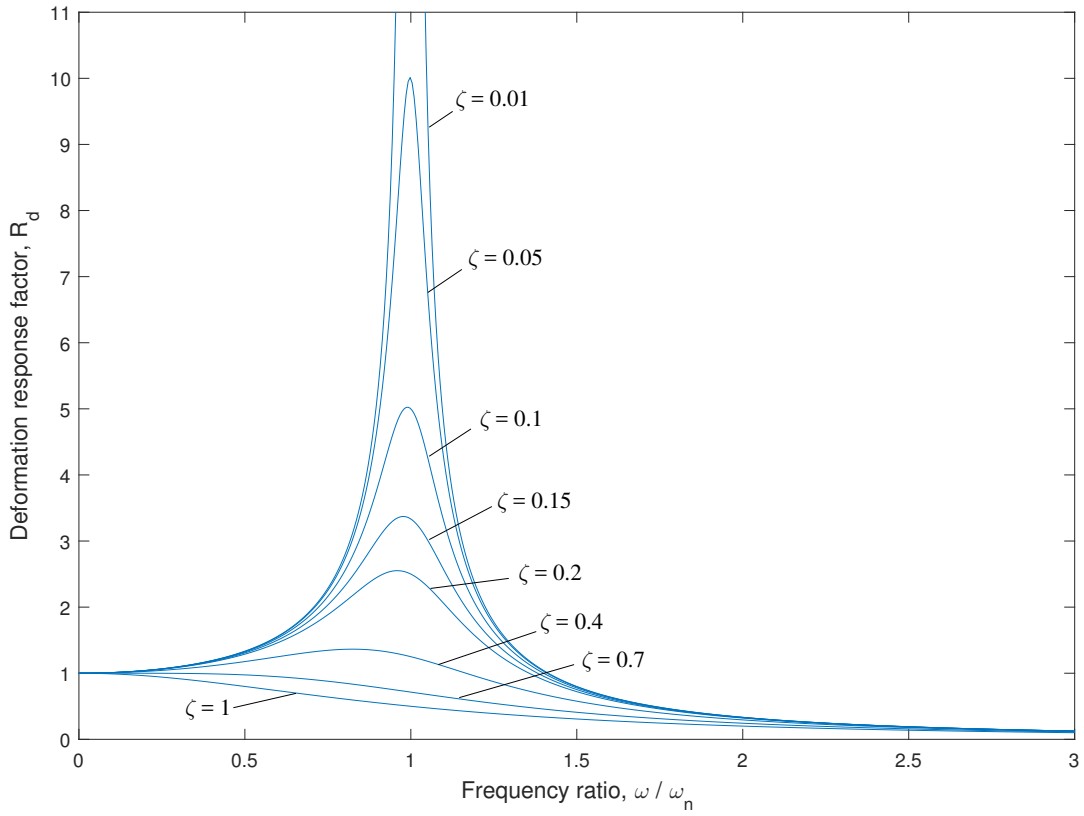


**Figure 2.4:** *The displacement response factor $R_d$, plotted for different values of the damping ratio $\zeta$.*

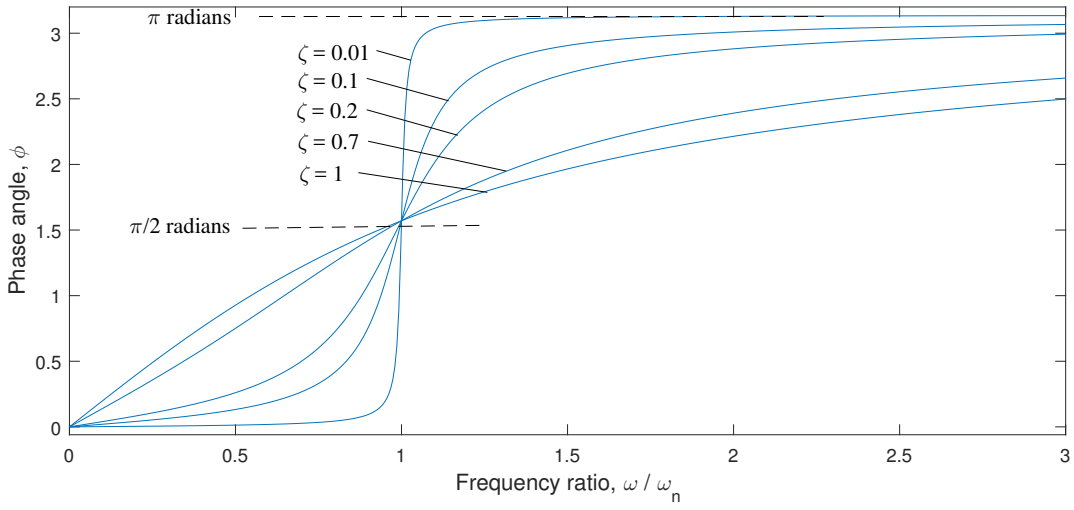


**Figure 2.5:** *The phase shift $\phi$, plotted for different values of the damping ratio $\zeta$.*

- At frequencies considerably below the natural frequency, i.e $\omega/\omega_n \ll 1$, the response of the system is controlled by the stiffness $k_\infty$. This means that there is no dynamic magnification of the signal and consequently the dynamic response factor $R_d \approx 1$. The phase shift is close to $\phi = 0°$, i.e the mass $m$ is moving in phase with the load.

- At frequencies around the natural frequency of the system, $\omega/\omega_n = 1$, the response is controlled by the damping. If no damping is incorporated in the system, $\zeta = 0\%$, the response is unbounded at resonance. At the natural frequency of the system $\omega = \omega_n$ there is a 90° phase shift between the load and the displacement of the mass. $\phi = 90°$ at $\omega = \omega_n$.
- At frequencies much higher than the natural frequency of the system the response is controlled by the mass $m$. As the frequency $\omega$ increases the displacement response factor $R_d$ goes towards zero. At these frequencies the phase shift between load and mass is $\phi = 180°$

## 2.3 Response to a half-sine pulse

The final topic of interest is the response of a dynamic system to a pulse load. In this case the pulse will have the shape of a half sine wave. The equation that governs the response is Eq.(2.5). A smart way to characterize a pulse is by relating the pulse duration $t_d$ to the natural vibration period of the studied system $T_n$. In Figure 2.7 the response of an *undamped* system to a half sine pulse is illustrated. Pulse durations ranging from $t_d = 0.125T_n$ to $t_d = 3T_n$ is included. At $t_d > 1.5T_n$ two peaks occur in the response during the pulse. At $t_d > 2.5T_n$ three peaks occur. Taking the maximum value of the response for a wide range of pulse-durations $t_d$, they can by combined into a *shock spectrum*. Figure 2.6 shows the shock spectrum of an undamped Kelvin system. For information on other types of pulse shapes see *Dynamics of structures* [1].

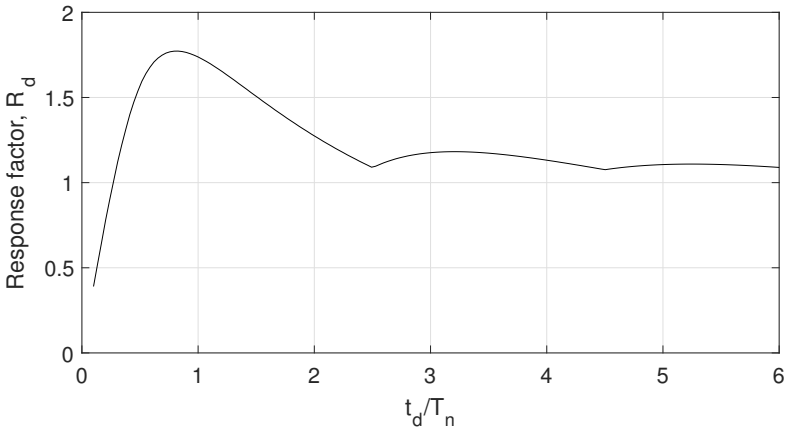


**Figure 2.6:** *Shock spectrum of an undamped Kelvin system*

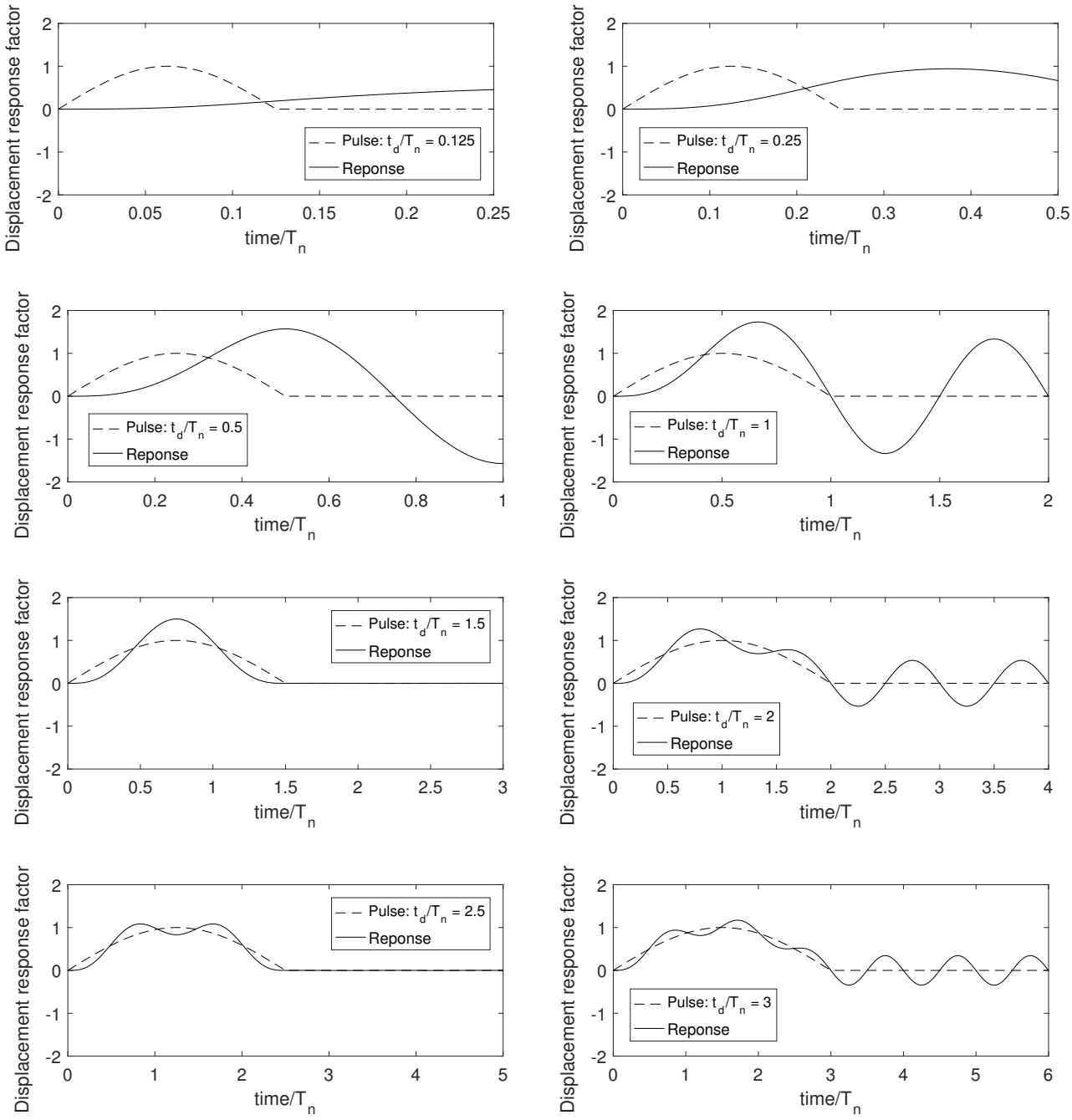


**Figure 2.7:** *The displacement response of an undamped Kelvin system to half-sine pulses with different duration times $t_d$.*

## 2.4 Energy

This section will describe the basics behind how energy is being dissipated in viscous damping. A more extensive presentation is found in *Dynamics of structures* [1].

As mentioned earlier: If the free vibration is disregarded then the displacement response to a sinusoidal force, $p_0 \sin \omega t$, will be

$$u(t) = u_0 \sin(\omega t - \phi) \tag{2.9}$$

The energy is being dissipated in the dashpot element and the force in this element is $f_D = c\dot{u}$. This means that the energy dissipated in one vibration cycle will be

$$E_D = \oint f_D \, du = \int_0^{2\pi/\omega} (c\dot{u})\dot{u} \, dt = \int_0^{2\pi/\omega} c\dot{u}^2 \, dt = c \int_0^{2\pi/\omega} [\omega u_0 \cos(\omega t - \phi)]^2 \, dt$$

Using the trigonometric identity $\cos(\omega t - \phi) = \cos\omega t \, \cos\phi + \sin\omega t \, \sin\phi$ and then the double angle formulas ($\cos(2\omega t) = 2\cos^2(\omega t) - 1 = 1 - 2\sin^2(\omega t)$ and $\sin(2\omega t) = 2\sin(\omega t)\cos(\omega t)$ one arrive at

$$E_D = \pi c \omega u_0^2 = 2\pi\zeta \frac{\omega}{\omega_n} k u_0^2 \tag{2.10}$$

The second identity, $2\pi\zeta(\omega/\omega_n)ku_0^2$, is obtained with use of $c = 2m\zeta\omega_n$ and $\omega_n^2 = k/m$. As one can see the amount of damping is proportional to the stiffness $k$, the driving angular frequency $\omega$ and to the square of the amplitude $u_0$.

When steady state vibrations are established the energy input $E_I$ will match the dissipated energy $E_D$. The energy input due to the applied force $p(t)$ will in one cycle of vibration become

$$E_I = \oint p(t) \, du = \int_0^{2\pi/\omega} p(t)\dot{u} \, dt = \int_0^{2\pi/\omega} [p_0 \sin\omega t][\omega u_0 \cos(\omega t - \phi)] \, dt = \pi p_0 u_0 \sin\phi$$

Before the steady state conditions occur more energy is entering the system than what is being dissipated. At $\omega = \omega_n$ and $\sin\phi = 1$ the energy input $E_I$ is a linear function of the displacement amplitude $u_0$, ($E_I = \pi p_0 u_0$) compared to the dissipated energy $E_D$ which is a quadratic function ($2\pi\zeta\frac{\omega}{\omega_n}ku_0^2$). At small amplitudes the linear function grows faster but eventually the two functions will match no matter how small the damping ratio $\zeta$ is. At the point where the functions match the system has reached *steady state*. Figure 2.8 shows this.

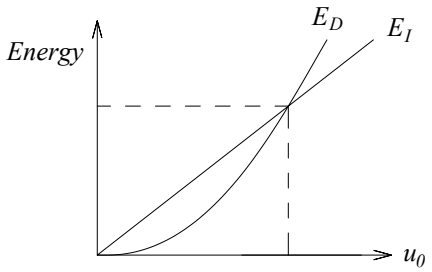


**Figure 2.8:** *At steady state the dissipated energy $E_D$ will match the energy input $E_I$. The dashed lines shows where $E_D = E_I$*

If the potential and the kinetic energy is studied during one cycle of vibration it is possible to conclude that the change in these quantities will be zero over the studied cycle.

Potential energy

$$E_s = \oint f_s \, du = \int_0^{2\pi/\omega} (ku)\dot{u} \, dt = \int_0^{2\pi/\omega} k[u_0 \sin(\omega t - \phi)][\omega u_0 \cos(\omega t - \phi)] \, dt = 0$$

Kinetic energy

$$E_K = \oint f_I \, du = \int_0^{2\pi/\omega} (m\ddot{u})\dot{u} \, dt = \int_0^{2\pi/\omega} m[-\omega^2 u_0 \sin(\omega t - \phi)][\omega u_0 \cos(\omega t - \phi)] \, dt = 0$$

Plotting the restoring force $f_s(t)$ and the displacement response $u(t)$ in a $(f_s, u)$-diagram an elliptical curve is obtained. This curve is often referred to as the *hysteresis loop*. The area enclosed by the ellipse will be equal to the dissipated energy $E_D$ in one vibration cycle of the system. Figure 2.9 shows this curve.

The restoring force for this simple material model was $f_s = k_\infty u + c\dot{u}$. This means that the tilted ellipse in Figure 2.9 is a superposition of the elastic and viscous response of the material, where the elastic force only determines the tilt. This means that the elliptical shape stems from the damping force, or more precisely, the relation between the displacement $u(t)$ and the displacement rate $\dot{u}(t)$. As the system has its maximum displacement the displacement rate is zero and vice versa. The following is a rewrite of the damping force $f_D$ in order to show this

$$f_D = c\dot{u}(t) = c\omega u_0 \cos(\omega t - \phi)$$

Using $\cos(x) = \sqrt{1 - \sin^2(x)}$ one obtains

$$f_D = c\omega\sqrt{u_0^2 - u_0^2 \sin^2(\omega t - \phi)} = c\omega\sqrt{u_0^2 - [u(t)]^2}$$

and this can be rewritten on elliptic form

$$\left(\frac{u(t)}{u_0}\right)^2 + \left(\frac{f_D}{c\omega u_0}\right)^2 = 1$$

This ellipse has the area $\pi(u_0)(c\omega u_0) = \pi c\omega u_0^2$ which is in accordance with the result in Equation (2.10). $u_0$ and $c\omega u_0$ are the semi-major and semi-minor axes of the ellipse.

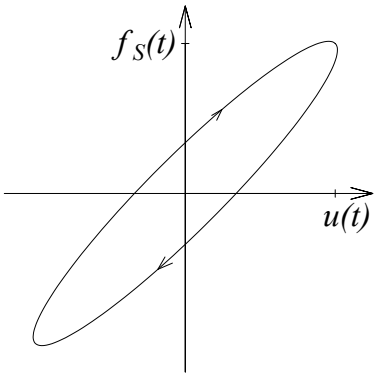


**Figure 2.9:** *Diagram showing the relation between the restoring force $f_S$ and the displacement $u(t)$.*

## 2.5 Equivalent viscous damping

Equivalent viscous damping is a concept commonly used to model the damping in actual structures. The main goal is to obtain a linear equation of motion in order to simplify the mathematical treatment. If all the damping mechanisms in the actual structure could be gathered into a corresponding equivalent damping coefficient, $c_{eq}$, the equation of motion could be expressed as

$$m\ddot{u} + c_{eq}\dot{u} + ku = p(t) \tag{2.11}$$

and the problem is possible to analyze with help of the well established methods used in linear dynamics. There exists a number of ways of doing this. Here one method is described, for more information on the subject see *Dynamics of structures* [1].

The most commonly used method is to measure the amount of dissipated energy during one vibration cycle in the actual structure, $E_{D(actual\ structure)}$. As described earlier the dissipated energy, during a cycle, is equal to the enclosed area of the hysteresis loop. Knowing this area, it is possible to determine an equal amount of dissipated energy, during a cycle, for a viscous system, $E_{D(viscous)}$. By putting

$$E_{D(viscous)} = E_{D(actual\ structure)} \tag{2.12}$$

it will be possible to determine an equivalent viscous damping ratio $\zeta_{eq}$.

Earlier, Eq.(2.10), it was shown that

$$E_{D(viscous)} = 2\pi\zeta\frac{\omega}{\omega_n}ku_0^2 \tag{2.13}$$

and by putting this equal to the dissipated energy of the actual structure the equivalent viscous damping ratio $\zeta_{eq}$ is obtained through

$$\zeta_{eq} = \frac{1}{2\pi} \frac{1}{\omega/\omega_n} \frac{E_{D(actual\ structure)}}{k u_0^2} \tag{2.14}$$

The experiment used to determine the force-displacement relation of the actual structure, and consequently the dissipated energy $E_D$, is a cyclic loading test with displacement amplitude $u_0$. Moreover, the experiment is conducted at $\omega = \omega_n$, i.e the natural frequency, and the stiffness parameter $k$ is the quasi-static stiffness of the structure. This quantity, $k$, is determined from a separate experiment.

Since the experiment is conducted at $\omega = \omega_n$ the determined damping ratio is only correct at this exciting frequency, but it is considered a good approximation also at other frequencies [1](p. 104).

For a *Multi Degree Of Freedom* system (MDOF), it is possible to assign an equivalent damping ratio $\zeta_{eq}$ to each natural mode of vibration of the structure.

# Chapter 3

# Method

Where analytical solutions does not exist or where they are hard to come by it is sometimes necessary to use numerical methods to obtain an approximation of the correct answer. In this thesis the *Central difference method* is used in these cases. This is an explicit time stepping method which relies on small time-steps in order to get accurate results. For more information on this method see *Dynamics of structures* [1].

## 3.1 Central difference method

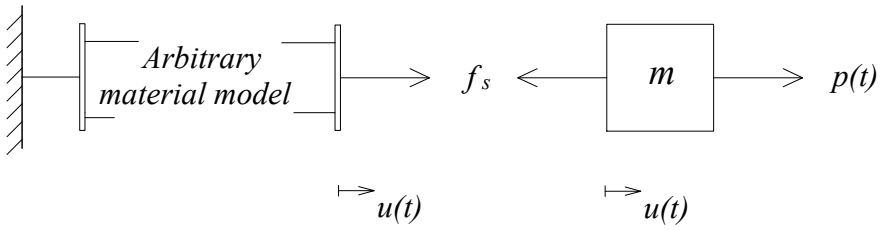


**Figure 3.1:** *Freebody diagram of a SDOF system described by an arbitrary material model.*

In order to evaluate the dynamic properties of the proposed material models the central difference method is used. The aim here is to obtain a displacement history from a given load history. The load history could be a sine function or a frequency sweep for instance. The equation that is to be solved is the following equation of motion. The equation is established from the free body diagram displayed in Figure 3.1

$$m\ddot{u} + (f_S) = p(t) \tag{3.1}$$

In the above equation, Eq.(3.1), at least the acceleration, $\ddot{u}$ needs to be approximated and for

most material models the restoring force $f_s$ is dependent on displacement $u$, velocity $\dot{u}$ or both. For instance the restoring force could be a function $f_s(u, \dot{u})$.

In the central difference method the first and second derivative of a function can be approximated by the following expressions

$$f'(x) = \frac{f(x+h) - f(x-h)}{2h} \qquad f''(x) = \frac{f(x+h) - 2f(x) + f(x-h)}{h^2} \tag{3.2}$$

Being that the first and second time derivative of the displacement $u$ corresponds to velocity and acceleration respectively, the expressions above, Eq.(3.2), translates into

$$\dot{u}_i = \frac{u_{i+1} - u_{i-1}}{2\Delta t} \qquad \ddot{u}_i = \frac{u_{i+1} - 2u_i + u_{i-1}}{(\Delta t)^2} \tag{3.3}$$

Now these expressions can be inserted into the equation of motion. For simplicity the time step length, $\Delta t$, is held constant throughout the time stepping.

$$m\left[\frac{u_{i+1} - 2u_i + u_{i-1}}{(\Delta t)^2}\right] + (f_S)_i = p_i \tag{3.4}$$

A rearrangement yields the following

$$\left[\frac{m}{(\Delta t)^2}\right] u_{i+1} = p_i - \left[\frac{m}{(\Delta t)^2}\right] u_{i-1} - \left[\frac{2m}{(\Delta t)^2}\right] u_i - (f_S)_i \tag{3.5}$$

Now a solution for the unknown displacement, $u_{i+1}$, is found and consequently the velocity as well as the acceleration can be updated in accordance with Eq.(3.3). The iteration scheme is then more or less established, but a few details are missing.

In order to find $u_{i+1}$ both $u_i$ and $u_{i-1}$ must be known. In the first iteration $u_1$ is sought, this means that $u_0$ and $u_{-1}$ needs to be calculated prior to the solution of $u_1$. To do this Eq.(3.3) is used, with $i = 0$

$$\dot{u}_0 = \frac{u_1 - u_{-1}}{2\Delta t} \qquad \ddot{u}_0 = \frac{u_1 - 2u_0 + u_{-1}}{(\Delta t)^2} \tag{3.6}$$

Since the equation of motion is an initial value problem, the displacement $u_0$ and the velocity $\dot{u}_0$ are known. This leaves three unknowns in the above equations, $u_{-1}$, $\ddot{u}_0$ and the sought quantity $u_1$. If the equation for $\dot{u}_0$ is solved for $u_1$ and the result is entered into the equation for $\ddot{u}_0$ the following expression is obtained

$$u_{-1} = u_0 - \Delta t(\dot{u}_0) + \frac{(\Delta t)^2}{2}\ddot{u}_0 \tag{3.7}$$

Now if the initial conditions $u_0$ and $\dot{u}_0$ are used to calculate the structure force $(f_S)_0$ at time $t_0 = 0$. The initial acceleration $\ddot{u}_0$ is given by

$$\ddot{u}_0 = \frac{p_0 - (f_S)_0}{m} \tag{3.8}$$

and consequently all the needed quantities can be determined and the iteration scheme is established.

According to Chopra [1] the stability requirement in the central difference method is

$$\frac{\Delta t}{T_n} < \frac{1}{\pi} \tag{3.9}$$

but the time step size $\Delta t$ should be smaller in order to dissolve the input signal in a good way and get accurate results.

## 3.2 Convergence

A convergence test was carried out in order to evaluate this solution method.

By calculating the displacement response factor $R_d$ of the Kelvin model analytically, for a large number of frequencies, the result could be compared to the numerical computations by studying the residual, $residual = R_{d,analytical} - R_{d,numerical}$. Both $R_{d,analytical}$ and $R_{d,numerical}$ are vectors and consequently the residual is a vector.

In Figure 3.2 the norm of the residual-vector, |residual|, is plotted for different time-step lengths $\Delta t$. The norm is also referred to as the magnitude of the vector, or length of the vector. The norm of the residual-vector is decreasing as the time-step length is decreased.

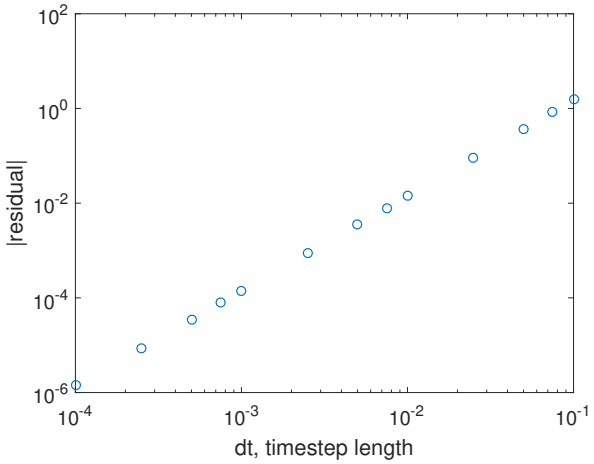


**Figure 3.2:** *Plot showing the decrease in the residual with decreasing time-step length.*

# Chapter 4

# Material models

Figure 4.1 shows how the shear modulus and the damping depends on the frequency, for a certain material. The material in question is HNBR which is a rubber material. The dots in the figure is the experimental results from material testing and the solid lines are the attempt to find a material model that can describe the behavior of the material.

A few things can be concluded. Both the shear modulus and the damping is increasing as the frequency is increased. Moreover damping is present even though the frequency is really low. Now look at Figure 4.2. Here displacement controlled cyclic loading has been used to test the material and it seems like the material is getting less stiff as the amplitude on the displacement is being increased.

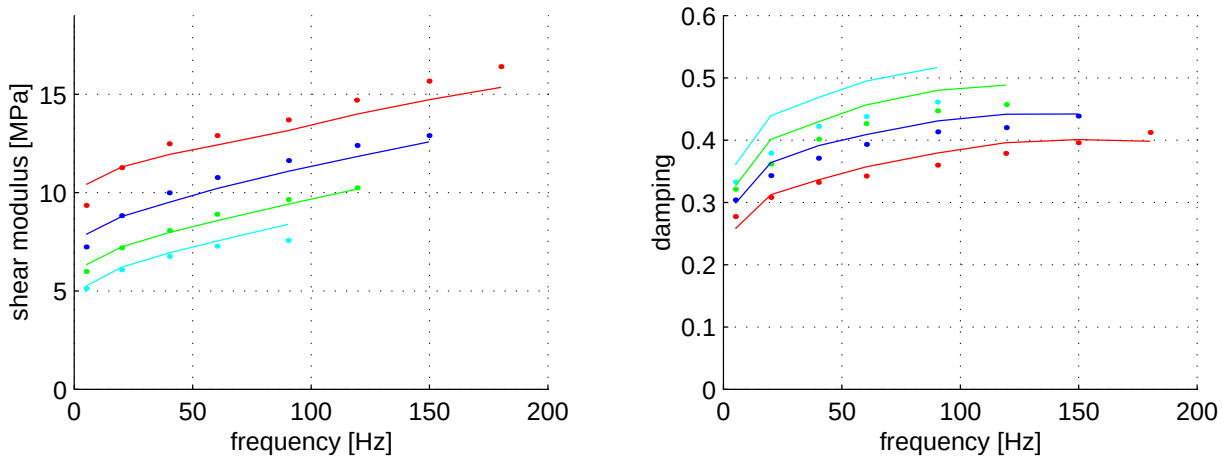


**Figure 4.1:** *Shear modulus and damping as functions of frequency for the rubber material, HNBR. The dots are the measurements and the solid lines are the fitted material models.*

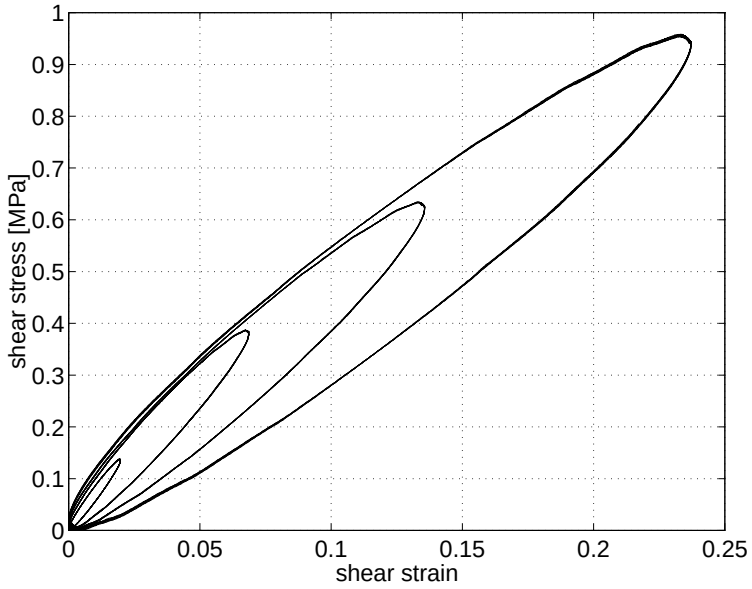


**Figure 4.2:** *Amplitude dependence of the hysteresis loop. Material: HNBR*

Or in other words: the shear modulus is decreasing as the displacement amplitude is being increased.

In order to incorporate all of these behaviors in one material model, the model will have to be both frequency dependent and amplitude dependent, Figure 4.3 shows the dynamic modulus and the damping of a material model that has these two properties. This is the *5-parameter model*. The figure shows that both the dynamic modulus and the damping is dependent on both frequency and amplitude. Frequency dependence is also referred to as rate dependence. The rate at which the load or displacement changes direction.

The following section will present different models that will have either of these features. Two rate dependent models will be presented in this first section about visco-elastic materials. Later two friction models will be presented in the section about amplitude dependent materials. Friction models can also be described in terms of plasticity theory.

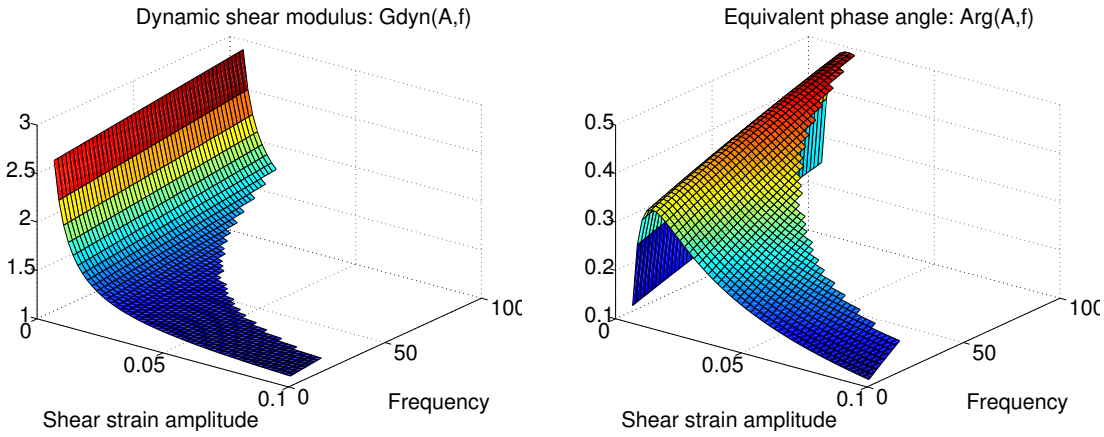


**(a)** *Dynamic shear modulus* **(b)** *The equivalent phase angle*

**Figure 4.3:** *Frequency and amplitude dependence of the shear modulus and the equivalent phase angle respectively. The model is the 5-parameter model, which is both rate- and amplitude dependent*

## 4.1 Visco-elastic materials

Since dynamic events are time dependent it would be of interest to investigate the time-dependency of the used material models. Two visco-elastic material models will be treated here: The *Kelvin-Voigt* model (or just *Kelvin* model) and the *Standard linear solid* model.

If not loaded too close to their ultimate strength polymers and concrete is two examples of materials that have viscoelastic response. Most of the material presented in this section is taken from *The mechanics of constitutive modeling* [3]. For a deeper presentation of viscous material models the reader is referred to this book.

Experimentally four tests are used to determine the time-dependent nature of a material: *creep test*, *relaxation test*, the response of the material to a constant *strain rate* i.e to push or pull at the material with a constant "velocity" and a *cyclic loading test* where the stress is evaluated from, for instance, a sinusoidal strain-history.

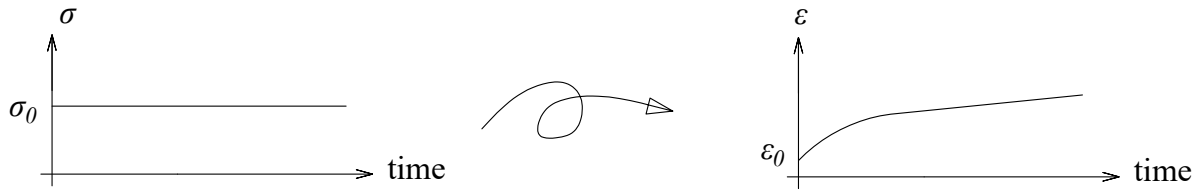


**Figure 4.4:** *Creep test*

In a *creep test* a constant stress, $\sigma_0$, is applied instantaneously to the material and the strain

response, $\varepsilon(t)$, which now may vary with time, is recorded. In addition to the initial strain $\epsilon_0$ a lot of material will now develop *creep* strain, see Figure 4.4. In order to model the *creep* strain the aim is to find a relationship on the form

$$\varepsilon(t) = J_C(t)\sigma_0$$

where $J_C(t)$ is called the *creep compliance*.

In a *relaxation test* the situation is reversed. Now a instantaneous step strain, $\varepsilon_0$ is applied to the material and held constant at this value. The material will experience an initial stress $\sigma_0$, this stress will however diminish with time, see Figure 4.5. This is due to the phenomena of relaxation, perhaps a less familiar phenomena compared to the *creep* behavior which may be more visibly present in everyday life. Relaxation is in a way the reversed situation compared to *creep* and in the same manner a similar relationship is sought, namely

$$\sigma(t) = E_R(t)\varepsilon_0$$

where $E_R(t)$ is called the *relaxation modulus*.

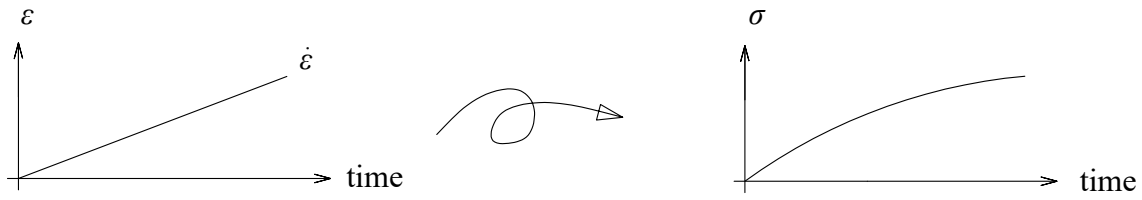


**Figure 4.6:** *Constant strain rate test*

In the third test the stress-response $\sigma(t)$ to a constant strain rate, $\dot{\varepsilon} = d\varepsilon/dt = c$, is recorded. A common feature among materials is that the material gets stiffer as the strain-rate is increased, i.e. the response is *rate-dependent*, see Figure 4.6. In analogy with a fluid, think of dragging

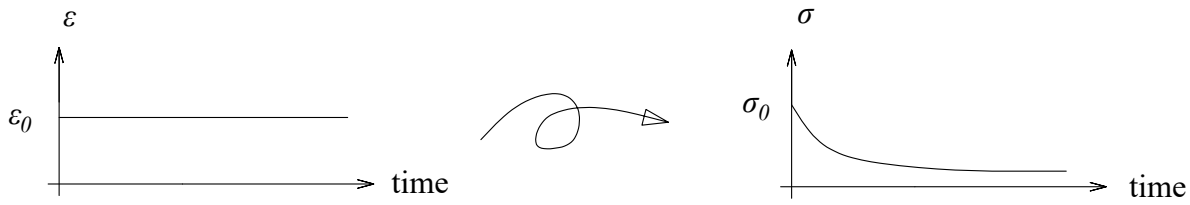


**Figure 4.5:** *Relaxation test*

your hand through water. If the you drag fast the resistance will be significant while dragging slow you'll experience almost no resistance at all.

And in a *cyclic loading test* the stress response, $\sigma(t)$, created by a displacement controlled loading of the test-specimen is recorded. The loading is often sinusoidal, i.e. the strain is on the form $\varepsilon(t) = \varepsilon_0 \sin(\omega t)$. If the material exhibits visco-elastic properties a phase-shift $\delta$ will be present between the strain input and stress output, see Figure 4.7. In other words: if the strain input is a steady-state sinusoidal strain history $\varepsilon_0 \sin(\omega t)$, the stress output will be a *phase-shifted* sinusoid with the same frequency $\sigma_0 \sin(\omega t + \delta)$. This will be shown later.

Plotting the strain input and stress output, for a purely visco-elastic material, in the $(\varepsilon, \sigma)$-plane an elliptic path is formed due to the phase-shift. The enclosed area inside the ellipse is equal to the dissipated energy, i.e the energy leaving the system. The formed path that encloses an area is known as a *hysteresis loop*, see Figure 4.8. With $\varepsilon = \varepsilon_0 \sin(\omega t)$ and the stress response being out-of-phase, $\sigma = \sigma_0 \sin(\omega t + \delta)$, the dissipated energy in one cycle can be determined.

$$U_c = \oint \sigma \, d\varepsilon = \int_0^T \sigma \frac{d\varepsilon}{dt} \, dt = \sigma_0 \varepsilon_0 \omega \int_0^T \cos(\omega t) \sin(\omega t + \delta) \, dt$$

Using the trigonometric formula $\sin(\omega t + \delta) = \sin(\omega t)\cos(\delta) + \cos(\omega t)\sin(\delta)$, the dissipated energy becomes

$$U_c = \pi \sigma_0 \varepsilon_0 \sin \delta$$

Moreover, with the use of complex calculus an equation on the form

$$\sigma^* = E^*(\omega)\varepsilon^* \tag{4.1}$$

can be obtained. Here the stress response $\sigma^*$ and the strain input $\varepsilon^*$ is a complex number in polar form and $E^*(\omega)$ is a complex function dependent of frequency $\omega$. $E^*(\omega)$ is called the *complex modulus*.

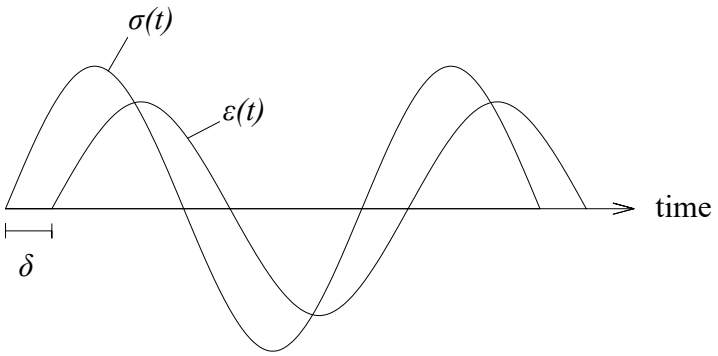


**Figure 4.7:** *Cyclic loading test*

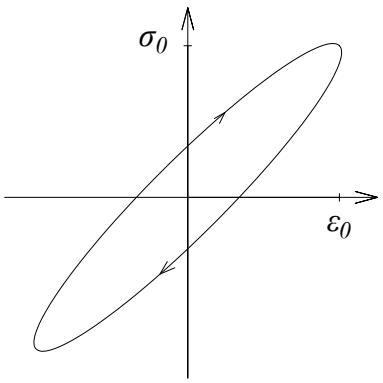


**Figure 4.8:** *The stress $\sigma$ and the strain $\varepsilon$ plotted in the ($\varepsilon$,$\sigma$)-plane, giving an elliptical hysteresis loop*

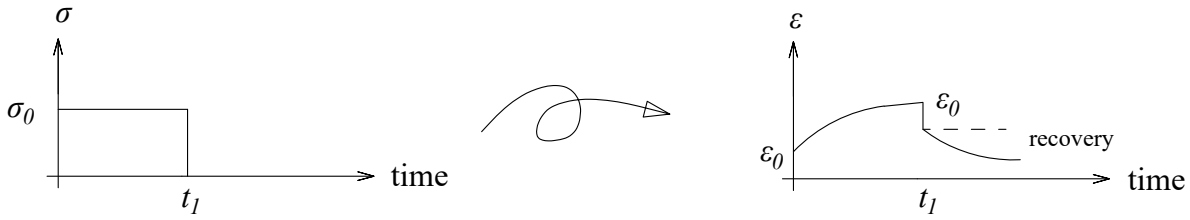


**Figure 4.9:** *Recovery test*

In addition to these four tests another phenomena could be worth mentioning. What happens if the stress $\sigma_0$ is instantaneously removed during a *creep test*? Here the phenomena of *recovery* is important. How much of the developed *creep* deformation will be permanent? See Figure 4.9.

Problem solving in structural mechanics largely evolves around the *Finite Element Method* and in this method the stresses in the system are evaluated from the current displacements. This would mean that, of the material-behaviors presented above, it is the ones that allows one to evaluate the stresses from the known displacements (strains) that, primarily, is of interest. More specifically the *relaxation* behavior and the stress response to a *cyclic* displacement.

Earlier the term visco-elasticity was mentioned and perhaps this requires an explanation. If a material is visco-elastic the principal of linearity will also hold for this material. This linearity principle can be described through the *creep behavior* of a material. If a step-stress $\sigma_0$ is applied to a visco-elastic material the strain response will be the elastic initial strain plus the developed creep strain.

$$\text{Step-stress:} \quad \sigma_0 \qquad \longrightarrow \qquad \text{Strain response:} \quad \varepsilon_{elastic} + \varepsilon_{creep}$$

Now if the step-stress is doubled, $2\sigma_0$, the two terms in the strain response will also be doubled.

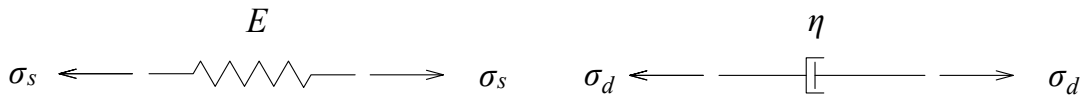


**Figure 4.10:** *A linear spring element (to the left) and a dashpot element (to the right).*

$$\text{Step-stress:} \quad 2\sigma_0 \qquad \longrightarrow \qquad \text{Strain response:} \quad 2\varepsilon_{elastic} + 2\varepsilon_{creep}$$

This linearity principal is not just valid for *creep*, but is assumed to be valid for any loading situation.

As mentioned earlier two visco-elastic material models will be treated: The *Kelvin-Voigt* model (or just *Kelvin* model) and the *Standard linear solid* model. Moreover there are two alternative ways to obtain constitutive relations for a visco-elastic material.

The first approach, and the only one to be used here, is to predefine a combination of linear springs and dashpots, see Figure 4.10. This will lead to the emergence of linear differential equations.

The other one is to use hereditary or convolution integrals. This approach is based on superposition which is a feature connected to the linearity principle mentioned earlier. The strength of this approach is that the desired material model is not limited to a certain combination of springs and dashpots.

The following are the constitutive relations that govern the linear spring and the dashpot respectively

$$\sigma_s = E\varepsilon_s \qquad\qquad \sigma_d = \eta\dot{\varepsilon}_d \tag{4.2}$$

where subscript $s$ refer to the spring and $d$ to the dashpot, Figure 4.10 gives a further explanation. The dashpot parameter $\eta$ has the dimension Pa·s. These structural elements can either be coupled in series or in parallel. For two structural elements coupled in parallel the strain will be the same in the two elements and consequently the total stress is given as the sum of the stress in each element

$$\text{Parallel:} \qquad \varepsilon = \varepsilon_1 = \varepsilon_2 \qquad\qquad \sigma = \sigma_1 + \sigma_2 \tag{4.3}$$

The reverse situation is having two structural elements coupled in series. This will lead to a constant stress throughout the chain of coupled elements, and the total strain then becomes the sum of the strain in each element.

$$\text{Series:} \qquad \sigma = \sigma_1 = \sigma_2 \qquad\qquad \varepsilon = \varepsilon_1 + \varepsilon_2 \tag{4.4}$$

As mentioned earlier complex calculus can be used to simplify derivations of particular expressions describing linear visco-elastic materials, for instance the *complex modulus*. An illustration of the connection between the complex plane and the $(\sigma, t)$-plane or the $(\varepsilon, t)$-plane is found in Figure 4.11. To the left in this figure a rotating vector diagram is found. The vectors are rotating with with an angular frequency, $\omega$, and with the phase shift, $\delta$, between them. This corresponds to the sine-time functions in the *time-amplitude* plane visible to the right in the figure.

This means that the harmonic loading can be expressed as a complex number in polar form.

$$\varepsilon^* = \varepsilon_0 e^{i\omega t} = \varepsilon_0(\cos\omega t + i\sin\omega t) \tag{4.5}$$

and consequently this can be used in order to express the complex stress response $\sigma^*$. Moreover, the first time-derivative becomes $\dot{\varepsilon}^* = i\omega\varepsilon^*$. This will prove very useful in the coming derivations.

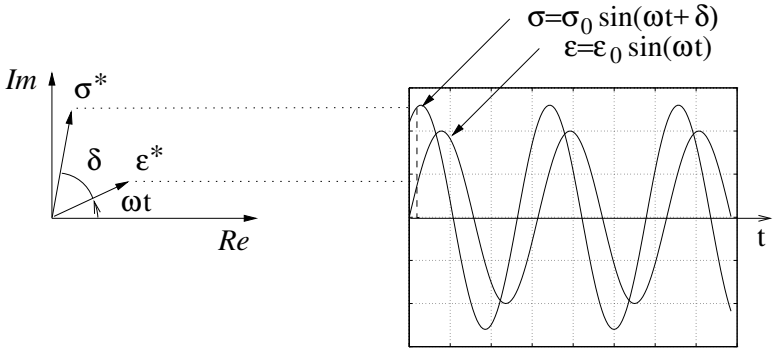


**Figure 4.11:** *Connection between frequency- and time-domain. To the left a rotating vector diagram and to the right we see sine-functions in the time domain.*

## 4.2 The Kelvin model

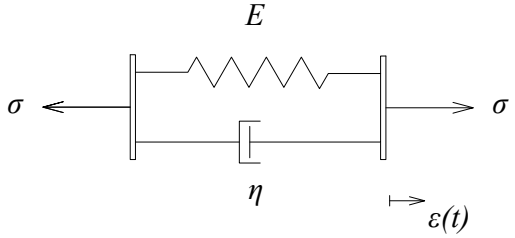


**Figure 4.12:** *The Kelvin material model.*

By putting a spring and dashpot in parallel the *Kelvin* model is obtained, see Figure 4.12. From before it is known that if two elements are coupled in parallel the total stress becomes the sum of the stress in the first element and the stress in the second element, Eq. (4.3). In this case

$$\varepsilon = \varepsilon_E = \varepsilon_\eta \qquad \sigma = \sigma_E + \sigma_\eta \tag{4.6}$$

With the equations for the spring ($\sigma_E = E\varepsilon_E$) and the dashpot ($\sigma_\eta = \eta\dot{\varepsilon_\eta}$) respectively the constitutive equation for the kelvin model becomes

$$\sigma = E\varepsilon + \eta\dot{\varepsilon} \tag{4.7}$$

Now that the constitutive equation is established its possible to study the behavior of the model. Examining the *relaxation* behavior and the response to *periodic* loading of the *Kelvin* model, a few irregularities will emerge.

### 4.2.1 Relaxation behavior

One of the presented main interest were to study how this model handles a relaxation test. So if a step-strain $\varepsilon_0$ is applied what will happen? During a step-strain $\varepsilon_0$ the strain-rate $\dot{\varepsilon}$ will be infinite and directly after the strain-rate returns to zero. This can be observed in Figure 4.13, during the step the slope of the curve is infinite, $\dot{\varepsilon} = \infty$, and at all other times the slope is zero, $\dot{\varepsilon} = 0$. If the step-strain occurs at $t = \tau$ this results in the following stress response

$$\sigma(t) = \infty \quad \text{at} \quad t = \tau \qquad \text{or} \qquad \sigma(t) = E\varepsilon_0 \quad \text{at} \quad t > \tau \tag{4.8}$$

Consequently the Kelvin model can not exhibit a realistic relaxation behavior.

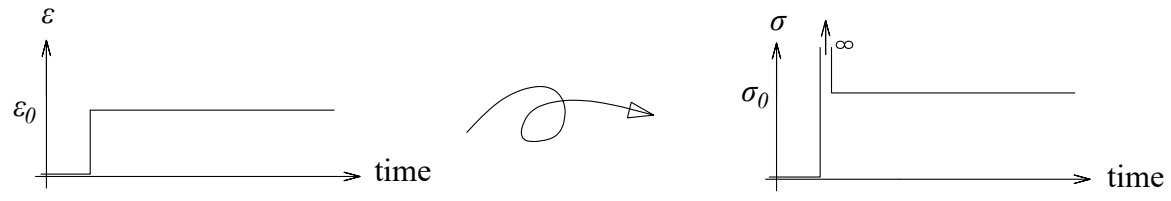


**Figure 4.13:** *Relaxation behavior of the Kelvin model. With $\dot{\varepsilon} = \infty$ during the step and $\dot{\varepsilon} = 0$ afterwards the stress goes from $\sigma = \infty$ during the step to $\sigma_0 = E\varepsilon_0$.*

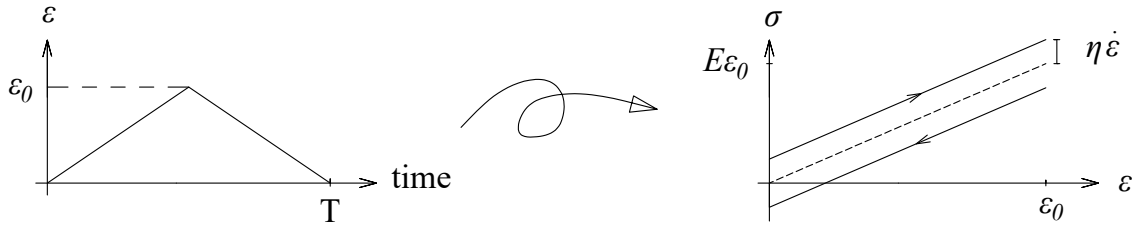


**Figure 4.14:** *A triangular strain-pulse creates a discontinuous stress response in the Kelvin model. This is due to the change in strain rate at $T/2$.*

### 4.2.2 Triangular pulse load

Before studying the harmonic excitation let's first look at a transient triangular pulse. Studying the left part of Figure 4.14 it can be viewed how the strain increases with a constant strain rate up to a maximum value $\varepsilon_0$ and then back to zero.

The strain rate is equal to either

$$\dot{\varepsilon} = \frac{\varepsilon_0}{(T/2)} = \frac{2\varepsilon_0}{T} \qquad \text{or} \qquad \dot{\varepsilon} = -\frac{2\varepsilon_0}{T} \quad \text{when} \quad t > T/2$$

with the strain-rate changing sign at $t = T/2$ and keeping the constitutive equation, Eq.(4.7) in mind its possible to conclude that the stress response will be discontinuous for a strain history of this kind, see left part of Figure 4.14.

The stress being discontinuous in a material is not very realistic and therefore a poor representation of the reality.

Moreover, studying the area enclosed by the *loading-unloading* path known as the hysteresis work, $U_c$, it gets clear that as the pulse-duration $T$ gets shorter the hysteresis work will grow infinitely large, see expression below and Figure 4.15.

$$U_c = \varepsilon_0 \cdot 2\eta\dot{\varepsilon} = \varepsilon_0 \cdot 2\eta\frac{2\varepsilon_0}{T}$$

### 4.2.3 Harmonic excitation and complex modulus

Now moving on to a harmonic loading, $\varepsilon_0 \sin(\omega t)$, it will be apparent that the equivalent to the pulse length, the periodic time $T$, will have a similar effect on the hysteresis work.

As was shown in Eq.(4.5) the harmonic loading could be expressed as a complex number in polar form $\varepsilon^* = \varepsilon_0 e^{i\omega t}$ with the following complex strain-rate $\dot{\varepsilon}^* = i\omega\varepsilon^*$. Inserting this in the constitutive equation (4.7) yields

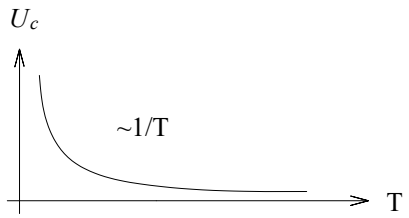


**Figure 4.15:** *The hysteresis work connected to a triangle pulse will be inversely proportional to the pulse-length, T, for the Kelvin model. For short enough pulses it will therefore grow without bound.*

$$\sigma^* = E\varepsilon^* + i\omega\eta\varepsilon^* = (E + i\omega\eta)\varepsilon^* \tag{4.9}$$

and a *complex modulus* on the form mentioned earlier is now found through

$$\sigma^* = E^*(\omega)\varepsilon^* \qquad \text{with} \qquad E^*(\omega) = (E + i\omega\eta) \tag{4.10}$$

this makes it possible to relate the stress response to a harmonic excitation through a multiplication with a complex function, $E^*(\omega)$. Earlier it was stated that the stress response to a sinusoidal strain, would be a phase-shifted sinusoid with the same frequency, i.e $\sigma_0 \sin(\omega t + \delta)$. This is now possible to show.

Expressing the stress response as a complex number in polar form in the same way the strain was expressed in (4.5) above, this would read

$$\sigma^* = \sigma_0 e^{i(\omega t+\delta)}$$

with $\delta$ being the phase angle. Now also express the complex modulus in polar form

$$E^*(\omega) = (E + i\omega\eta) = |E^*|e^{i\,arg(E^*)}$$

Multiplying with the strain then gives

$$\sigma_0 e^{i(\omega t+\delta)} = |E^*|e^{i\,arg(E^*)}\varepsilon_0 e^{i\omega t} = |E^*|\varepsilon_0 e^{i(\omega t+arg(E^*))} \tag{4.11}$$

It turns out that the magnitude of the complex modulus $|E^*|$ represents a scaling between the stress and strain amplitudes. This quantity is often referred to as the *dynamic modulus*. The argument of the complex modulus represents the *phase angle*, $\delta$. Both the dynamic modulus and the phase angle $\delta$ are possible to measure in experiments.

$$\sigma_0 = |E^*|\varepsilon_0 \qquad \text{and} \qquad arg(E^*) = \delta \tag{4.12}$$

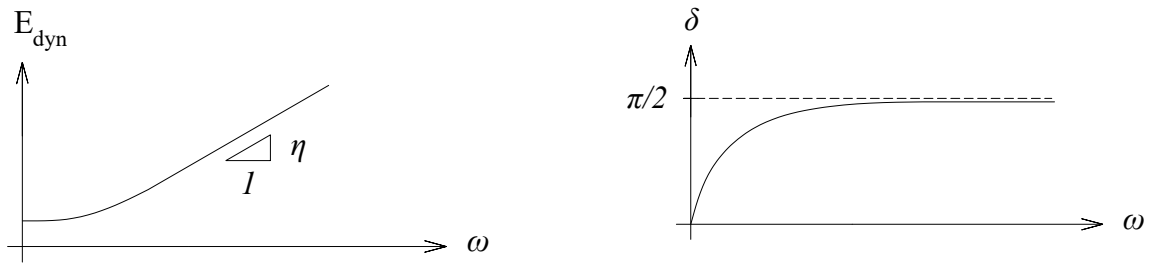


**Figure 4.16:** *To the left it can be seen how the dynamic modulus $E_{dyn}$ increases without bound as the frequency gets higher. To the right it can be seen how the phase angle grows to towards $\pi/2$ with increasing frequency*

Evaluating the above expressions in terms of the E-modulus, frequency and dashpot-coefficient gives

$$E_{dyn} = |E^*| = \sqrt{E^2 + \omega^2\eta^2} \qquad \text{and} \qquad \tan\delta = \frac{\eta}{E}\omega \tag{4.13}$$

It turns out that the dynamic modulus grow without bound when the frequency increases, meaning that the material will get infinitely stiff for a high enough frequency. The phase angle grows towards $\pi/2$ for an increasing frequency, see Figure 4.16 where the two quantities are plotted. Both of these behavior seems unrealistic.

Now the question arise: how does this effect the hysteresis loop. As mentioned: visco-elastic materials dissipate energy under cyclic loading. Previously the dissipated energy in one cycle $U_c$ was determined, Eq.(4.1)

$$U_c = \pi\sigma_0\varepsilon_0 \sin\delta$$

Substituting the stress amplitude $\sigma_0$ for $E_{dyn}\varepsilon_0$ and increasing the frequency it is possible to see how the hysteresis loop is affected. It turns out that the hysteresis work will become infinitely large as the frequency is increased

$$U_c = \pi E_{dyn}\varepsilon_0^2 \to \infty \qquad \text{as} \qquad \omega \to \infty$$

since the dynamic modulus is function that grows with increasing frequency. At low frequencies visco-elastic materials dissipate no energy. This behavior is visualized in Figure 4.17.

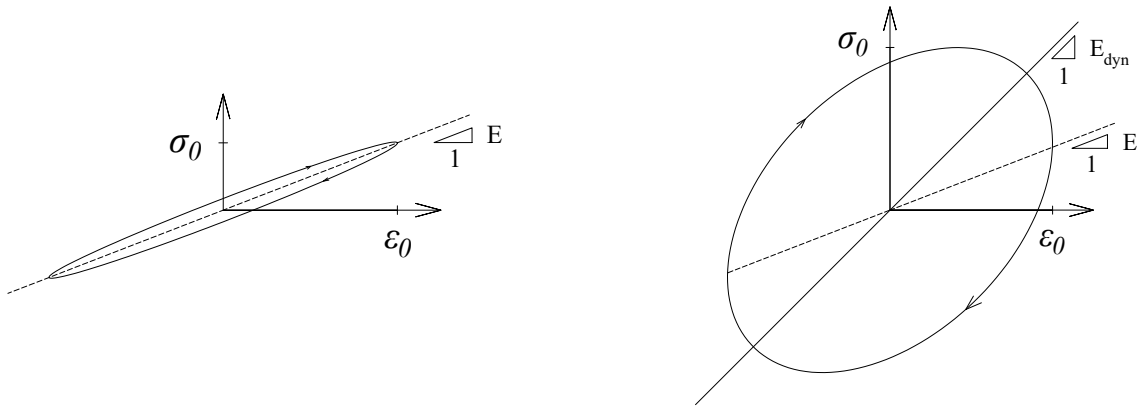


**(a)** *Low frequency, $\omega$.* **(b)** *High frequency, $\omega$.*

**Figure 4.17:** *The influence of frequency on the dissipated energy, $U_c$, for the Kelvin model*

### 4.2.4 Kelvin model: Summary

Below follows a summary of the irregularities associated with the Kelvin model.

- Discontinuous stress response to a step-strain and consequently an inability to exhibit relaxation behavior.
- Discontinuous stress response to strain functions with non-smooth shifts in the strain rate $\dot{\varepsilon}$, for instance a triangular pulse.
- Unbounded dynamic modulus $E_{dyn}$ for large frequencies $\omega$.
- And consequently an unbounded hysteresis work $U_c$ for large frequencies.

## 4.3 SLS: Standard linear solid model

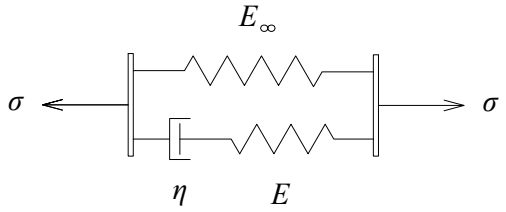


**Figure 4.18:** *The Standard linear solid model*

In the previous section a few different irregularities of the *Kelvin*-model were presented. Amongst these were the inability to exhibit relaxation behavior, the stress-discontinuity that appeared after a triangular pulse and the unbounded *dynamic modulus* $E_{dyn}$, which resulted in an unbounded area of the hysteresis loop as the frequency increased. Naturally it is of interest to find a material model which does not exhibit these flaws.

The least complex such model is the *Standard linear solid* model, from here on referred to as the *SLS* model. This model is obtained by taking the *Kelvin* model but also adding a linear spring in series with the dashpot, i.e the model consist of a spring coupled in parallel with a dashpot and another spring. Figure 4.18 shows the combinations of springs and dashpots.

Having a spring coupled in series with a dashpot constitutes a *Maxwell element*. In order to obtain an expression for the relaxation modulus, $E_R(t)$, as well as the complex modulus, $E^*(\omega)$, of the *SLS* model, it is a good decision to start of with the *Maxwell element* and then add the extra spring in parallel at the very end.

### 4.3.1 The Maxwell model

The *Maxwell element* is a model of a linear viscoelastic fluid. This will become apparent later when the relaxation behavior of the model is studied, but first the constitutive equation will be presented. Figure 4.19 shows the *Maxwell element*.

As the dashpot and spring are coupled in series, in the *Maxwell model*, the total strain in the element is given by

$$\varepsilon = \varepsilon_{spring} + \varepsilon_{dashpot} \tag{4.14}$$

and consequently the time derivative becomes

$$\dot{\varepsilon} = \dot{\varepsilon}_{spring} + \dot{\varepsilon}_{dashpot} \tag{4.15}$$

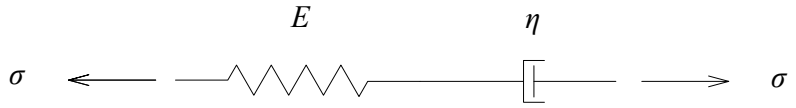


**Figure 4.19:** *The Maxwell element*

With the the use of

$$\dot{\sigma} = E\dot{\varepsilon}_{spring} \qquad \text{and} \qquad \sigma = \eta\dot{\varepsilon}_{dashpot} \tag{4.16}$$

the constitutive equation can now be written as follows

$$\dot{\sigma} + \frac{E}{\eta}\sigma = E\dot{\varepsilon} \tag{4.17}$$

Now the relaxation behavior can be studied.

**Maxwell model: Relaxation modulus**

The normalized relaxation behavior $E_R(t)$ can be derived by solving (4.17) for a step strain. For $t > 0$ the time-derivative of the strain is zero, $\dot{\varepsilon}(t) = 0$. (4.17) then turns into

$$\dot{\sigma} + \frac{E}{\eta}\sigma = 0 \qquad\qquad t > 0 \tag{4.18}$$

The above equation has the following solution

$$\frac{d}{dt}\left(\sigma e^{\frac{E}{\eta}t}\right) = 0 \quad \Rightarrow \quad \sigma(t) = Ce^{-\frac{E}{\eta}t} \tag{4.19}$$

During the step strain the strain rate, $\dot{\varepsilon}$, is infinite and consequently the dashpot becomes infinitely stiff. This means that the stress response at $t = 0$ is governed entirely by the elastic spring, giving $\sigma(0) = E\varepsilon_0$ and consequently the integration constant $C$ is equal to $E\varepsilon_0$. Thus the full solution becomes

$$\sigma(t) = E\varepsilon_0 e^{-\frac{E}{\eta}t} \tag{4.20}$$

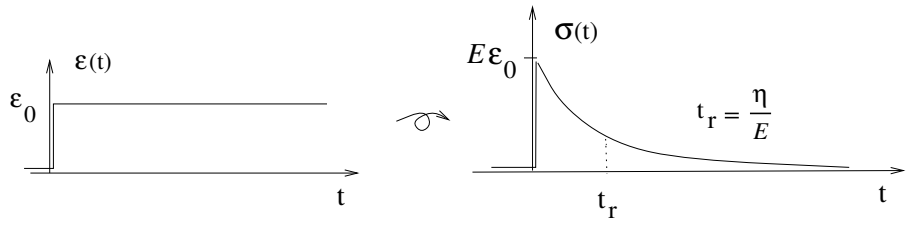


**Figure 4.20:** *Relaxation behavior of the Maxwell element. After some time the stress-response approaches zero.*

With the relaxation time $t_r$ defined as $t_r = \eta/E$ the relaxation behavior of the Maxwell model can now be expressed through the relaxation modulus $E_R(t)$ as

$$\sigma(t) = E_R(t)\varepsilon_0 = Ee^{-\frac{t}{t_r}}\varepsilon_0 \tag{4.21}$$

With the relaxation modulus being

$$E_R(t) = Ee^{-\frac{t}{t_r}} \tag{4.22}$$

Figure 4.20 shows the relaxation behavior of the Maxwell element. The stress-response will after some time be approximately zero. This is a model of a viscoelastic fluid.

Now moving on to find an expression for the complex modulus of the *Maxwell model*

### Maxwell model: Complex modulus

In the previous section handling the *Kelvin model* the main idea behind the complex modulus was presented. The aim was to relate the complex strain to the complex stress through the multiplication with a complex function termed the complex modulus, $E^*(\omega)$.

By solving the constitutive equation of the Maxwell model (4.17) for a steady-state sinusoidal strain history the complex modulus can be obtained.

Like before the sinusoidal strain history in complex form can be expressed in the following way

$$\varepsilon^* = \varepsilon_0 e^{i\omega t} = \varepsilon_0(\cos\omega t + i\sin\omega t) \tag{4.23}$$

Using this and inserting the following trial solution for the complex stress

$$\sigma^* = Ce^{i\omega t}$$

into the constitutive equation (4.17) yields

$$\dot{\sigma} + \frac{E}{\eta}\sigma = E\dot{\varepsilon} \quad \Rightarrow \quad i\omega C e^{i\omega t} + \frac{E}{\eta} C e^{i\omega t} = i\omega E \varepsilon_0 e^{i\omega t} \tag{4.24}$$

Now the unknown $C$ can be determined

$$C = E\frac{i\omega}{i\omega + E/\eta}\varepsilon_0 \quad \text{or} \quad C = E\frac{i\omega t_r}{i\omega t_r + 1}\varepsilon_0 \tag{4.25}$$

and consequently the sought relation can be established

$$\sigma^* = E\frac{i\omega t_r}{i\omega t_r + 1}\underbrace{\varepsilon_0 e^{i\omega t}}_{\varepsilon^*} \quad \Rightarrow \quad \sigma^* = E^*(\omega)\varepsilon^* \tag{4.26}$$

where the complex modulus is found to be

$$E^*(\omega) = E\frac{i\omega t_r}{i\omega t_r + 1} \tag{4.27}$$

With the derived expressions for the relaxation- and complex modulus of the Maxwell model, all that is left in order to obtain the equivalent expressions for the SLS model, is to add a spring in parallel to the Maxwell element.

### 4.3.2 Adding the spring: Relaxation modulus, harmonic excitation and complex modulus of the SLS model

Adding a spring in parallel will generate a model with solid properties. Before the stress relaxed all the way down to zero, which is the case for a linear visco-elastic fluid, now however a limit of the relaxation has been introduced. This limit is equal to the E-modulus of the added spring, denoted by $E_\infty$, see Figure 4.21.

Adding the spring in parallel with the Maxwell element means that the total stress will be the sum of the stress in the added spring and the stress in the Maxwell element like this

$$\sigma = \sigma_\infty + \sigma_M \tag{4.28}$$

where subscript $M$ denotes the Maxwell element and the subscript $\infty$ denotes the spring. Now in order to obtain the relaxation modulus for the SLS model it is just to add the response to a step strain of a linear spring to the relaxation modulus of the Maxwell model. The response to a step strain for a linear spring with $E$-modulus $E_\infty$ is

$$\sigma(t) = E_\infty \varepsilon_0 \tag{4.29}$$

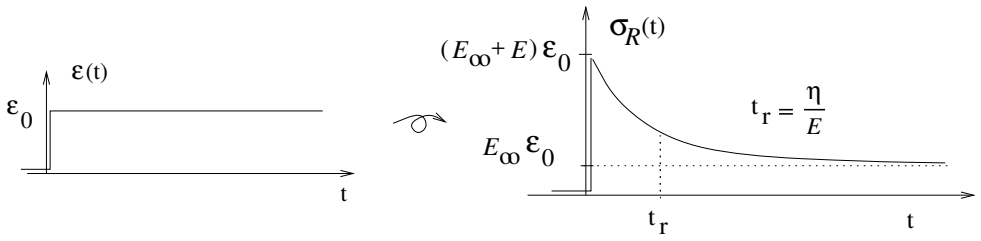


**Figure 4.21:** *Relaxation behavior of the SLS model. After some time the stress-response approaches $E_\infty \varepsilon_0$.*

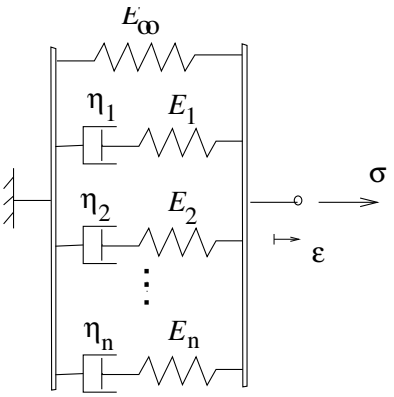


**Figure 4.22:** *The generalized Maxwell model*

Adding this to the response of the Maxwell model one obtains

$$\sigma(t) = E_R(t)\varepsilon_0 = \left(E_\infty + Ee^{-\frac{t}{t_r}}\right)\varepsilon_0 \tag{4.30}$$

and consequently the relaxation modulus of the SLS model is written

$$E_R(t) = E_\infty \left(1 + \frac{E}{E_\infty} e^{-\frac{t}{t_r}}\right) \tag{4.31}$$

Many materials have more than one relaxation mechanism. In order to capture this in the material model it is possible to put several Maxwell elements in parallel, each Maxwell element could represent a relaxation mechanism with a unique relaxation time $t_r$. Figure 4.22 shows the generalized Maxwell model with $n$ Maxwell elements coupled in parallel.

### Complex modulus, SLS model

Moving on to the complex modulus and the strategy here is the same.

The response of a linear spring to a sinusoidal strain is

$$\sigma^* = E_\infty \varepsilon^* \tag{4.32}$$

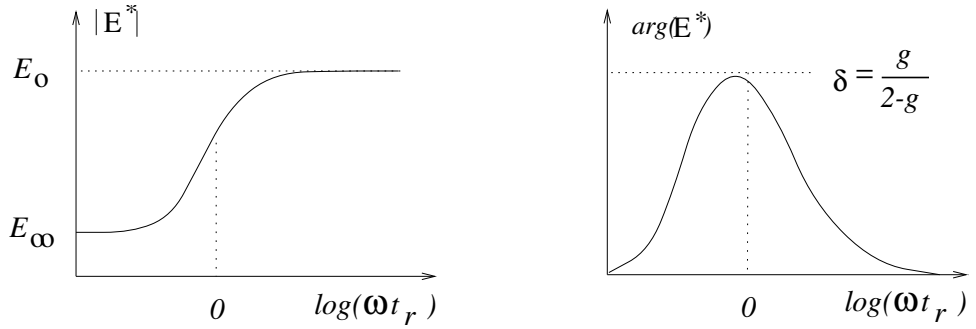


**Figure 4.23:** *$E_{dyn} = |E^*|$ and $\delta = arg(E^*)$ plotted against the logarithmic normalized frequency $\omega t_r$, for $g = 0.5$. Maximum phase angle occur at $\omega t_r \approx 1$ (note the logarithmic x-axis)*

Now adding this response to the response of the Maxwell element one arrive at

$$\sigma^* = E_\infty \varepsilon^* + E \frac{i\omega t_r}{i\omega t_r + 1} \varepsilon^* \tag{4.33}$$

And the complex modulus of the SLS model is found to be

$$E^*(\omega) = E_\infty \left(1 + \frac{E}{E_\infty} \frac{i\omega t_r}{i\omega t_r + 1}\right) \tag{4.34}$$

In the section discussing the Kelvin model it was concluded that the magnitude of the complex modulus represented a scaling between the stress and strain amplitudes, a quantity called the dynamic modulus, and that the argument represented the phase angle, $\delta$. This holds also for the SLS model. Eq. (4.35) shows the relationships again.

$$\sigma_0 = |E^*|\varepsilon_0 \qquad \text{and} \qquad \arg(E^*) = \delta \tag{4.35}$$

To summarize: The response to a steady-state sinusoidal strain is a steady state sinusoidal stress with the same frequency, but out of phase.

One of the strongest objections to the Kelvin model was directed towards its behavior at high frequencies, see Figure 4.16.

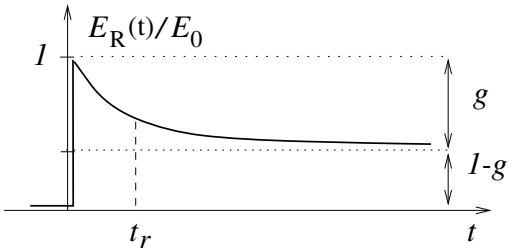


**Figure 4.24:** *Relating the normalized relaxation modulus $E_R(t)/E_0$ to the introduced parameters $E_0$, $g$ and $t_r$. $E_0 = E_\infty + E$, $g = E/E_0$ and $t_r = \eta/E$.*

With the SLS model a more realistic behavior is therefore anticipated. Defining the new quantity $g$, the relative amount of relaxation (see Figure 4.24 for an explanation), and reminding ourselves of the definition of the relaxation time , $t_r$

$$g = \frac{E}{E_\infty + E} \qquad t_r = \frac{\eta}{E}$$

the *dynamic modulus* and the *phase shift* can be plotted against the normalized frequency $\omega t_r$. Earlier the complex modulus was found to be

$$E^*(\omega) = E_\infty + E\frac{i\omega t_r}{i\omega t_r + 1} \qquad \text{and consequently} \quad E_{dyn} = |E^*| \quad \text{and} \quad \delta = \arg(E^*)$$

Figure 4.23 shows this plot for $g = 0.5$ i.e $E_\infty = E$. Note that the axis with the normalized frequency $\omega t_r$ is logarithmic, so the maximum phase angle occur at approximately $\omega t_r = 1$. For $g \leq 0.5$ and the assumption $\tan\delta \approx \delta$ an approximation of the maximum phase angle can be obtained through

$$\delta_{max} = \frac{g}{2-g} \qquad \text{for} \quad \omega t_r \approx 1 \quad \text{and} \quad g \leq 0.5 \tag{4.36}$$

Maximum phase angle $\delta$ also means maximum dissipation of energy, $U_c$. Remember

$$U_c = \pi\sigma_0\varepsilon_0 \sin\delta$$

Studying Figure 4.23 it is possible to conclude that

$$\delta \to 0 \quad \text{and} \quad E_{dyn} \to E_\infty \qquad \text{as} \quad \omega t_r \to 0 \tag{4.37}$$

and

$$\delta \to 0 \quad \text{and} \quad E_{dyn} \to E_\infty + E \qquad \text{as} \quad \omega t_r \to \infty \tag{4.38}$$

This means that the response is basically elastic for low and high frequencies. When the behavior is elastic the dissipated energy $U_c$ is equal to zero.

Figure 4.25 shows the hysteresis and dynamic stiffness of the model for a low, intermediate and high normalized frequency $\omega t_r$

$$1) \quad \omega t_r \ll 1 \qquad 2) \quad \omega t_r \approx 1 \qquad 3) \quad \omega t_r \gg 1$$

As mentioned, the area of the hysteresis loop is small for low and high frequencies i.e the response is approximately elastic.

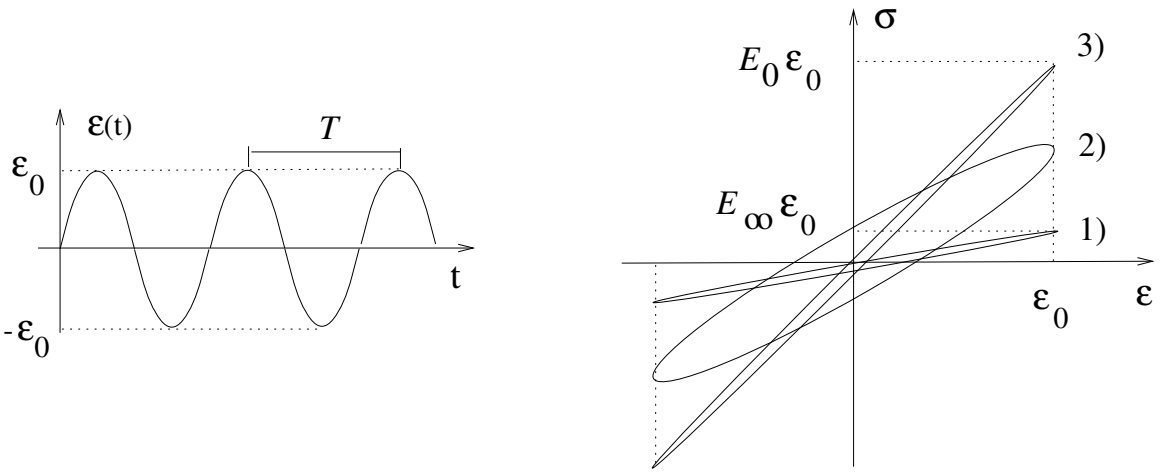


**Figure 4.25:** *Hysteresis work and dynamic stiffness for a low, intermediate and high frequency. 1) $\omega t_r \ll 1$ 2) $\omega t_r \approx 1$ 3) $\omega t_r \gg 1$. $E_0 = E_\infty + E$*

As a last topic in this section we study the normalized dynamic modulus $|E^*|/(E_\infty + E)$ and the phase angle $\arg(E^*)$ as functions o normalized frequency $\omega t_r$ and how different values of $g$ effect these quantities. Figure 4.26 shows this.

The parameter $g$ was defined as $g = E/(E_\infty + E)$. In the following dynamic analysis, SLS models with a normalized relaxation of $g = 0.5$ and downwards will be studied. Moreover the models will be studied in a frequency range where the upper limit is situated well below $\omega t_r = 1$, since this upper limit constitutes a physically reasonable frequency range for a real material.

### 4.3.3 SLS model: Numerical evaluation of stress

In a time stepping procedure the following expression could be used to evaluate the stress in the Maxwell element $\sigma_M$

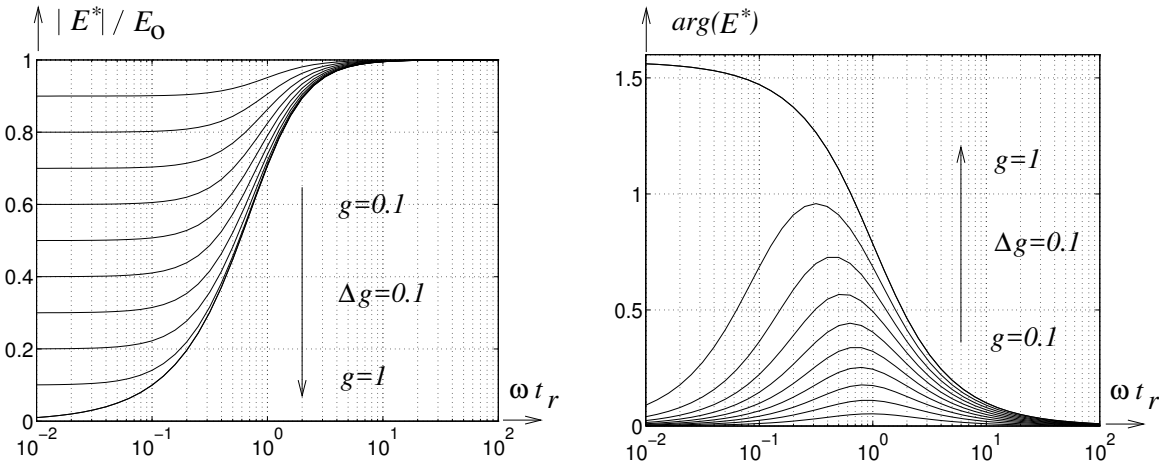


**Figure 4.26:** *The absolute value and the phase of $E^*$ as functions of normalized frequency $\omega t_r$ for different values of normalized relaxation $g$*

$$\Delta\sigma_M = \sigma_M \left( e^{\frac{-\Delta t}{t_r}} - 1 \right) + \frac{1}{2} E \left( 1 + e^{\frac{-\Delta t}{t_r}} \right) \Delta\varepsilon \tag{4.39}$$

The calculated stress increment is then added to the last known value according to

$$\sigma_{M,i+1} = \sigma_{M,i} + \Delta\sigma_M$$

It should be pointed out that the evaluation of the stress increment contains approximations which are dependent on the time-step length $\Delta t$. The approximations become better for smaller time-steps. See *Notes on linear viscoelasticity* [4] for further details.

### 4.3.4 SLS model: Summary

Below follows a summary of the improvements obtained with the SLS model compared to the previously discussed Kelvin model.

- The SLS model can exhibit relaxation behavior.
- The spring in the Maxwell element prevents discontinuous stress response at non-smooth shifts in the strain rate $\dot{\varepsilon}$
- The dynamic modulus $E_{dyn}$ is bounded at large frequencies $\omega$.
- And consequently the response is almost elastic at high frequencies, i.e the hysteresis work $U_c$ is bounded.

## 4.4 Friction models

In this section two material models which are rate independent, i.e independent of load frequency, will be presented. Moreover the materials are amplitude dependent which is in contrast to the visco-elastic models previously discussed. The amplitude dependence could be described as caused by friction or as plasticity. Both view-points are valid. Friction materials could typically be soils. Friction soils such as sand or gravel. Cracked concrete could also be an example of a material which is amplitude dependent. Dyrbye [5] justified the use of the SFS model, which will be presented here, by referring to bridge research. Studies had showed that the logarithmic decrement was amplitude dependent in a way that could not be explained by any simpler friction model. Kalmar-Nagy and Shekhawat [6] points to beam column connections as an example of amplitude-dependent structural behavior. Such connections have bi-linear hysteresis, something that will be covered here.

## 4.5 Coulomb friction model

The material presented in this section is mostly based on unpublished writings put together by my supervisor Per Erik Austrell (personal communication, spring 2017).

The least complex way to model a *rate-independent* damping behavior is by putting a spring in parallel with a friction element or a friction block, see Figure 4.27.

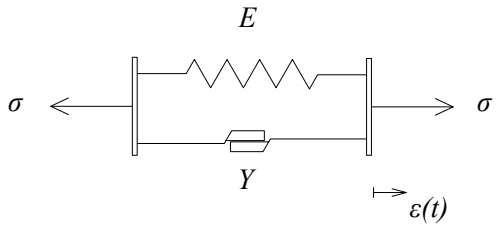


**Figure 4.27:** *Coulomb friction material model*

Having the spring and the block coupled in parallel yields

$$\sigma = \sigma_E + \sigma_F \tag{4.40}$$

where subscript $E$ refers to the elastic spring and the subscript $F$ refers to the block. This is in a way analogous to the Kelvin model, with the dashpot exchanged for a friction block. Figure 4.28 gives an explanation to the behavior of the block. As the node to the right in the figure moves to the right (i.e the strain-rate is directed to the right) the block reacts with a constant stress directed to the left. As the node moves to the left the stress in the block is directed to the right.

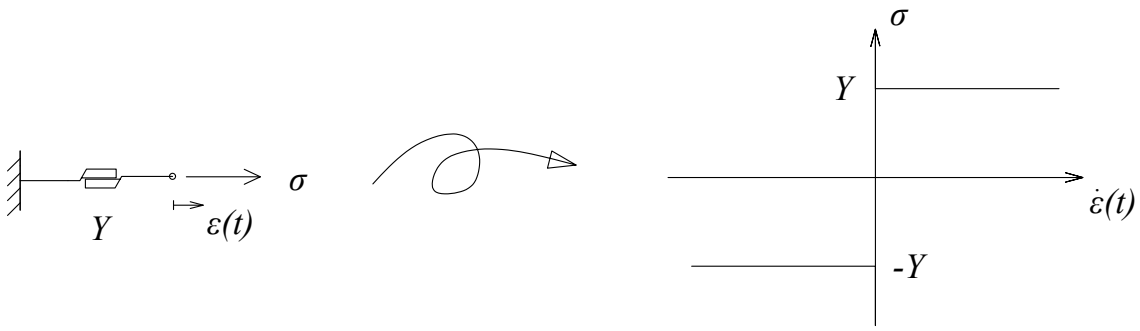


**Figure 4.28:** *The stress in the friction block related to the direction of movement of the node to the right, i.e the strainrate. Movement to the right is chosen as the positive direction.*

The following equation gives the total strain in the material. First term is the elastic part and the second term describes the stress in the friction block as explained above.

$$\sigma = E\varepsilon + Y\,\mathrm{sign}(\dot{\varepsilon}) \qquad \mathrm{sign}(\dot{\varepsilon}) = \begin{cases} 1 & \text{if} \quad \dot{\varepsilon} > 0 \\ -1 & \text{if} \quad \dot{\varepsilon} < 0 \end{cases} \tag{4.41}$$

In order to see the physical irregularities connected with the proposed model one can return to the triangular pulse presented in the previous section where the Kelvin model was discussed.

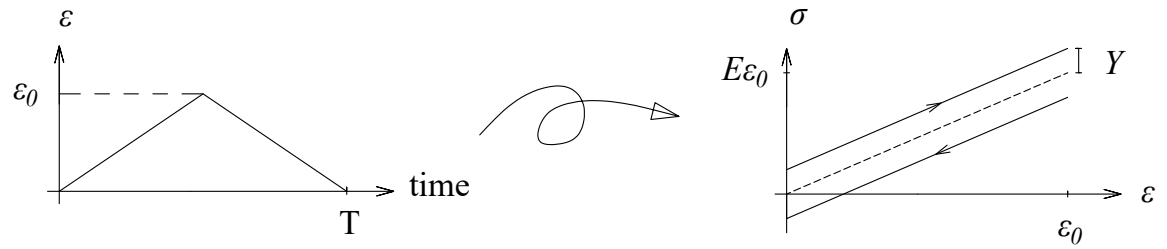


**Figure 4.29:** *A triangular strain yields a discontinuous stress response.*

Studying Figure 4.29 it can be noted that the model, through the friction block, is able to dissipate energy. The area of the hysteresis loop, which is equal to the dissipated energy during the pulse, is

$$U_c = 2Y\varepsilon_0 \tag{4.42}$$

So far everything is in order, but looking at the stress-response it can be noted that it is discontinuous at the point where the strainrate $\dot{\varepsilon}$ changes direction. The point where the

change of direction occur is (T/2, $\varepsilon_0$). In this point the strainrate is discontinuous but even with a smooth strain function $\varepsilon(t)$ with a continuous strain rate the stress response will be discontinuous.

Take the strain function $\varepsilon = \varepsilon_0 \sin(\omega t)$. Inserting this function into equation (4.41) gives the following stress response

$$\sigma = E\varepsilon_0 \sin(\omega t) + Y \,\mathrm{sign}(\cos \omega t) \tag{4.43}$$

and it gets clear that the strain rate changes direction when the strain is at its maximum $\varepsilon_0$, giving a discontinuous stress response even for this smooth strain function. Figure 4.30 below shows this.

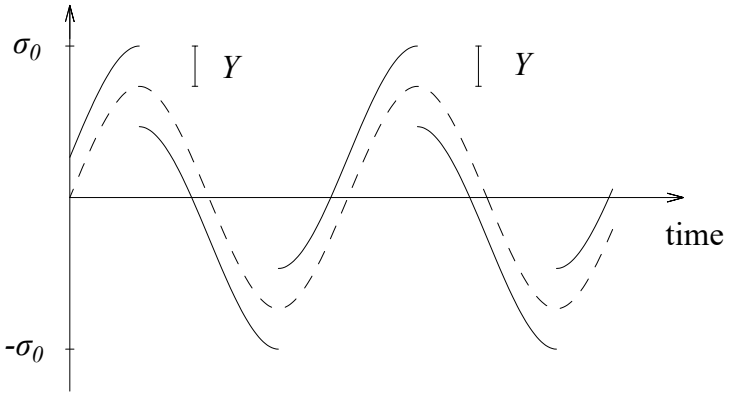


**Figure 4.30:** *Discontinuous stress response (solid line) to a continuous smooth strain function (dashed line).*

The stress response is therefore a periodic but non-harmonic discontinuous function.

Doing a *Fast Fourier Transform* (*FFT*) on the stress response $\sigma(t)$ one can see that the response contains odd multiples of the fundamental frequency. In other words: A harmonic strain generates a stress-response that contains the strain frequency, $\omega$, plus odd multiples of this frequency i.e $3\omega, 5\omega, 7\omega$, etc.

The *FFT* is a way to investigate if the response to a sinusoidal strain is linear or non-linear respectively.

- If the response to a sinusoidal strain with the frequency $\omega$ only contains this frequency then the response is linear.
- If the response contains the frequency $\omega$ plus other frequencies the response is non-linear

In Figure 4.31 the non-linear response of the Coulomb model can be studied.

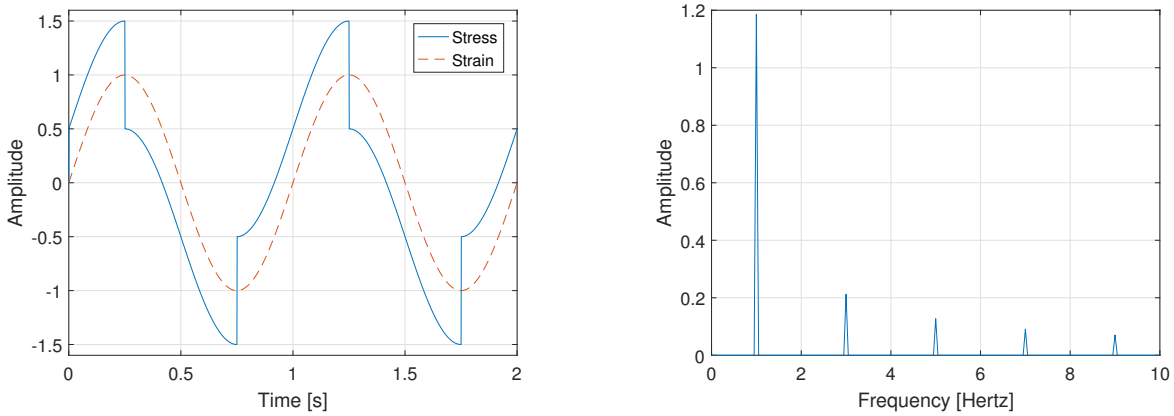


**(a)** $\sigma(t) = \sin(2\pi t) + 0.5\, sign(\cos(2\pi t))$ **(b)** *Frequency content of the stress response* $\sigma(t)$

**Figure 4.31:** *Division of the stress response into its different frequency components. Model parameters:* $E = 1$, $Y = 0.5$. *Applied strain:* $\varepsilon(t) = \sin(2\pi t)$, *i.e* $f = 1$ *Hz*

The hysteresis loop associated with the cyclic straining $\varepsilon(t) = \varepsilon_0 \sin(\omega t)$ of the model is shown in Figure 4.32. Maximum strain $\varepsilon_0$ and maximum stress $\sigma_0$ occur at the same time, i.e stress and strain are in phase (phase angle is zero). All periodic strain functions generates the same hysteresis work as long as the strain amplitude $\varepsilon_0$ is the same. The dissipated energy in one cycle is

$$U_c = 2Y2\varepsilon_0$$

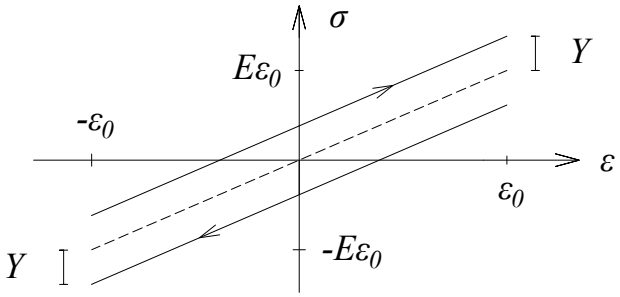


**Figure 4.32:** *Hysteresis loop associated with a periodic strain function with amplitude* $\varepsilon_0$

Again the reader is reminded of the discontinuous stress response that occur when the strain changes direction. In previous section a quantity called the dynamic modulus $E_{dyn}$ was determined for viscoelastic models. It was defined as the relation connecting the maximum stress to the maximum strain, $\sigma_0 = E_{dyn}\varepsilon_0$. In this model, with maximum stress being $E\varepsilon_0 + Y$, the expression for the dynamic modulus becomes

$$E_{dyn} = \frac{\sigma_0}{\varepsilon_0} = \frac{E\varepsilon_0 + Y}{\varepsilon_0} = E + \frac{Y}{\varepsilon_0} \tag{4.44}$$

The strain-amplitude dependence of the dynamic modulus is illustrated further in Figure 4.33. What is troubling here is that the dynamic modulus approaches infinity as the strain amplitude approaches zero, i.e

$$E_{dyn} = E + \frac{Y}{\varepsilon_0} \;\rightarrow\; \infty \qquad \text{as} \qquad \varepsilon_0 \;\rightarrow\; 0$$

This shows the need for a more sophisticated material model describing strain-amplitude dependence i materials.

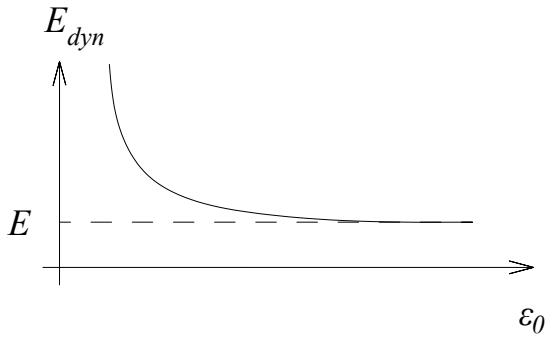


**Figure 4.33:** *Amplitude dependence of the dynamic modulus $E_{dyn}$*

### 4.5.1 Coulomb friction model: Summary

Below follows a summary of the irregularities associated with this friction model.

- The stress response to a known strain will be discontinuous if the strain changes direction.

$$\sigma = E\varepsilon + Y\,\text{sign}(\dot{\varepsilon}) \qquad \text{sign}(\dot{\varepsilon}) = \begin{cases} 1 & \text{if} \quad \dot{\varepsilon} > 0 \\ -1 & \text{if} \quad \dot{\varepsilon} < 0 \end{cases} \tag{4.45}$$

- The dynamic modulus approaches infinity as the strain amplitude approaches zero

$$E_{dyn} = E + \frac{Y}{\varepsilon_0} \;\rightarrow\; \infty \qquad \text{as} \qquad \varepsilon_0 \;\rightarrow\; 0$$

## 4.6 SFS: Simple frictional solid model

The material presented in this section is basically a rewrite of chapter 10 in the thesis *Modeling of elasticity and damping for filled elastomers* [7]. The reader is referred here for further information.

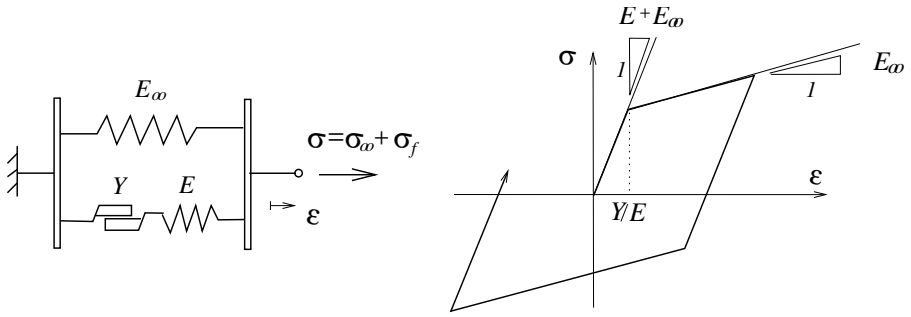


**Figure 4.34:** *The SFS model to the left and the associated hysteresis loop to the right.*

If the dashpot in a SLS-element is exchanged for a pair of friction blocks one obtain a model that describes a solid with frictional damping. In contrast to the *rate-dependence* of the dashpot, the friction blocks are *rate-independent*. Since the upper spring with stiffness $E_\infty$ and the lower friction-spring element is coupled in parallel the total stress is the sum of the stress in the upper spring $\sigma_\infty$ and the stress in the lower friction-spring element $\sigma_f$, i.e

$$\sigma = \sigma_\infty + \sigma_f \tag{4.46}$$

Figure 4.34 shows this relation and the hysteresis loop associated with a periodic strain. This hysteresis loop is only dependent on the strain amplitude of the periodic strain. Consequently a sine, sawtooth or square shaped periodic strain function yields the same hysteresis work, regardless of frequency, if the strain amplitude $\varepsilon_0$ is the same.

### 4.6.1 Evaluating the stress in the friction element

The friction-spring element acts like a linear elastic perfectly plastic spring, here referred to as the friction element. Since the stress-strain curve of such a spring is bilinear a check is required to find out if the current displacement is in the elastic or plastic region, see Figure 4.35.

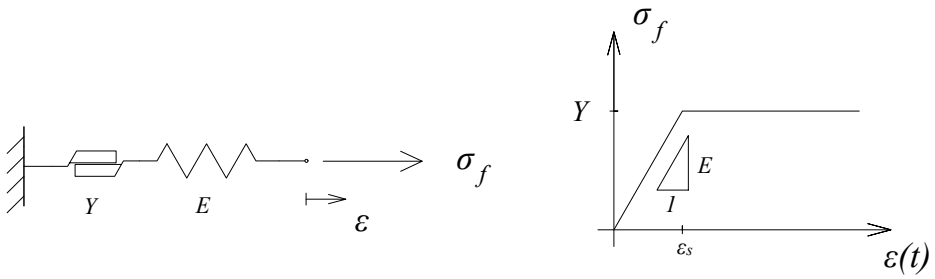


**Figure 4.35:** *The elastic perfectly plastic spring, referred to as the friction element and the associated load-curve.*

The strain in the friction element will be the sum of elastic and (frictional) plastic strain, $\varepsilon = \varepsilon_e + \varepsilon_p$. To obtain an algorithm which evaluates the stress in the friction element $\sigma_f$ it is necessary to know when the strain transitions from the elastic to the plastic region. If a small strain $\Delta\varepsilon$ is added to the existing strain $\varepsilon$ and knowing that the maximum stress in the friction element is $Y$ it is possible to determine this. Therefore a strain increment is defined

$$\Delta\varepsilon = \Delta\varepsilon_e + \Delta\varepsilon_p$$

The aim is to determine a stress increment $\Delta\sigma_f$. Since the stress is the same throughout the whole friction element it is possible to determine the stress only from the elastic spring $\sigma_f = E\varepsilon_e$. The expression for the stress increment then becomes

$$\Delta\sigma_f = E\Delta\varepsilon_e \tag{4.47}$$

Suppose that the current stress $\sigma_f$ is known, then a trial stress can be defined under the assumption that the strain increment is purely elastic

$$\sigma^{trail} = \sigma_f + E\Delta\varepsilon$$

The total stress in the element $\sigma_f$ is limited to

$$-Y < \sigma_f < Y$$

and this condition is tested for each increment, $\Delta\varepsilon_e$. If the trial stress $\sigma^{trial}$ is larger than the yield stress , then at least a part of the strain increment is plastic. Eventually there is $\Delta\varepsilon_e = 0$, if the strain increment is purely plastic. This leads to the condition:

$$\text{if} \quad |\sigma^{trial}| > Y \quad \text{then} \quad \sigma_f = \pm Y \tag{4.48}$$

An algorithm for evaluating the stress in the element can now be written as follows

**Table 4.1:** *The algorithm used to evaluate the stress $\sigma_f$ in the friction element*

$i$=1,2,3...

1. $\Delta\varepsilon = \varepsilon_{i+1} - \varepsilon_i$
2. $\sigma^{trial} = (\sigma_f)_i + E\Delta\varepsilon$
3. $\alpha = Y/\sigma^{trial}$
4. if $\alpha > 1$ then $\alpha = 1$
5. $(\sigma_f)_{i+1} = \alpha\sigma^{trial}$

For the simpler friction model presented in the previous section it was shown that the stress response to a sinusoidal strain $\varepsilon(t) = \varepsilon_0 \sin(\omega t)$ was discontinuous. Figure 4.36 shows how the SFS model responds to a sinusoidal strain and the frequency content of that response. Just like the simpler model the stress response contains odd multiples of the fundamental frequency $\omega = 2\pi f$. The used model parameters were: $E_\infty = 1$ Pa, $E = 1.5$ Pa and $E_\infty = 0.5$ Pa. The strain amplitude was $\varepsilon_0 = 1$

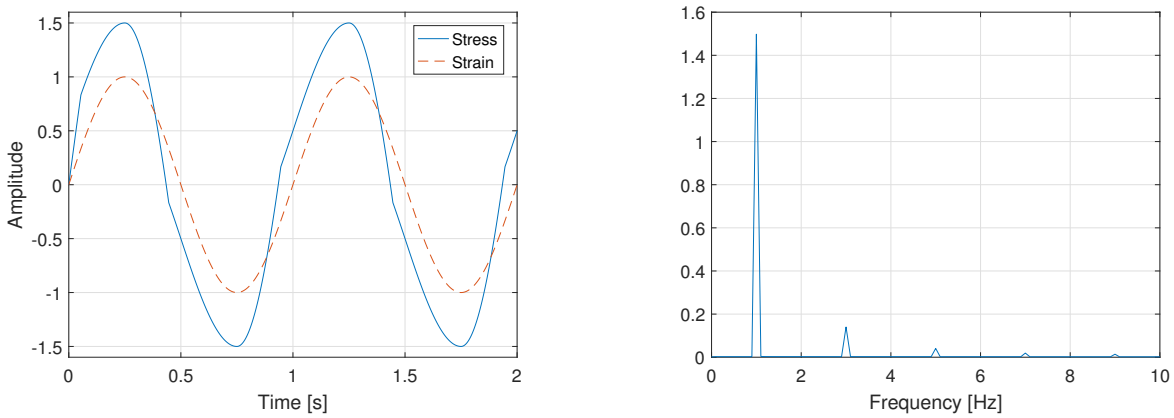


**Figure 4.36:** *Frequency content of the stress-response. Plotting parameters: $E_\infty = 1$ Pa, $E = 1.5$ Pa and $E_\infty = 0.5$ Pa. The used strain amplitude was $\varepsilon_0 = 1$*

Now moving on to study the dynamic modulus of the SFS model

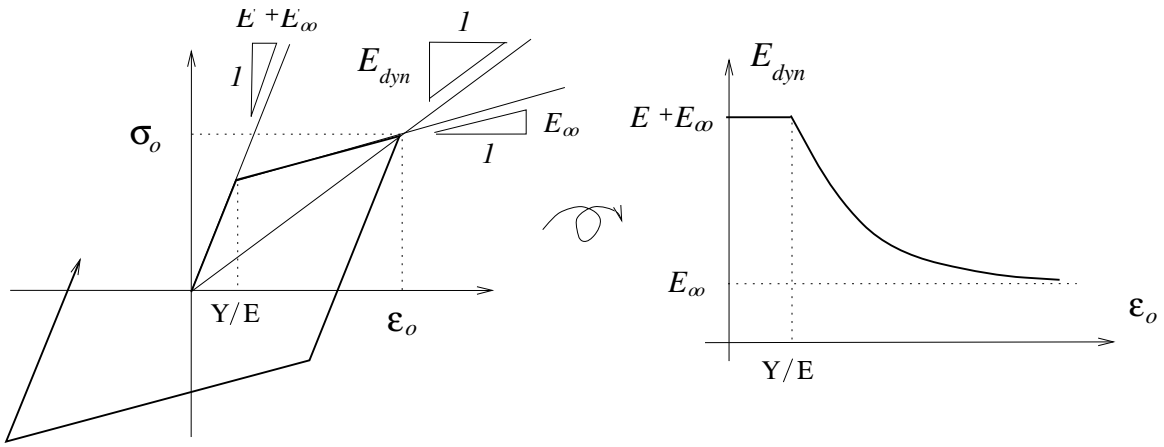


**Figure 4.37:** *Definition of the dynamic modulus $E_{dyn}$ from the hysteresis loop. Maximum stress and maximum strain occur simultaneously.*

The amplitude dependence of the SFS model is illustrated in Figure 4.37. Maximum stress and maximum strain occur at the same time, and the dynamic modulus is calculated at this point as $E_{dyn} = \sigma_0/\varepsilon_0$. If the strain amplitude is below the yield limit $\varepsilon_s = Y/E$ the model is fully elastic with a constant modulus $E + E_\infty$. When the strain amplitude exceeds the yield limit we have $\sigma_0 = Y + E_\infty \varepsilon_0$. This gives the following expression for the dynamic modulus in the strain range $\varepsilon_0 > \varepsilon_s$

$$E_{dyn} = \frac{\sigma_0}{\varepsilon_0} = \frac{Y + E_\infty \varepsilon_0}{\varepsilon_0} = E_\infty + \frac{Y}{\varepsilon_0} \qquad \varepsilon_0 > \varepsilon_s \tag{4.49}$$

In contrast to the simpler friction model the dynamic modulus of the SFS model is not unbounded when the strain-amplitude approaches zero, Figure 4.37 shows the dynamic modulus as a function of strain amplitude $\varepsilon_0$.

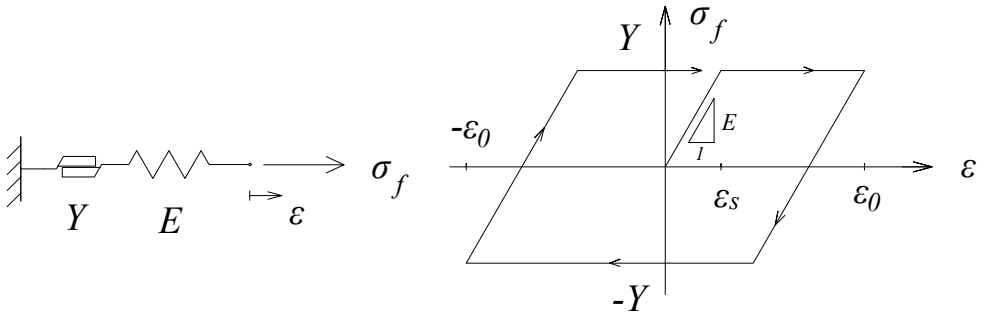


**Figure 4.38:** *The hysteresis loop associated with the friction element.*

Now the focus is directed towards the damping of the model. The linear spring does not contribute to the damping so it is only necessary to look at the friction element. Figure 4.38 shows the hysteresis loop associated with a periodic strain with amplitude $\varepsilon_0$. The area enclosed in one period, i.e the dissipated energy is

$$U_c = 2Y \cdot 2(\varepsilon_0 - \varepsilon_s) \tag{4.50}$$

If $\varepsilon_0 < \varepsilon_s$ the response is elastic and the dissipated energy is zero. Using the following definition of normalized damping

$$d = \frac{U_c}{\pi \sigma_0 \varepsilon_0} \tag{4.51}$$

and inserting the expression for the stress amplitude $\sigma_0 = Y + E_\infty \varepsilon_0$, an expression for $d$ can be obtained

$$d = \frac{4}{\pi} \frac{\varepsilon_0 - \varepsilon_s}{\left(1 + \frac{E_\infty}{Y}\varepsilon_0\right)\varepsilon_0} \qquad \varepsilon_0 > \varepsilon_s \tag{4.52}$$

Defining a normalized strain as $\alpha = \varepsilon_0/\varepsilon_s$ and inserting this into Eq. (4.52) yields

$$\frac{E_{dyn}}{E_\infty} = 1 + \frac{E}{E_\infty}\frac{1}{\alpha} \qquad \text{and} \qquad d = \frac{4}{\pi}\frac{\alpha - 1}{\left(1 + \frac{E_\infty}{E}\alpha\right)\alpha} \tag{4.53}$$

With the introduction of the parameter $h = E/E_\infty$ these expressions can be plotted as functions of the normalized strain $\alpha$ for different values of $h$, Figure 4.39 shows this. An increase in $h$ leads to an increase in damping and maximum damping occur around $\alpha = 2 - 3$.

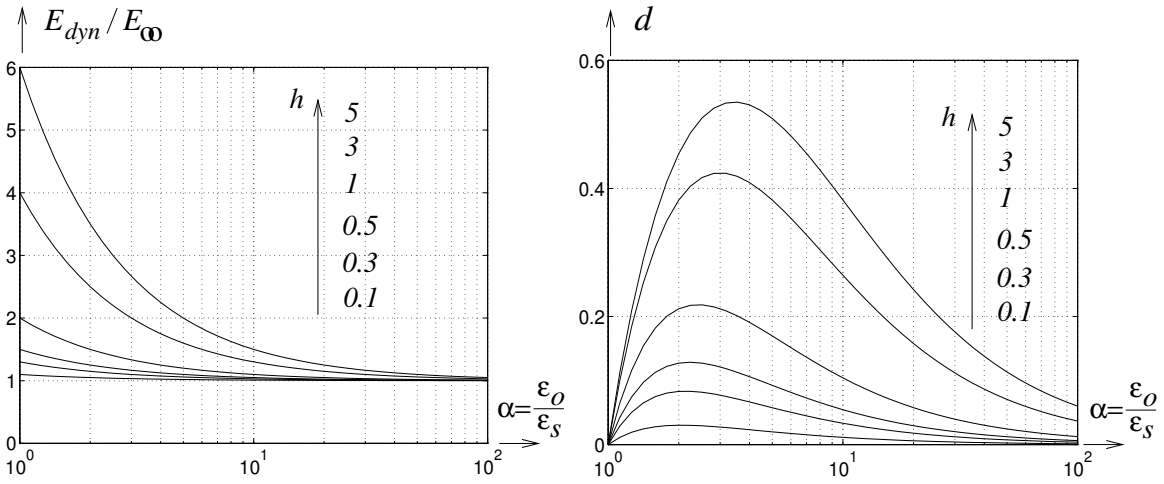


**Figure 4.39:** *To the left: the dynamic modulus as a function of the normalized strain for different values on h. To the right: the equivalent phase angle d as a function of the normalized strain for different values on h. The phase angle is equal to the damping.*

Similar to the generalized maxwell model, Figure 4.22, where several Maxwell elements were coupled in parallel it is possible to couple several friction elements in parallel to get a better fit to the experimental results. Figure 4.40 shows this and the obtained model behavior.

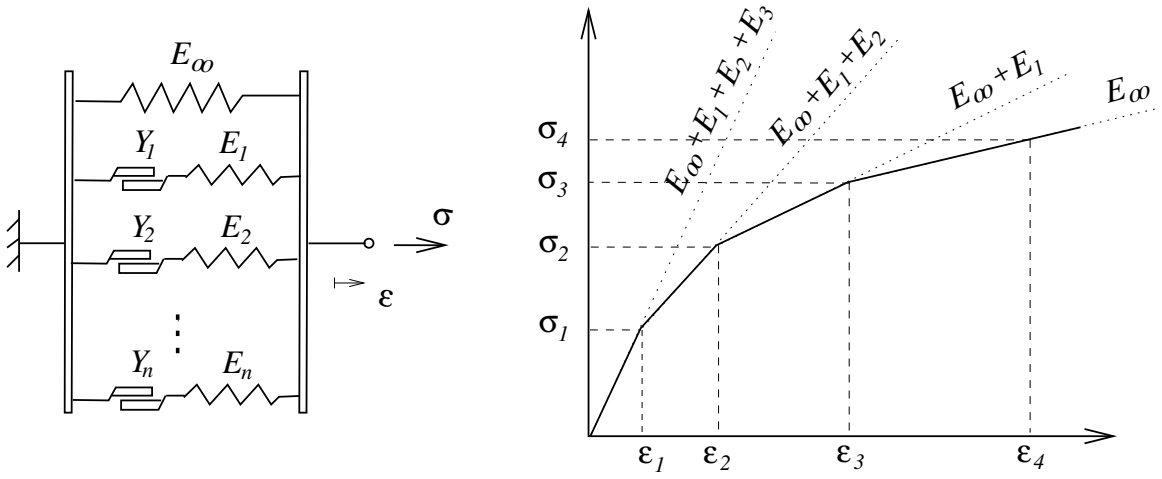


**Figure 4.40:** *Generalized friction model and the obtained load-curve*

### 4.6.2 SFS model: Summary

Below follows a summary of the improvements obtained with the SFS model compared to the simpler friction model.

- No discontinuities in the stress response regardless of strain type.
- An upper bound on the dynamic modulus is introduced due to the spring in the friction element. For strain amplitudes smaller than the yield-strain limit $\varepsilon_s = Y/E$ the response is purely elastic with the constant modulus $E_\infty + E$.

## 4.7 Concluding remarks

An introduction to visco-elastic and frictional material models has now been given. Both the linear visco-elastic SLS model and the non-linear friction SFS model was introduced in order to obtain visco-elastic and friction models without discontinuities in the stress-response.

If the SLS and the SFS model is combined one obtains a material model which is both rate- and amplitude dependent. This model was referred to as the *5-parameter model*, see Figure 4.41. Such a model can be used in order to model the material that was presented in the introduction to this chapter, see Figure 4.1 and 4.2. Moreover the model can be extended with more *Maxwell* and *friction elements* in order to better capture the behavior of a real material.

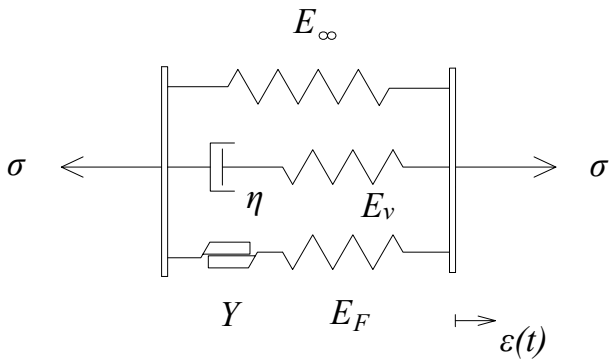


**Figure 4.41:** *The 5-parameter model*

# Chapter 5

# Load definition and structural formulation

The following chapter defines the conditions for the dynamic analyses of the presented material models. Initially a fictitious test-specimen is defined in terms of geometry and then a realistic frequency range, in which to conduct the dynamic analyses, is determined.

## 5.1 Geometry-dependent structural formulation

In order to investigate the dynamic properties of the material models a transition from a material formulation, independent of geometry, into geometry-dependent structural formulation is needed. Figure 5.1 shows the idea.

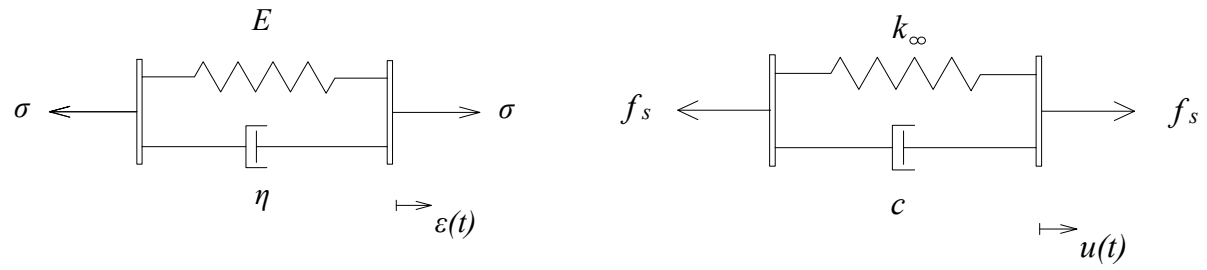


**(a)** *Kelvin material model* **(b)** *Kelvin structure model*

**Figure 5.1:** *Transition from material to structure.*

To keep it simple a fictitious bar-shaped test specimen could be used. A bar is a structural element used when the load is applied mainly in the axial-direction of the structural element i.e

in the length direction of the bar. The fictitious test-specimen is given the following dimensions. Moreover it is assumed that the bar-structure is **weightless**.

$$\begin{aligned} &\text{Bar length:} && L = 10 \text{ cm} \\ &\text{Area of bar cross-section} && A = 1 \text{ cm}^2 \end{aligned}$$

The aim is now to move from a material-formulation where the strains $\varepsilon$ are related to the stresses $\sigma$ into the structural-formulation where displacements $u$ are related to forces in the structure $f_s$. It should be noted that the Poisson effect will be neglected.

$$\begin{aligned} E\varepsilon = \sigma \qquad &\Rightarrow \qquad ku = f_S \\ \eta\dot{\varepsilon} = \sigma \qquad &\Rightarrow \qquad c\dot{u} = f_s \end{aligned}$$

Doing this requires multiplication with the determined dimensions of the structure. With $u = \varepsilon L$ and $f = \sigma A$ the stiffness $k$ [N/m] can be obtained through

$$\frac{E \cdot A}{L} \cdot \varepsilon \cdot L = \sigma \cdot A \qquad \Rightarrow \qquad \frac{EA}{L} u = f_s \tag{5.1}$$

in the same way the $c$-parameter can be determined

$$\frac{\eta \cdot A}{L} \cdot \dot{\varepsilon} \cdot L = \sigma \cdot A \qquad \Rightarrow \qquad \frac{\eta A}{L} \dot{u} = f_S \tag{5.2}$$

Consequently the $k$- and $c$-parameters becomes

$$k = \frac{EA}{L} \text{ [N/m]} \qquad \text{and} \qquad c = \frac{\eta A}{L} \text{ [kg/s]}$$

## 5.2 Load definition

In order to find a reasonable frequency range in which to conduct the studies the decision was taken to let pulses with different duration times, $t_d$, define the endpoints of the frequency interval.

A pulse with a duration time of $t_d = 5$ ms is considered a short pulse. The upper boundary of the pulse duration was chosen to be $t_d = 50$ ms.

If the pulse has the shape of a half-sine function, the period-time of the sine function would be $2t_d$. Utilizing this, it is possible to estimate the highest frequency to be triggered by a pulse of a certain duration.

$$f = \frac{1}{2t_d} \tag{5.3}$$

This will give the following boundaries of the frequency range of interest

$$t_d = 50\,\text{ms} \Rightarrow f = 10\,\text{Hz} \qquad t_d = 5\,\text{ms} \Rightarrow f = 100\,\text{Hz}$$

Now for a certain material it is possible to connect a mass to the structure which will make the eigen-frequency of the *Single degree of freedom* (SDOF) system fall within the desired frequency interval $[10, 100]$ Hz.

Using the described, *weightless*, test specimen with length $L = 0.1$ m and cross-sectional area $A = 1$ cm$^2$ and wanting the first natural frequency to appear at 10 Hz with an added mass $m = 1$ kg gives a numerical value on the E-modulus: $E_\infty \approx 4$ MPa (3.948 MPa). This is a reasonable E-modulus for a rubber material. Figure 5.2 shows a free body diagram of the structure with the added mass $m$.

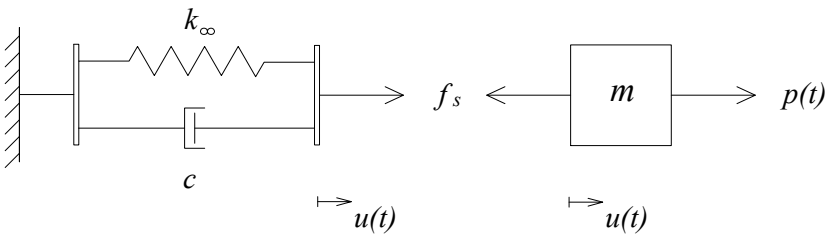


**Figure 5.2:** *Freebody diagram of the Kelvin system*

# Chapter 6

# Linear Dynamic systems

In order to compare the dynamic behavior of the SLS model to the Kelvin model two approaches are possible. Figure 6.1 shows the two dynamic systems respectively.

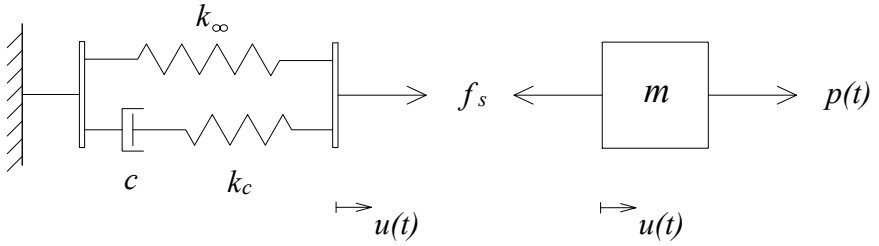


**(a)** *A dynamic SLS system*

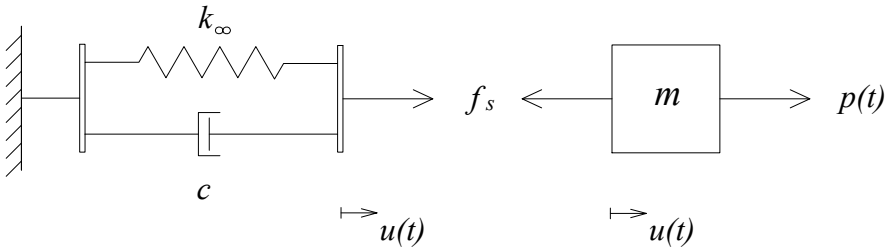


**(b)** *A dynamic Kelvin system*

**Figure 6.1:** *The two studied linear dynamic systems*

The most common one would be to use equivalent viscous damping as described in Section 2.5. For a SDOF-system the material behavior will in a way be equivalent at the natural frequency of the system but not at any other frequency. This approach is always a possibility when the displacement are within the linear-elastic regime of the structure. The down side of this approach is that for a real structure a measurement would be required in order to determine the damping parameter and this parameter would only guarantee a good result at the specific

natural frequency. I.e if the mass of the structure or the mass applied to the structure would change the determined damping parameter would not be correct [1].

The other approach, and perhaps the more interesting of the two, would be to try to fit the *2-parameter* Kelvin model to the *material* behavior of the *3-parameter* SLS model for a wide range of frequencies. The fit would be carried out without an attached mass, $m$. The Kelvin model could be fitted to the SLS model in the desired frequency interval $[10, 100]$ Hz, in terms of *dynamic modulus* and *phase angle*.

If this is possible, two material models are obtained which have a similar behavior on a certain frequency range. What will now happen if a mass $m$ is attached to the materials? Will the fitted Kelvin model behave in accordance with the SLS model also with the mass attached? Altering the mass will change the natural frequency. Could the fitted Kelvin model also be used to model the *dynamic behavior* of the SLS model for a wide range of natural frequencies? Adding different masses the natural frequency could be made to appear at for instance 10, 50 and 90 Hz.

## 6.1 Fitted material approach

Picking a SLS material with $g = 0.5$ translates into

$$E_\infty = E$$

In a previous section the stiffness of the upper linear spring (see Figure 5.1) was set to $E_\infty \approx 4$ MPa (3.948 MPa). This is a reasonable E-modulus for a rubber material. Setting the relaxation time to $t_r = 0.0005$ s one obtains a model which also has a reasonable amount of damping in the studied frequency range. Remember the definition of the relaxation time $t_r = \eta/E$.

Now a least squares fit can be carried out in order to find the $\eta$-parameter of the Kelvin model. Since the internal damping of a material is closely connected to the phase angle $\delta$, the starting point will be to try to fit the expression for the phase angle of the Kelvin model to that of the SLS model. The phase angle $\delta$ is equal to the argument of the complex modulus $\arg(E^*(\omega))$. For the SLS model and Kelvin model respectively we have

$$\delta_{SLS} = \arg(E_\infty + E\frac{i\omega t_r}{1 + i\omega t_r}) \qquad \delta_{Kelvin} = \arg(E_\infty + i\omega c) \tag{6.1}$$

Numerically the above expressions can be plotted for different frequencies $\omega$. The best fit in a least square sense would be $|r| = |\delta_{SLS} - \delta_{Kelvin}|$ where $r$ is the residual vector and $|r|$ is the length of this vector. Table 6.1 shows the fitting procedure.

**Table 6.1:** *Least squares fit of the phase angle $\delta$ of a Kelvin model to a SLS model.*

| $\eta$-parameter | $\|\|\delta_{SLS} - \delta_{Kelvin}\|\|$ |
|---|---|
| 1790 | 0.1921 |
| 1800 | 0.18809 |
| 1810 | 0.18782 |
| 1820 | 0.19129 |
| 1830 | 0.19831 |

Apparently $\eta = 1810$ Pa·s provides the best fit to a SLS-material with relaxation parameter $g = 0.5$ and relaxation time $t_r = 0.0005$ s, in the frequency range $[10, 90]$ Hz. Figure 6.2 shows the fitted curves.

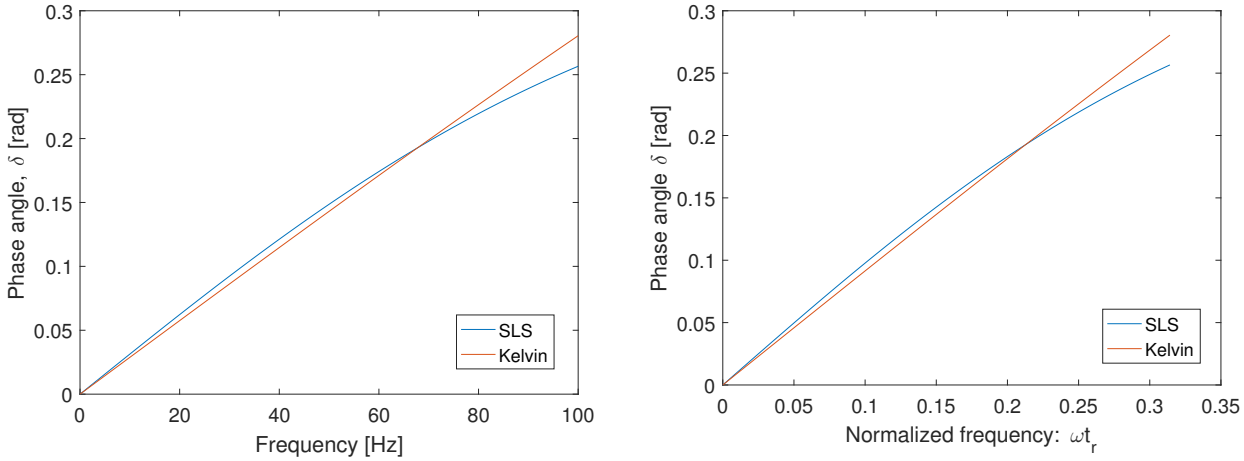


**Figure 6.2:** *To the left we have the phase angle $\delta$ plotted for the two models in the chosen frequency range. To the right the same curves are plotted as functions of normalized frequency. SLS-parameters: $g = 0.5$, $t_r = 0.0005$. Kelvin-parameters: $E_\infty = 3.948$ MPa $\eta = 1810$ Pa·s*

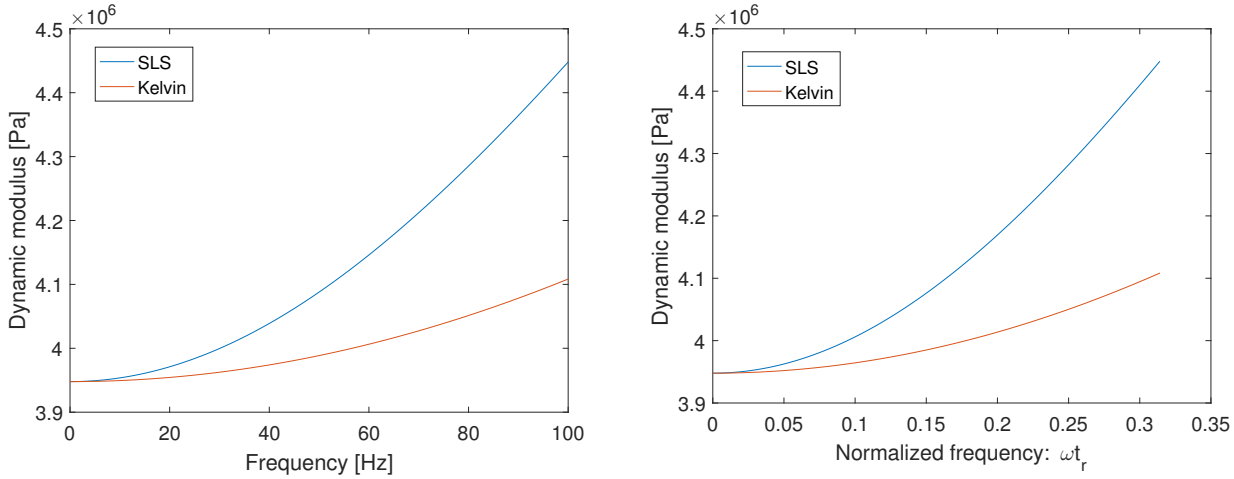


**Figure 6.3:** *To the left we have the dynamic modulus $E_{dyn}$ plotted for the two models in the chosen frequency range. To the right the same curves are plotted as functions of normalized frequency. SLS-parameters: $g = 0.5$, $t_r = 0.0005$. Kelvin-parameters: $E_\infty = 3.948$ MPa $\eta = 1810$ Pa·s*

Figure 6.3 shows the dynamic modulus $E_{dyn}$ of the reference SLS material and the fitted Kelvin material plotted against the frequency and the normalized frequency respectively. The used damping parameter $\eta$ in the Kelvin model is the parameter determined from the curve-fitting, $\eta = 1810$ Pa·s. At high frequencies the dynamic modulus of the Kelvin model deviates significantly from the dynamic modulus of the SLS reference model. The SLS material gets much stiffer at high frequencies.

Figure 6.4 shows what happens if the frequency range is extended further. At higher frequencies, $f > 100$ Hz, it is no longer possible to fit a Kelvin model, in a satisfactory way, to a SLS model with these particular parameters ($g = 0.5$, $t_r = 0.0005$ s). Note that the frequency-axis is logarithmic.

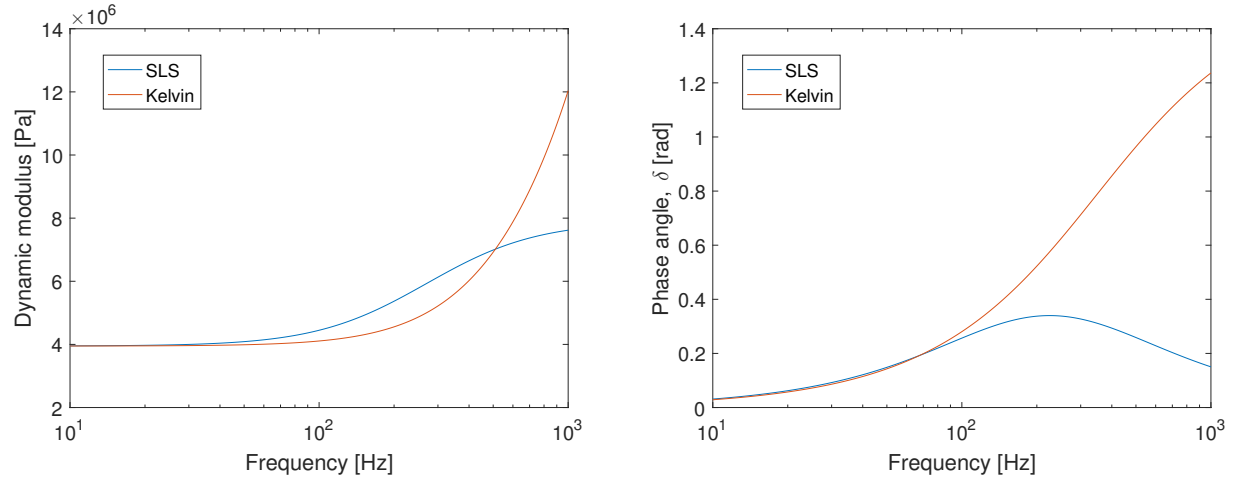


**(a)** *Dynamic modulus as a function of frequency* **(b)** *Phase angle as function frequency*

**Figure 6.4:** *The dynamic modulus and phase angle of the two models plotted in a wider frequency interval. Note that the frequency-axis is logarithmic.*

## 6.2 Steady-state response: Fitted material approach

As presented before (see Figure 5.1): Transitioning from a material-formulation in terms of stresses and strains into a structural-formulation, where displacements are related to forces, yields

$$k_\infty = \frac{E_\infty A}{L}, \qquad c = \frac{\eta A}{L}, \tag{6.2}$$

The chosen test bar had the following dimensions:

Length: $L = 10$ cm, cross-section area: $A = 1$ cm$^2$

The numerical values on the structural-parameters then becomes:

$$\begin{aligned} k_\infty &\quad 3948 \text{ [N/m]} \\ k_c &\quad 3948 \text{ [N/m]} \\ c &\quad 1.81 \text{ [kg/s]} \end{aligned}$$

For a sinusoidal steady-state excitation, $p^* = p_0 e^{i\omega t}$, the steady state displacement amplitude $u_0$ can be expressed analytically for these two material models, since they are linear. As shown before Eq.(2.8), the expression for the *steady state* displacement amplitude of the Kelvin system is

$$\text{Kelvin}: \quad u_0 = \frac{p_0}{|-\omega^2 m + k_\infty + i\omega c|} \tag{6.3}$$

where $p^* = p_0$ i.e $p^*$ is placed along the real-axis. $k^* = k_\infty + i\omega c$ is called the complex stiffness of the system. Clearly the complex stiffness $k^*(\omega)$ is the structural equivalent to the complex modulus $E^*(\omega)$. Consequently the *steady state* displacement amplitude $u_0$ of the SLS system can be determined in the same manner since we know the complex modulus of the SLS model. For the dynamic SLS system we get

$$\text{SLS}: \quad u_0 = \frac{p_0}{\left|-\omega^2 m + k_\infty + k_c \frac{i\omega t_r}{1+i\omega t_r}\right|} \tag{6.4}$$

The quasi-static displacement, $u_{qs}$, is equal to $p_0/k_\infty$ for both models. When the loading is slow the dashpots generates no resistance at all. The quantity of interest here is the displacement response-factor $R_d$, which is a scale factor between the quasi-static displacement $u_{qs}$ and the displacement caused by the dynamic loading $u_0$

$$R_d = \frac{u_0}{u_{qs}} \tag{6.5}$$

If the fitted structural parameter $c$ is inserted into Eq.(6.3) a comparison between the two models is possible.

By attaching different masses to the structure the resonant frequency will appear at different places in the frequency interval [10, 90] Hz. Starting off with a mass $m = 1$ kg and using the following definition

$$f_{n,\infty} = \frac{1}{2\pi}\sqrt{\frac{k_\infty}{m}} \tag{6.6}$$

the first system will have a resonance peak at around 10 Hz ($k_\infty = 3948$ N/m). With the same stiffness parameter and a desired resonance-peak at 50 Hz the second system will have a mass $m = 0.04$ kg and to have the peak appear at 90 Hz in the third and last system the attached mass $m$ would have to be $m = 0.012346$ kg. To summarize:

| Added mass | | $f_{n,\infty}$ |
|---|---|---|
| $m = 1$ kg | $\rightarrow$ | 10 Hz |
| $m = 0.04$ kg | $\rightarrow$ | 50 Hz |
| $m = 0.0123$ kg | $\rightarrow$ | 90 Hz |

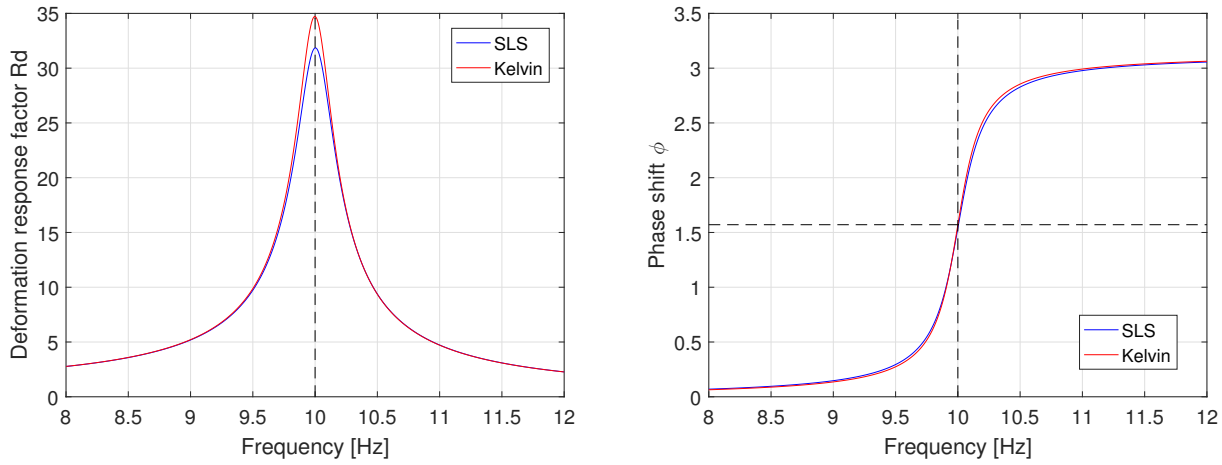


**Figure 6.5:** *Steady-state response of the SLS and the Kelvin system respectively. Attached mass $m = 1$ kg*

The steady-state response of the system with the attached mass $m = 1$ kg in terms of displacement response factor $R_d$ and corresponding phase-shift $\phi$ can be studied in Figure 6.5. Both models have a peak in the response factor $R_d$ at roughly the same frequency, this is also indicated by the phase-shift $\phi$ which is plotted to the right in Figure 6.5 for different frequencies. In linear dynamics the phase-shift $\phi$ is equal to $\pi/2$ at the natural frequency of the system [1] (Page: 88).

However, the two models differ significantly in the magnitude of the response factor $R_d$. For the Kelvin system, $R_d$ is around 35 compared to an $R_d$-value of 32 for the SLS-system. This

indicates that the two models does not have the same amount of damping at this frequency and that the damping is low in both systems.

Mathematically, the damping is what keeps the displacement from going towards infinity at resonance. One way of comparing the amount damping at a certain frequency is to study the phase-angle $\delta$ of the material at this particular frequency, see Equation (6.1).

The other option would be to compare the damping of the models in terms of the damping ratio $\zeta$. Through the relation $c = 2m\zeta\omega_n$ a specific damping ratio $\zeta_K$ is connected to the fitted $c$-parameter of the Kelvin system. Using equivalent viscous damping as described earlier an approximate damping ratio could be connected to the SLS system, $\zeta_{eq,SLS}$, as well. How this is done is described in detail in Appendix A.

Let us present both in order to get a feeling for the relation between the two quantities. Remember that $\zeta_{eq,SLS}$ is an approximation.

**Table 6.2:** *Damping parameters of the SLS and the Kelvin system respectively. Attached mass* $m = 1\ kg$

| | $\delta$ [rad] | $\zeta$ |
|---|---|---|
| SLS: | 0.0313 | 1.57 % |
| Kelvin: | 0.0288 | 1.44 % |

Even though the difference in phase-angle between the two material models is not larger than 0.0025 radians this results in the quite severe difference in the response-factor $R_d$. To illustrate this further we look at an arbitrary Kelvin system.

For $\zeta = 1\%$ the response factor becomes $R_d = 50$ at resonance

For $\zeta = 2\%$ the response factor becomes $R_d = 25$ at resonance

Obviously both models are very sensitive to the value of the chosen damping-parameters when the damping is **small**. 1 % or 2 % makes a big difference, and consequently this is something to think about when analyzing results from simulations.

A last observation before moving on: Looking at the Kelvin model primarily, there is a factor 2 between phase-angle $\delta$ and the damping ratio $\zeta$. Approximately this is true also for the SLS-system when the phase angle is compared to the equivalent viscous damping ratio $\zeta_{eq}$.

We will return to this observation later. Perhaps it will be helpful in an attempt to estimate an equivalent damping parameter $\zeta_{eq}$ that could be used to fit the *steady state* response of a Kelvin system to the *steady state* response of a SLS system.

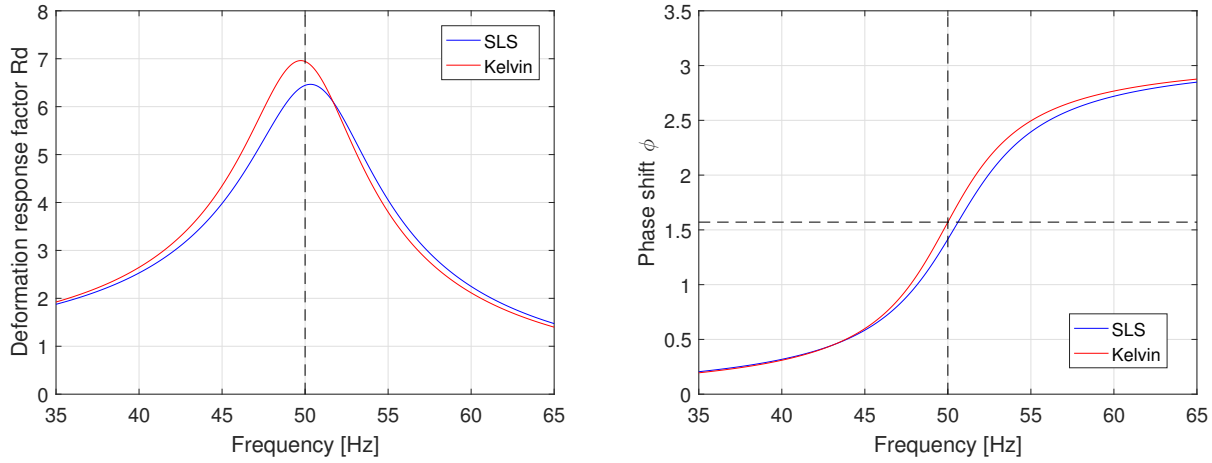


**Figure 6.6:** *Steady-state response of the SLS and the Kelvin system respectively. Attached mass* $m = 0.04$ *kg*

In the next two systems the resonance peaks occur at roughly 50 Hz, see Figure 6.6. The fitted Kelvin system is close in terms of magnitude of the response factor $R_d$. Both systems have a response factor $R_d$ between 6 and 7. A small horizontal drift of the respective peaks is visible however. The peak of the Kelvin system occur at a frequency slightly below the natural frequency of the system, $f_n = 50$ Hz. This is a characteristic feature of a Kelvin system. The more damping, the more the peak drifts towards a lower frequency. The displacement resonance frequency for a Kelvin system is $\omega_n\sqrt{1-2\zeta^2}$ [1] (Page: 82)

The SLS system have a small drift to the right instead. This seems reasonable since the maxwell element adds an extra spring to the system. At 50.62 Hz the phase shift $\phi$ is $\pi/2$, see Table 6.3. In linear dynamics the undamped natural frequency is defined as the frequency at which the phase shift $\phi$ is $\pi/2$. If this is true also for the SLS system (which is linear) then its behavior is similar to that of the Kelvin system: the phase shift is $\pi/2$ at 50.62 Hz and the peak in the response factor occur at a slightly lower frequency, $f = 50.32$ Hz.

Since the material models were fitted only with regard to the phase angle $\delta$ of the materials, the dynamic modulus $E_{dyn}$ could differ significantly as the frequency gets higher. This quantity is now included in the table below. As a reminder: $E_{dyn}$ is the magnitude of the complex modulus $|E^*(\omega)|$.

**Table 6.3:** *Damping parameters and dynamic modulus of the SLS and the Kelvin system respectively. Attached mass* $m = 0.04$ *kg*

| | $\delta$ [rad] | $\zeta$ | $E_{dyn}$ [MPa] | $f(\phi = \pi/2)$ | $f(\max(R_d))$ |
|---|---|---|---|---|---|
| SLS: | 0.14858 | 7.68 % | 4.088 | 50.62 Hz | 50.32 Hz |
| Kelvin: | 0.14305 | 7.20 % | 3.989 | 50.00 Hz | 49.74 Hz |

Table 6.3 shows that the quotient $\delta/\zeta$ is close to 2 also for these two systems. The forth column

shows at which frequency $f$ the phase shift is $\pi/2$ and the fifth column shows at which frequency the response factor has its maximum value.

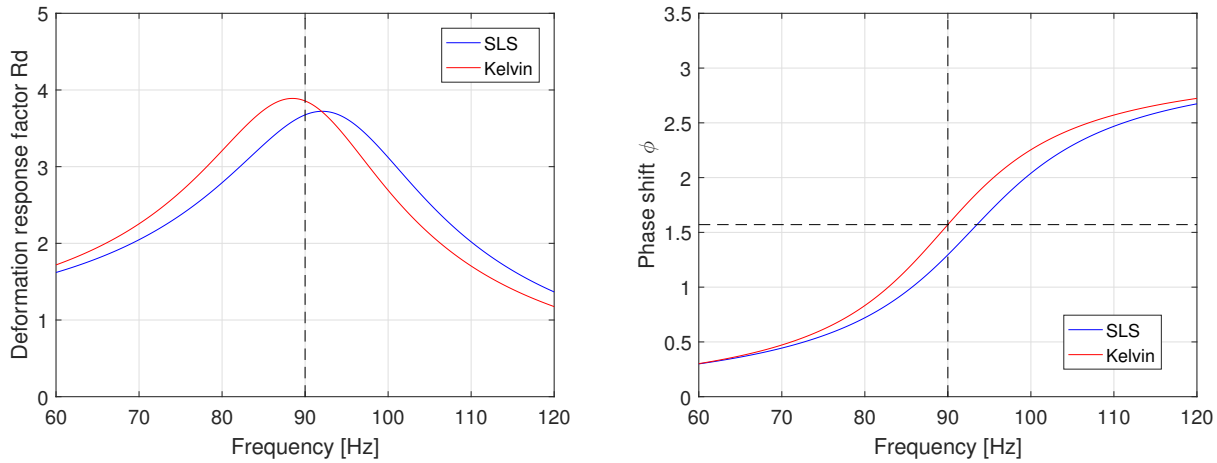


**Figure 6.7:** *Steady-state response of the SLS and the Kelvin system respectively. Attached mass* $m = 0.0123$ *kg*

With an attached mass of $m = 0.0123$ kg the two studied systems have their respective natural frequencies at around 90 Hz, see Figure 6.7. The general behavior of the two systems is similar to the behavior of the systems showed in the previous Figure 6.6, but here the behavior is more accentuated. The respective peaks in the response factor is closer to each other in terms of the magnitude, slightly below $R_d = 4$, but further apart in terms of frequency. These two systems are the most highly damped systems showed so far. Looking at Table 6.4 we see that the phase angle $\delta$ is around 0.25 [rad] which translates into a damping ratio of about $\zeta = 13\%$. This is a significant amount of damping.

**Table 6.4:** *Damping parameters and dynamic modulus of the SLS and the Kelvin system respectively. Attached mass* $m = 0.0123$ *kg*

| | $\delta$ [rad] | $\zeta$ | $E_{dyn}$ [MPa] | $f(\phi = \pi/2)$ | $f(\max(R_d))$ |
|---|---|---|---|---|---|
| SLS: | 0.23910 | 13.137 % | 4.364245 | 93.51 Hz | 92.20 Hz |
| Kelvin: | 0.25368 | 12.963 % | 4.078366 | 90.00 Hz | 88.47 Hz |

In Table 6.4 it is noticeable that the SLS system has its peak in response factor $R_d$ at a frequency slightly lower than the frequency at which the phase shift $\phi$ is $\pi/2$. This is consistent with the results presented in Table 6.3 earlier.

### 6.2.1 Summary of the Fitted material approach

Below follows a summary of the findings presented in this section.

- At low damping, Figure 6.5, the systems deviate mainly in terms of the magnitude of the peaks. A damping ratio of $\zeta = 2\%$ rather than 1% makes a huge difference in terms of the magnitude of the response factor $R_d$.
- At low damping the systems seem to have the same stiffness since the peaks in response factor occur at the same frequency.
- At high damping the situation is reversed. The systems are close in magnitude of the response factor, but the peaks are further apart in terms of frequency
- At high frequencies the SLS system gets stiffer and its natural frequency start to deviate from $f_n = (\sqrt{k_\infty/m})/2\pi$. The Kelvin system also gets stiffer in terms of dynamic stiffness but this does not effect the resonance frequency.
- When fitting the Kelvin material model to the SLS model the focus should lie on the phase angle $\delta$. The reason for this is that the dynamic modulus $E_{dyn}$ of the Kelvin model does not influence the natural frequency of the Kelvin system anyway. The Kelvin model lacks what is called a *modulus effect*, due to the fact that the model only contains one spring element.

All in all, this seems like a fairly successful method to capture the behavior of a material described by the SLS model. The desire to use the Kelvin model in computations stems from the simplistic mathematical treatment.

It was no problem to extend this approach to different reference materials described by a SLS model. Starting with a material with the same normalized relaxation parameter $g$ but lowering the relaxation time $t_r$ resulted in a SLS model to which a Kelvin model could be fitted easily in terms of the phase angle $\delta$

With the following material parameters

| $g$ | $E_\infty$ [MPa] | $E$ [MPa] | $t_r$ [s] |
|---|---|---|---|
| 0.5 | 3.948 | 3.948 | 0.00025 |

a least squares fit of the phase angle could be carried out. The following table shows the fitted $\eta$-parameter

| $\eta$-parameter | $\|\|\delta_{SLS} - \delta_{Kelvin}\|\|$ |
|---|---|
| 950 | 0.046963256076712 |
| 960 | 0.029224836191831 |
| 970 | 0.031711273210136 |

Figure 6.8 shows the fitted curves in terms of the dynamic modulus $E_{dyn}$ (to the left) and phase angle $\delta$ (to the right). Focusing on the phase angle the fit is really good, which was already indicated by the small residual, $|\delta_{SLS} - \delta_{Kelvin}|$.

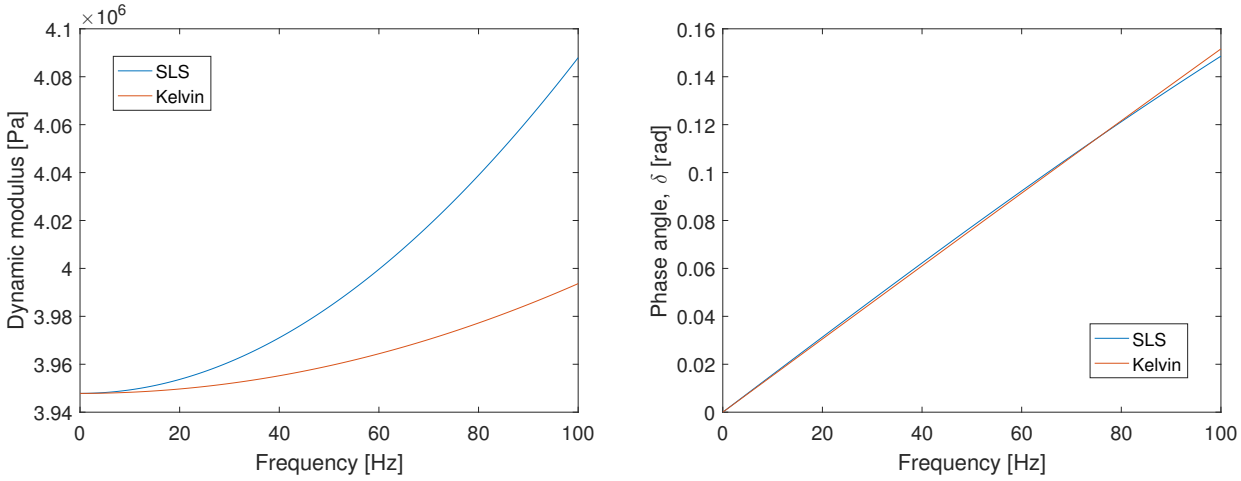


**Figure 6.8:** *The dynamic modulus and the phase angle of the two models respectively. SLS-parameters:* $g = 0.5$, $t_r = 0.00025$ *s. Kelvin-parameters:* $E_\infty = 3.948$ *MPa,* $\eta = 960$ *Pa·s*

Now the steady-state dynamic analysis with the three different masses can be repeated with this new material and the new fitted Kelvin model. The results will not be presented explicitly but a summary of the findings follows here:

The fitted Kelvin model proved to be a good approximation to the SLS reference system. The systems were studied at $f_{n,1} = 10$ Hz ($m = 1$ kg), $f_{n,2} = 50$ ($m = 0.04$ kg) and $f_{n,3} = 90$ Hz ($m = 0.0123$ kg). As before $f_n$ is defined as $(\sqrt{k_\infty/m})/2\pi$.

The two systems had peaks in the response factor that were similar in magnitude. And the peaks occurred at roughly the same frequency. It is safe to conclude that a good fit in terms of the phase angle of the materials will generate quite accurate approximations in terms of the dynamic behavior.

Now what if the relaxation time $t_r$ was increased rather than decreased? Will it be harder to find a damping parameter $\eta$ to use in the Kelvin model.

Imagine a new material with the same parameters as the previous except for the relaxation time $t_r$ which is now increased to $t_r = 0.00075$ [s].

| $g$ | $E_\infty$ [MPa] | $E$ [MPa] | $t_r$ [s] |
|---|---|---|---|
| 0.5 | 3.948 | 3.948 | 0.00075 |

A least squares fit of the phase angle gives the $\eta$-parameter

| $\eta$-parameter | $\|\|\delta_{SLS} - \delta_{Kelvin}\|\|$ |
|---|---|
| 2450 | 0.515797681130279 |
| 2460 | 0.515078177791386 |
| 2470 | 0.515647547929513 |

Already now we see that the residual is bigger in this case. Figure ( 6.9 shows the fitted curves in terms of the dynamic modulus $E_{dyn}$ (to the left) and phase angle $\delta$ (to the right).

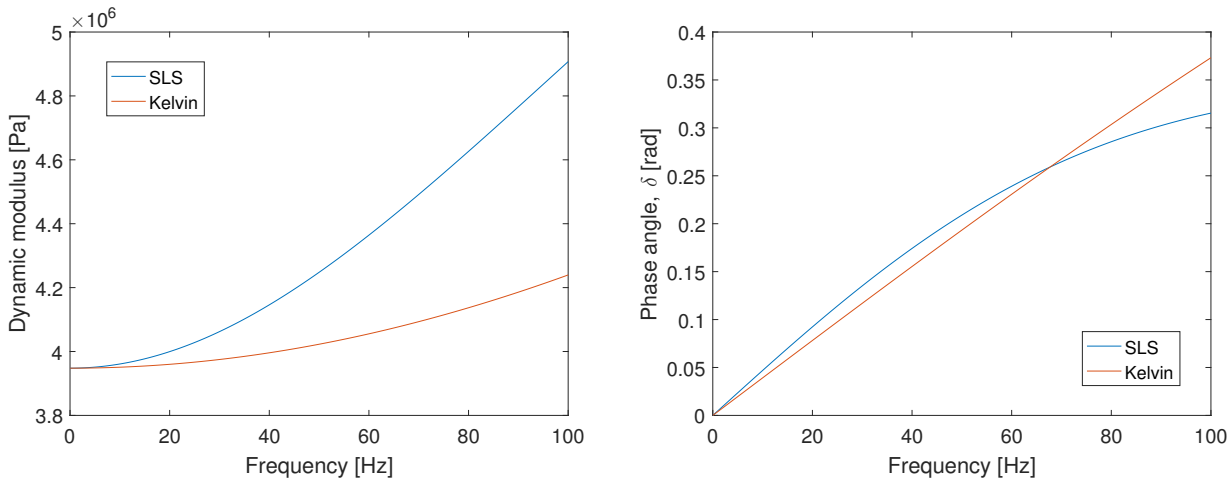


**Figure 6.9:** *The dynamic modulus and the phase angle of the two models respectively. SLS-parameters:* $g = 0.5$, $t_r = 0.00075$ *s. Kelvin-parameters:* $E_\infty = 3.948$ *MPa,* $\eta = 2460$ *Pa·s*

The conclusion is that as the relaxation time increases the harder it will be to fit a Kelvin model to the SLS reference model and consequently the approximation to the dynamic SLS system will be poor.

The aim in this section was to fit the material behavior of the Kelvin model to the SLS reference model over the frequency interval $[10, 90]$ Hz and the corresponding interval of the normalized frequency $\omega t_r$. Then compare the *steady state* response of the fitted Kelvin system to the reference SLS system.

As the relaxation time decreases the normalized frequency interval gets shorter making it easier to fit the Kelvin model over this frequency interval.

An example:

- At $f = 100$ Hz the normalized frequency $\omega t_r$ of the current material is equal to $2\pi f t_r = 0.47$ for $t_r = 0.00075$ s (Figure 6.9).
- At $f = 100$ Hz the previous material, with $t_r = 0.00025$ s, only has a normalized relaxation-value of $\omega t_r = 0.16$ s (Figure 6.8)
- On the normalized frequency interval $[0, 0.16]$ the function describing the phase angle $\delta$ of the SLS model will basically be a straight line. And it is easy to fit curves to straight lines.

So for certain materials this is a good approach.

## 6.3 Steady-state response: "New Kelvin" approach

By the dynamic analyses it was indicated that, at resonance, the relation between the phase angle of the materials $\delta$ and the damping ratio of the systems $\zeta$ was

$$\delta = 2\zeta \tag{6.7}$$

see Table 6.2, 6.3 and 6.4 respectively.

The phase angle of the SLS reference material $\delta$ is known for all frequencies. If the relation $\delta = 2\zeta$ holds for all SLS materials it would be possible to fit a dynamic Kelvin system with the damping ratio $\zeta = \delta/2$ to a dynamic SLS reference system.

Another observation was that the dynamic SLS system was slightly stiffer than the Kelvin system at high frequencies, i.e the resonance occurred at a slightly higher frequency than $f_n$. To obtain this behavior for the Kelvin system, the single spring that governs the stiffness will have to be made stiffer in some controlled way.

One quantity that is known prior to the dynamic analysis, i.e at the material stage, is the dynamic modulus of the material $E_{dyn}$. Translating this into a normal stiffness of a bar yields

$$k_{dyn} = \frac{E_{dyn}A}{L} \tag{6.8}$$

Through numerical testing it was concluded that for the SLS system the frequency

$$f_{n,dyn} = \frac{1}{2\pi}\sqrt{\frac{k_{dyn}}{m}} \tag{6.9}$$

represented an upper limit for the resonance peak. In other words: the resonance will occur in the frequency interval

$$[f_{n,\infty},\ f_{n,dyn}] \tag{6.10}$$

which means that the stiffness of the Kelvin system should be somewhere in the interval

$$[k_\infty, k_{dyn}] \tag{6.11}$$

With this information at hand it is perhaps possible to create a Kelvin system which approximates a dynamic reference SLS system by just knowing the phase angle $\delta$ and the dynamic modulus $E_{dyn}$ of the SLS model.

In the next section an extensive examination of the natural frequency of the SLS system will be presented. How is the relaxation time $t_r$ and $g$-factor effecting the natural frequency?

Now, the following is an example of how a dynamic SLS system with a natural frequency around $f_n$ could be approximated by a Kelvin system, using the method that was just presented.

- Start by determining the dynamic stiffness at $f = f_n$ where $f_n$ is $\frac{1}{2\pi}(\sqrt{k_\infty/m})$

$$k_{dyn} = \frac{A}{L} E_{dyn}(2\pi f_n) = \frac{A}{L} \left| E_\infty + E \frac{i2\pi f_n t_r}{1 + i2\pi f_n t_r} \right|$$

  Since it is unknown at this point what the real natural frequency of the system is, the above estimation of the stiffness just serves as a starting point for this method.

- Determine an angular frequency using the dynamic stiffness $k_{dyn}$

$$\omega_{n,dyn} = \sqrt{\frac{k_{dyn}}{m}}$$

- Use this angular frequency to determine the phase angle $\delta$

$$\delta(\omega_{n,dyn}) = \arg\left( E_\infty + E \frac{i\omega_{n,dyn} t_r}{1 + i\omega_{n,dyn} t_r} \right)$$

- The damping ratio becomes

$$\zeta = \frac{1}{2}\delta(\omega_{n,dyn}) \qquad \rightarrow \qquad c = 2m\zeta\omega_{n,dyn}$$

- Pick a suitable stiffness in the stiffness interval, $[k_\infty, k_{dyn}]$ to apply to the Kelvin system. This will simulate a modulus effect which is not present in the Kelvin model. It turned out that the results became better if the picked stiffness was closer to $k_{dyn}$ than to $k_\infty$, however this is not something that can be known at this point. An example of a weighted stiffness could be

$$k_{Kel} = \frac{1}{5}\left(4 \cdot k_{dyn} + k_\infty\right)$$

  A clue to how to make a better estimation of the stiffness is presented in the next section.

- Insert this stiffness $k_{Kel}$ into the expressions for the displacement response factor $R_d$ and the phase shift $\phi$. Use $c = 2m\left(\frac{1}{2}\delta\right)\omega_{n,dyn}$ as the damping parameter

$$R_d = \frac{u_0}{u_{qs}} = \frac{1}{|-\omega^2 m + k_{Kel} + i\omega c|} \qquad \text{and} \qquad \phi = -\arg\left(-\omega^2 m + k_{Kel} + i\omega c\right)$$

The following plots shows the steady-state response to sinusoidal excitation for the SLS reference system together with the two approximations termed "Old Kelvin" and "New Kelvin". "Old Kelvin" refers to the approximation obtained by the "fitted curve" - the approach that was presented in the previous section. Again this curve is plotted in red, see Figure 6.5, 6.6 and 6.7. "New Kelvin" refers to the approximation method that was just presented, where use was made of the relation between the phase angle $\delta$ and the damping ratio $\zeta$. This curve is plotted as a black dashed line. The used material parameters for the SLS model are:

| $g$ | $E_\infty$ [MPa] | $E$ [MPa] | $t_r$ [s] |
|---|---|---|---|
| 0.5 | 3.948 | 3.948 | 0.0005 |

Like before $c = 1.81$ kg/s was used in the "Old Kelvin" system.

At first a mass $m = 1$ kg was attached to the structures generating the following result.

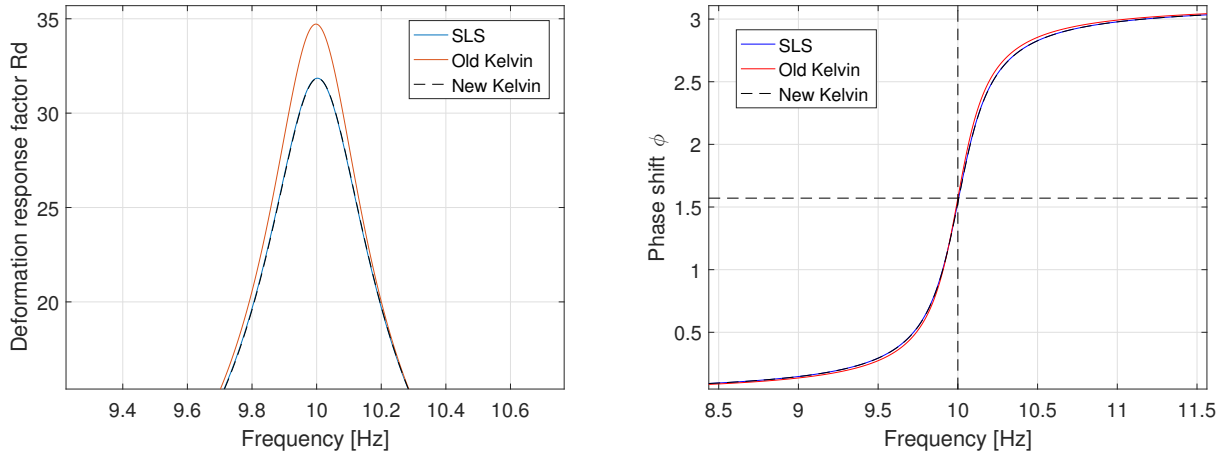


**Figure 6.10:** *Steady-state response of the reference SLS system and the two approximations ("Old Kelvin" and "New Kelvin"). Attached mass $m = 1$ kg*

Studying Figure 6.10 closely it can be noted that the "New Kelvin" approximation has basically the same damping as the reference system, i.e the magnitude of the response factor is almost identical at resonance. The respective damping ratio $\zeta$ of the two approximations is presented in the following table as a comparison. The phase angle $\delta$ for the three materials is also presented. The phase angle is evaluated at $f_n = 10$ Hz.

**Table 6.5:** *Damping parameters of the three systems respectively. Attached mass $m = 1$ kg*

| | $\delta$ [rad] | $\zeta$ |
|---|---|---|
| SLS | 0.031343 | - |
| "Old Kelvin": | 0.028799 | 1.568 % |
| "New Kelvin": | 0.031342 | 1.440 % |

In the next figure, Figure 6.11, a mass $m = 0.04$ kg has been attached to the structures generating the following result.

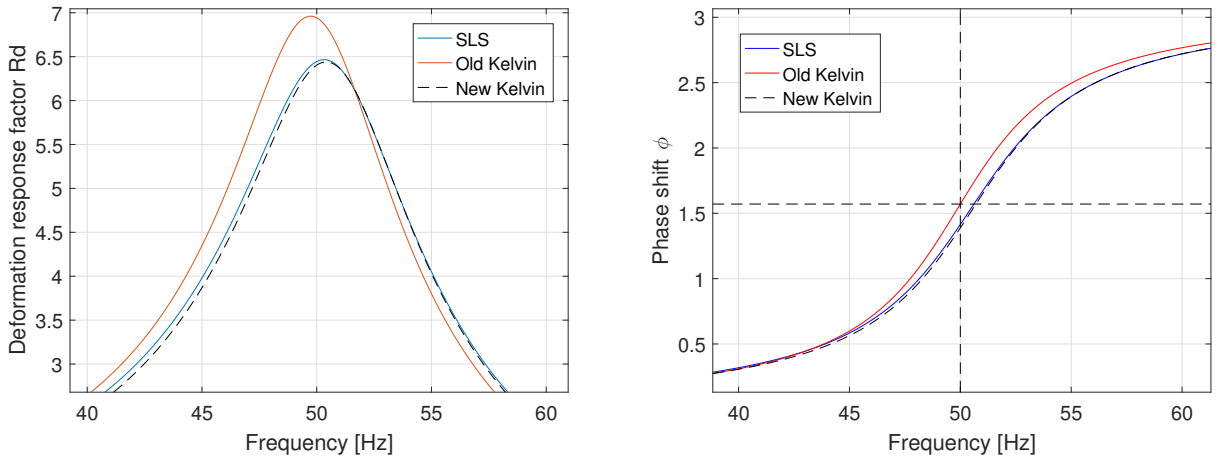


**Figure 6.11:** *Steady-state response of the reference SLS system and the two approximations ("Old Kelvin" and "New Kelvin"). Attached mass $m = 0.04$ kg*

Again the "New Kelvin"-approach matches the response of the SLS reference system in terms of magnitude of the response factor, but now also in terms of the damped natural frequency. The damping ratio of the approximations $\zeta$ and phase angle $\delta$ for the three materials is presented in the following table (Table 6.6). The phase angle is evaluated at $f_n = 50$ Hz. Note the close approximation of the phase angle $\delta$ generated by the "New Kelvin"-approach.

**Table 6.6:** *Damping parameters of the three systems respectively. Attached mass $m = 0.04$ kg*

| | $\delta$ [rad] | $\zeta$ |
|---|---|---|
| SLS | 0.148589 | - |
| "Old Kelvin": | 0.143051 | 7.202 % |
| "New Kelvin": | 0.148235 | 7.546 % |

Lastly a mass $m = 0.0123$ kg was attached to the structures generating the following result.

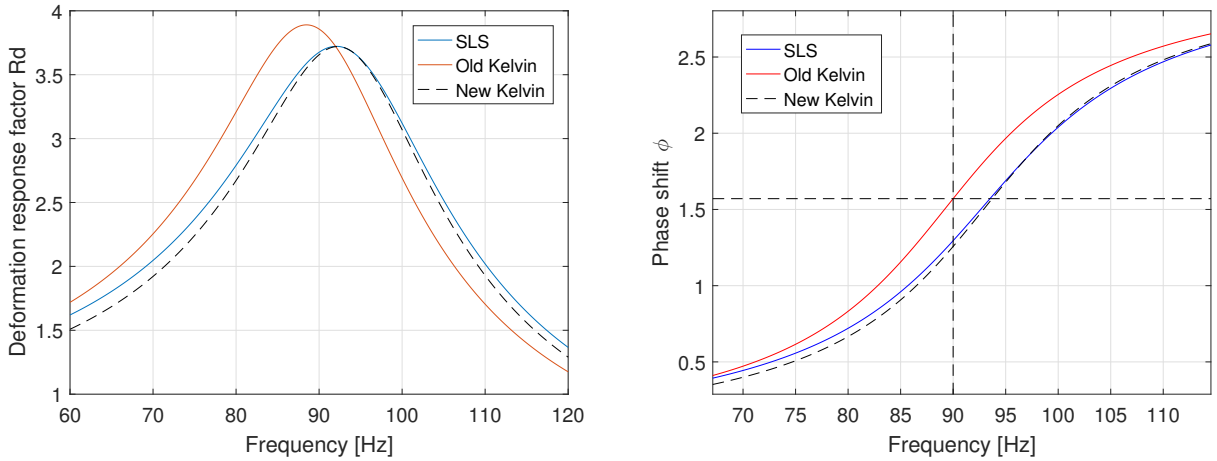


**Figure 6.12:** *Steady-state response of the reference SLS system and the two approximations ("Old Kelvin" and "New Kelvin"). Attached mass* $m = 0.0123$ *kg*

Studying Figure 6.12 it can be concluded that the "New Kelvin"-approach is a fairly successful way to approximate the response of a SLS system. Now looking at Table 6.7 it can be noted that the damping of the "Old Kelvin"-system is actually higher than the damping of the SLS reference system which would indicate that the SLS system should have a bigger response factor than the "Old Kelvin" system. Theory says that in a Kelvin system the response at resonance is controlled solely by the damping of the system. Can this be the case also for the SLS system? Looking at Figure 6.2 the Kelvin model has a bigger phase angle in a wide range around 90 Hz, so it is not a question of at which particular frequency the phase angle $\delta$ was evaluated. There must be something else effecting the SLS system.

Now this is perhaps where the modulus effect comes in. Both the Kelvin model and the SLS model have an increasing dynamic modulus $E_{dyn}$ in terms of the material, but this fact only effects the SLS model when the respective dynamic systems is studied. For higher frequencies the dynamic SLS system gets stiffer resulting in a resonance frequency slightly higher than $f_n = (\sqrt{\frac{k_\infty}{m}})/2\pi$, whereas for an unmodified but damped Kelvin system the resonance frequency always occur slightly below $f_n = (\sqrt{\frac{k_\infty}{m}})/2\pi$. In other words: the increase in dynamic stiffness of the Kelvin material model does not effect the dynamic system where a mass has been attached.

If the response at resonance for a SLS system is not just controlled by the damping of the system but also by the extra stiffness, connected to the modulus effect, this could explain why the response of the SLS system is smaller.

**Table 6.7:** *Damping parameters of the three systems respectively. Attached mass* $m = 0.0123$ *kg*

| | $\delta$ [rad] | $\zeta$ |
|---|---|---|
| SLS | 0.239105 | - |
| "Old Kelvin": | 0.253678 | 12.96 % |
| "New Kelvin": | 0.235477 | 12.37 % |

### 6.3.1 Summary of the "New Kelvin"-approach

By using the approach presented in this section it will perhaps be possible to model a material, using the more physically correct SLS material model, and from the fitted SLS model estimate the damping ratio $\zeta$. This damping ratio can then be applied to a dynamic Kelvin system in order to model the dynamic response of the examined material.

Now you have made an estimation of the damping ratio of a material purely based on measurements of the dynamic modulus $E_{dyn}$ and phase angle $\delta$ of the material in question.

This is obviously a short-cut compared to the widely used concept of *equivalent viscous damping* where dynamic testing of a structure is needed to estimate a damping ratio $\zeta$.

Now it is possible to carry out the dynamic steady state calculations without having to involve a more complex material model than the Kelvin model.

## 6.4 Free vibration response of dynamic SLS systems

In this section it is examined how the relaxation time $t_r$ and the stiffness relation between the Maxwell element and the spring element is affecting the natural frequency of the SLS system.

The stiffness relation between the Maxwell element and the spring element is expressed through the parameter $g$, where

$$g = \frac{E}{E_\infty + E}$$

Earlier it could be noted that the resonance frequency of the SLS system occurred at a slightly higher frequency than $f_n$, where $f_n$ was defined as $(\sqrt{\frac{k_\infty}{m}})/2\pi$. This behavior was traced back to the "modulus effect" which was something that the more crude Kelvin model was lacking due to the fact that the model only contains one spring element.

By keeping the $g$-parameter constant and altering the relaxation time $t_r$ the effect of this quantity on the natural frequency of the system can be studied. The situation is then reversed by keeping the relaxation time $t_r$ constant and altering the $g$-parameter. The natural frequency is calculated by doing a free vibration simulation of the dynamic system and taking the mean value of the period time $T_n$ of three consecutive periods. The simulation is carried out using the *central difference method* with a time-step length $\Delta t$ of $5 \cdot 10^{-6}$ s.

First the effect of the $g$-parameter was studied. Three different parameters was used creating three different models. The following table contains the details.

| Model | $g$ | $E_\infty$ [MPa] | $t_r$ [s] |
|---|---|---|---|
| 1 | 0.5 | 3.948 | 0.0005 |
| 2 | 0.3 | 3.948 | 0.0005 |
| 3 | 0.1 | 3.948 | 0.0005 |

Figure 6.13 shows the dynamic modulus $E_{dyn}$ and phase angle $\delta$ as a function of frequency for the three respective models. At low frequencies the stiffness is basically the same. At 90 Hz Model 1 ($g = 0.5$) is by far the stiffest. The suspicion is then that the dynamic system based on Model 1 one will have the highest *damped* natural frequency, because of the mentioned modulus effect.

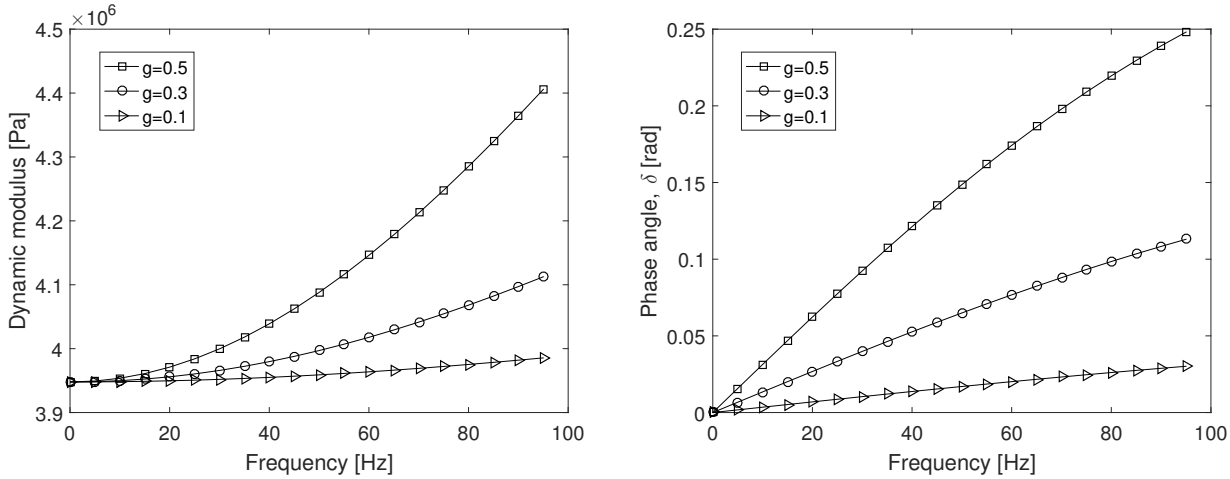


**Figure 6.13:** $g = 0.5$ $g = 0.3$ $g = 0.1$

Making the transition from the material formulation into the structural formulation and attaching different masses makes it possible to obtain the natural frequency of the current system.

Nine different masses are attached so that $f_n$ goes from 10 Hz to 90 Hz with intervals of 10 Hz. This is shown in the left column of Table 6.8. The other columns shows the natural frequency of each system for the nine different masses. At low frequencies the deviation from $f_n$ is negligible, this is also something that was reflected when looking at the dynamic modulus $E_{dyn}$, see Figure 6.13. At higher frequencies, most notable around 90 Hz, the difference in dynamic modulus is significant, resulting in a slight increase of the natural frequency. Remember that the natural frequency of any system is proportional to the square-root of the stiffness. That's why the difference in natural frequency will not become that dramatic even though the difference in dynamic modulus is big.

**Table 6.8:** *Natural damped frequency of three different SLS systems. The systems have different normalized relaxation factors, g*

| $f_n$ [Hz] | $f(g = 0.5)[Hz]$ | $f(g = 0.2)[Hz]$ | $f(g = 0.1)[Hz]$ |
|---|---|---|---|
| 10 | 10.0040 | 10.0033 | 10.0000 |
| 20 | 20.0267 | 20.0133 | 20.0000 |
| 30 | 30.1114 | 30.0601 | 30.0300 |
| 40 | 40.2414 | 40.1070 | 40.0534 |
| 50 | 50.4796 | 50.2513 | 50.0835 |
| 60 | 60.8273 | 60.4839 | 60.1202 |
| 70 | 71.3436 | 70.5882 | 70.2576 |
| 80 | 82.0277 | 80.8625 | 80.3213 |
| 90 | 92.9440 | 91.3659 | 90.3614 |

In the following each model has the same relaxation parameter $g$ but the relaxation time $t_r$ is different. The following table shows the details of the models.

| Model | $g$ | $E_\infty$ [MPa] | $t_r$ [s] |
|---|---|---|---|
| 1 | 0.5 | 3.948 | 0.00075 |
| 2 | 0.5 | 3.948 | 0.00050 |
| 3 | 0.5 | 3.948 | 0.00025 |

Studying Figure 6.14 it can be noted that the longest relaxation time, $t_r = 0.00075$ s, results in the highest dynamic modulus.

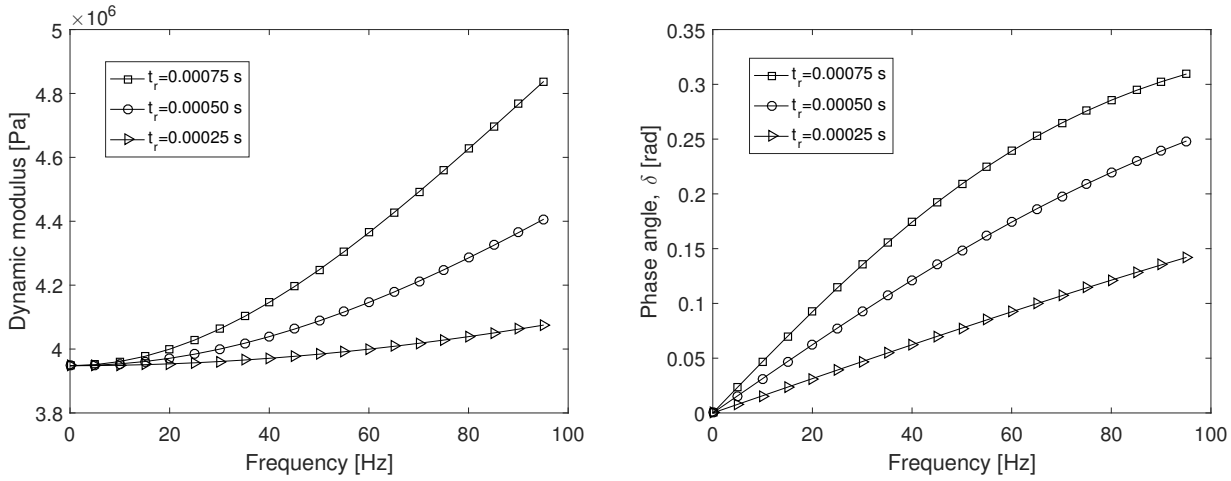


**Figure 6.14:** $tr = 0.00075\ s\ tr = 0.0005\ s\ tr = 0.00025\ s$

As for the natural frequency, the conclusion made previously holds for this situation as well: a big dynamic modulus will result in a relatively high natural frequency. Table 6.9 shows this. At high frequencies the system with $t_r = 0.00075$ s has a substantially higher natural frequency.

**Table 6.9:** *Natural damped frequency of three different SLS systems. The systems have different relaxation times, $t_r$*

| $f_n$ [Hz] | $f(t_r = 0.00075)$ [Hz] | $f(t_r = 0.00050)$ [Hz] | $f(t_r = 0.00025)$ [Hz] |
|---|---|---|---|
| 10 | 10.0067 | 10.0040 | 10.0000 |
| 20 | 20.0736 | 20.0267 | 20.0133 |
| 30 | 30.2115 | 30.1114 | 30.0300 |
| 40 | 40.5570 | 40.2414 | 40.0748 |
| 50 | 51.1073 | 50.4796 | 50.1295 |
| 60 | 61.9707 | 60.8273 | 60.2047 |
| 70 | 73.2064 | 71.3436 | 70.3120 |
| 80 | 84.9269 | 82.0277 | 80.4807 |
| 90 | 97.1943 | 92.9440 | 90.6947 |

With the information provided in Table 6.13 and 6.14 it might be possible to obtain an analytical expression to determine the natural frequency of an SLS system. And perhaps it will be possible to do a better estimate of the stiffness $k_{Kel}$ used in the "New Kelvin"-approach, which was presented in section 6.3.

### 6.4.1 Free vibration response: Summary

By plotting the quotient $f_{n,SLS}/f_n$ at each natural frequency $f_n$ (10,20, ... , 90 Hz) it is revealed that the curve describing the increase in natural frequency has the same shape as the curve describing the increase in dynamic modulus. This perhaps comes as no surprise. Figure 6.15 shows the increase in natural frequency in percent compared to $f_n$. For instance: for a system with $t_r = 0.00075$ s the natural frequency is 8 % higher than $f_n = 90$ Hz for the same attached mass. The increase gets bigger at high frequencies, generally it looks like it follows the behavior of the dynamic modulus $E_{dyn}$.

To summarize: If a parameter is changed, whether it is $t_r$ or $g$, and this leads to an increase in the dynamic modulus $E_{dyn}$ this will cause an increase in the natural frequency of the system $f_{n,SLS}$.

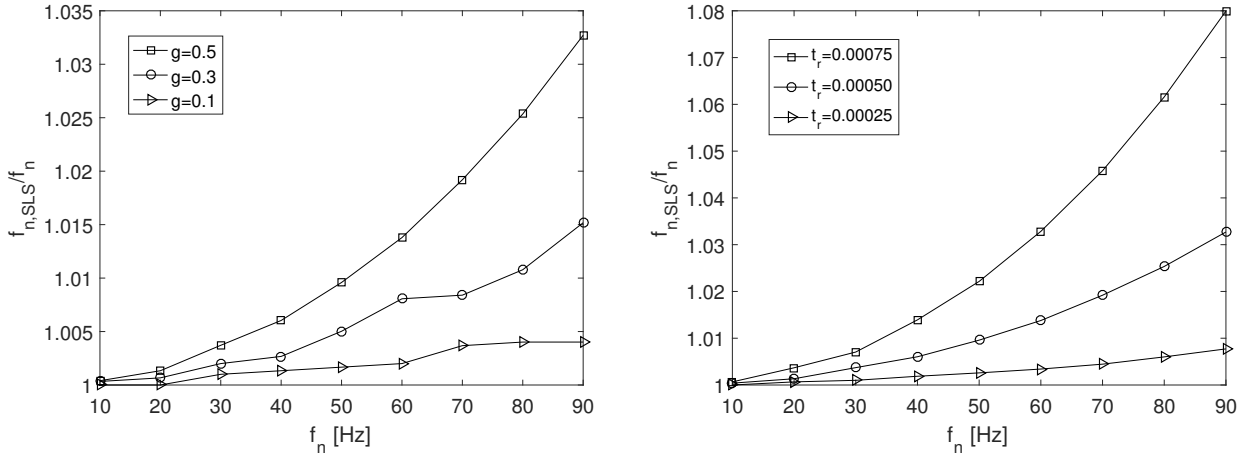


**(a)** *The effect of the relaxation parameter g* **(b)** *The effect of the relaxation time $t_r$*

**Figure 6.15:** *This figure shows how much the natural frequencies of the SLS systems deviates from $f_n$ in percent.*

## 6.5 Half sine pulse response: A comparison

In *Dynamics of structures* [1] the response to a half sine pulse is derived without taking damping of the structural model into account. This simplifies the mathematical treatment of the problem. Moreover it is said that damping has a small influence on the structural-response to an impulse-load. Here the response to a half-sine impulse is tested numerically through a time stepping procedure, *the central difference method*, which makes it possible to study the influence of damping on the response.

The half-sine pulse is characterized by its amplitude $p_0$ and the pulse duration $t_d$. The pulse $p(t)$ is defined as

$$p(t) = \begin{cases} p_0 \sin(\pi t/t_d) & t \leq t_d \\ 0 & t > t_d; \end{cases}$$

This pulse determines the magnitude of the displacement response-factor $R_d$ of the visco-elastic model.

The response-factor is often presented in terms of the quotient $t_d/T_n$ which relates the pulse-duration $t_d$ to the natural period-time of the structure $T_n$ (the natural period time is of course connected to the natural frequency of the system). Here a number of numerical simulations of pulses with different pulse-durations $t_d$ was carried out and the corresponding maximum of the response factor $R_d$ was stored. If each maximum of the response factor $R_d$ is plotted against the corresponding $t_d$-value a shock-spectrum is generated. It tells the reader what pulse-length generates the biggest response of a particular dynamic system, defined by its period time $T_n$.

In this thesis two pulse-durations $t_d$ were used to define the frequency range in which to conduct the studies of the material models and the related dynamic systems. These pulses were

$$t_d = 50\,\text{ms} \Rightarrow f = 10\,\text{Hz} \qquad t_d = 5\,\text{ms} \Rightarrow f = 100\,\text{Hz}$$

The lower pulse-duration time, 5 ms, will now serve as a lower limit of the pulse-duration during the study of the response of the systems to a pulse load.

Again the interest falls on comparing a dynamic SLS system to a Kelvin system. Two SLS materials will be tested: one with $g = 0.5$, $t_r = 0.0005$ s and one with $g = 0.2$, $t_r = 0.001$ s. To each SLS material a Kelvin material will be fitted in terms of the phase angle $\delta$ of the SLS material. This procedure has been described in Section 6.1. The aim is to assign a suitable $\eta$-paramater to the Kelvin model which will generate a Kelvin material model with approximately the same amount of damping in the material as the reference SLS model. The $\eta$-parameter is then converted into a $c$-parameter which governs the viscous damping of the dynamic Kelvin system.

The material parameters of the first SLS system to be tested is presented in the following table. The parameters of the Kelvin approximation is also presented, moreover a second Kelvin system, with no damping, is included in the analysis to show the impact of damping on the dynamic response.

| Material | $g$ | $k_\infty$ [N/m] | $t_r$ [s] | $c$ [kg/s] |
|---|---|---|---|---|
| SLS reference | 0.5 | 3948 | 0.0005 | - |
| Kelvin (damped) | - | 3948 | - | 1.81 |
| Kelvin (undamped) | - | 3948 | - | 0.0 |

In Figure 6.16(a) a mass of $m = 1$ kg was attached to the structures giving the systems a period time of approximately $T_n = 0.1$ s ($f_n \approx 10$ Hz). Half sine pulses of different durations generated the shock-spectrum shown in the figure. Figure 6.16(b) shows a zoom in at the first peak in the shock-spectrum.

A few things can be noted. The damping of the SLS system and the corresponding Kelvin system is low, therefore the difference in response compared to the purely elastic system is small. In Table 6.2 numeric values on the damping are presented for the two systems. Moreover the maximum response seems to occur at around $t_d/T_n = 0.8$ which with $T_n = 0.1$ s would mean a pulse duration of $t_d = 80$ ms. A pulse with such long duration generates a relatively slow impact which does not create a resisting force in the dashpots, and consequently there is almost no damping (note: in a dashpot the force $f_D$ is proprotional to the velocity $\dot{u}$). Moreover the stiffness of the systems is basically the same since the spring in the Maxwell element in the SLS system does not contribute since the dashpot is inactive.

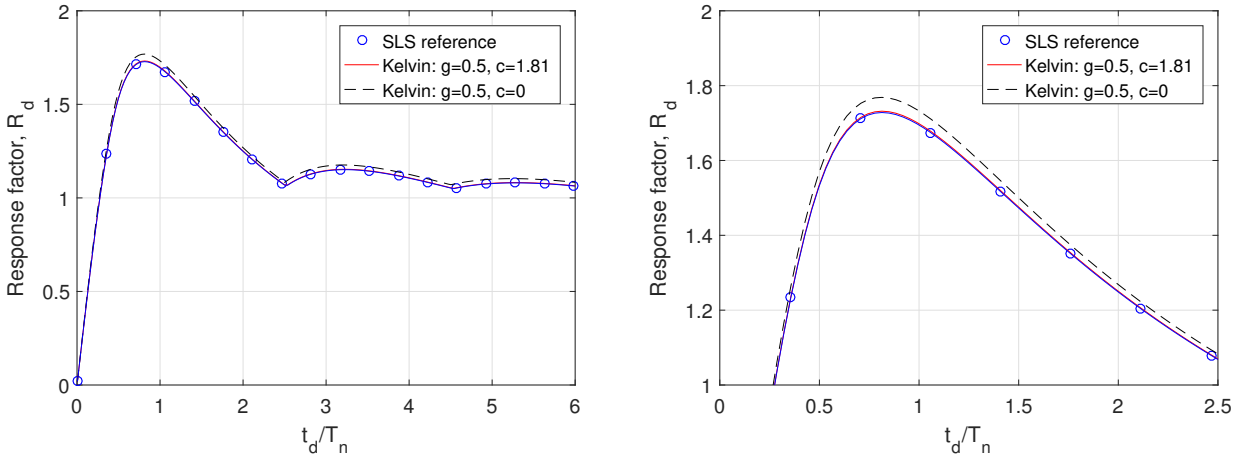


**(a)** **(b)** *Zoom in on the first peak*

**Figure 6.16:** *The Shock-spectrum of the three systems respectively. The SLS reference system ($g = 0.5$) is compared to both a damped ($c = 1.81kg/s$) and undamped ($c = 0kg/s$) Kelvin system. $T_n = 0.1$ s, attached mass $m = 1$ kg*

The next system is more interesting. Here a mass $m = 0.0123$ kg has been attached to the bar-structures resulting in a period time around $T_n = 0.0111$ s ($f_n \approx 90$ Hz). Figure 6.17(a) shows the shock spectrum, and (b) shows the zoom in on the peak. The response of the SLS system is slightly smaller compared to the damped Kelvin system. From the steady state analysis it was shown that the models had similar damping at 90 Hz, see Table 6.4, so perhaps this difference could be ascribed to the modulus effect that is present in the SLS system. So if the SLS system is stiffer this could explain the slightly smaller response. The relative increase in natural frequency of the SLS systems, caused by the increase in stiffness, was studied in Section 6.4. Figure 6.18(a) shows that the SLS system is stiffer, i.e higher natural frequency, and that the decay of the response is similar, i.e the damping ratios corresponds.

Returning to Figure 6.17 and studying the response of the undamped Kelvin system it can be noted that the damping of the two other systems plays a significant role when the pulse durations are short. The resposne of the damped systems is smaller throughout the whole spectrum but more so around $t_d/T_n = 0.5$ to $t_d/T_n = 1.5$. These quotients corresponds to pulse-durations of

$$t_d = 0.5T_n = 5.6\,\text{ms} \qquad t_d = 1.5T_n = 16.7\,\text{ms}$$

which is slightly above the lower limit of pulse durations of interest, which was 5 ms.

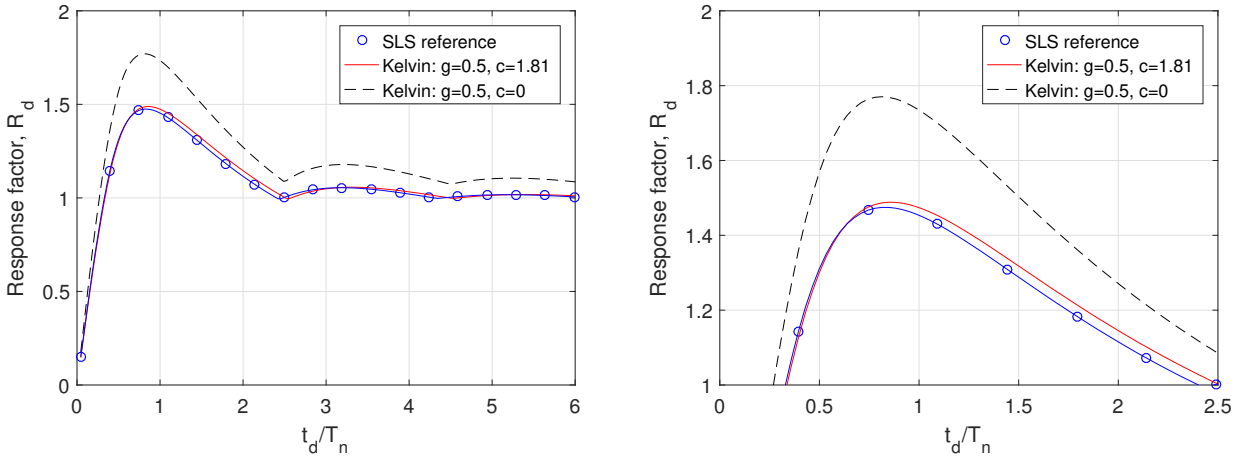


**(a)** **(b)** *Zoom in on the first peak*

**Figure 6.17:** *The Shock-spectrum of the three systems respectively. The SLS reference system ($g = 0.5$) is compared to both a damped ($c = 1.81$ kg/s) and undamped ($c = 0$ kg/s) Kelvin system. $T_n = 0.0111$ s, attached mass $m = 0.0123$ kg*

Figure 6.18(a) shows the response in time of the SLS and Kelvin system to a pulse with $t_d = 0.8T_n = 8.9$ ms. The pulse is plotted as a solid black line to the left in the figure. Figure 6.18(b) shows the response of the systems to a pulse with $t_d = 2.5T_n = 27.8$ ms. At $1.5 < t_d/T_n < 2.5$ two peaks develops in the response during the pulse. When $t_d/T_n < 2.5$ the first of the peaks is the biggest. At $t_d/T_n = 2.5$ the two peaks are roughly the same size which the figure shows. At $t_d/T_n > 2.5$ the second peak is the biggest, moreover a third smaller peak develops during the pulse.

If $t_d/T_n = 1.5, 2.5...$, and the system is undamped, the mass stays still after the for pulse ends. The mass has zero velocity and no displacement. For a system with damping this is clearly not the case, the velocity and displacement are small though, see Figure 6.18(b).

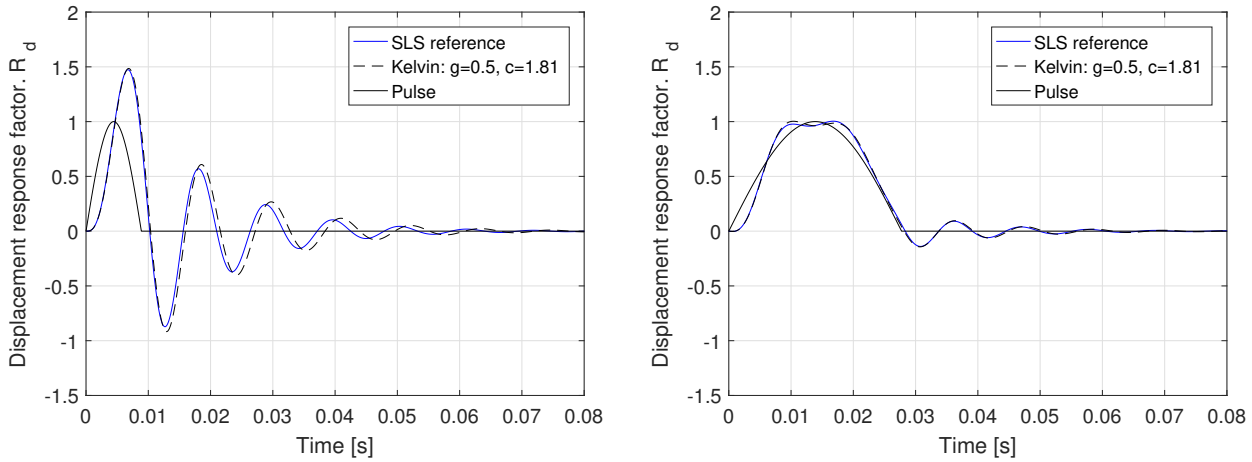


**(a)** *Pulseduration:* $t_d = 0.8T_n = 0.0089$ *s* **(b)** *Pulseduration:* $t_d = 2.5T_n = 0.0278$ *s*

**Figure 6.18:** *SLS parameters: $g = 0.5$, $t_r = 0.0005$ s. Kelvin parameters: $k_\infty = 3948$ N/m, $c = 1.81$ kg/s. Period time: $T_n = 0.0111$ s, attached mass $m = 0.0123$ kg*

Now a new SLS material is introduced. The material has the relaxation parameter $g = 0.2$ and relaxation time $t_r = 0.001$s. Following the procedure described in Section 6.1 a damping parameter $\eta$ can be assigned to a Kelvin model in order to make the model fit the curve of the phase angle of the SLS model.

A least squares fit of the curves describing the phase angle of the materials resulted in the following damping parameter $\eta$

| $\eta$-parameter | $\|\|\delta_{SLS} - \delta_{Kelvin}\|\|$ |
|---|---|
| 790 | 0.196356045429581 |
| 800 | 0.193626450554188 |
| 810 | 0.194779809724235 |

Figure 6.19 shows the phase angle plotted against the frequency (to the left) and normalized frequency $\omega t_r$ (to the right).

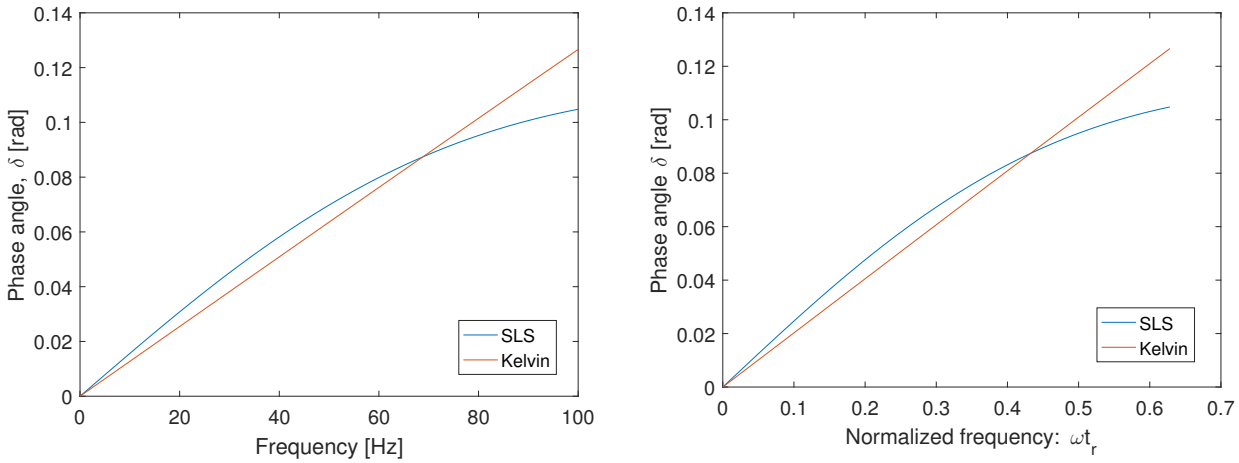


**Figure 6.19:** *To the left we have the phase angle $\delta$ plotted for the two models in the chosen frequency range. To the right the same curves are plotted as functions of normalized frequency. SLS-parameters: $g = 0.2$, $t_r = 0.001$. Kelvin-parameters: $E_\infty = 3.948$ MPa $\eta = 800$ Pa·s*

In terms of the structure, $\eta = 800$ Pa·s corresponds to $c = 0.8$ kg/s. The bar-length is again 10 cm and the area of the cross-section is 1 cm$^2$. The following table contains material parameters of the systems. An undamped Kelvin system is also included.

| Material | $g$ | $k_\infty$ [N/m] | $t_r$ [s] | $c$ [kg/s] |
|---|---|---|---|---|
| SLS reference | 0.2 | 3948 | 0.001 | - |
| Kelvin (damped) | - | 3948 | - | 0.8 |
| Kelvin (undamped) | - | 3948 | - | 0.0 |

Like before a mass of $m = 1$ kg was attached to the structures giving the systems a period time of approximately $T_n = 0.1$ s ($f_n \approx 10$ Hz). Figure 6.20(a) and (b) shows the shock spectrum

where (b) is a zoom in of the first peak which is of most interest. The results are similar to those shown in Figure 6.16. The damping is low in both systems since the pulse durations are long, giving a slow impact. A slow impact does not generate a resting force from the dashpots.

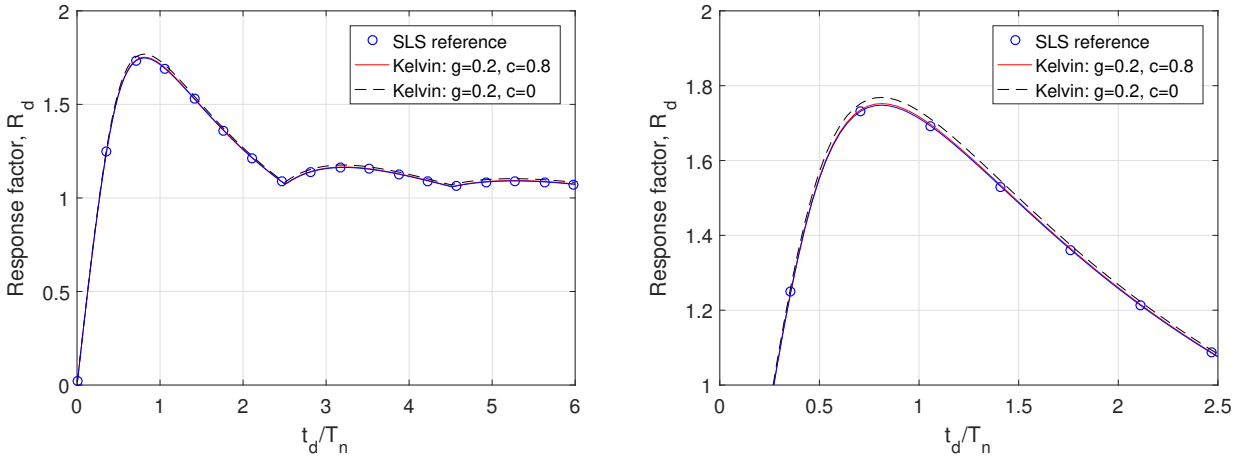


**(a)** **(b)** *Zoom in on the first peak*

**Figure 6.20:** *The Shock-spectrum of the three systems respectively. The SLS reference system ($g = 0.2$) is compared to both a damped ($c = 0.80kg/s$) and undamped ($c = 0kg/s$) Kelvin system. $T_n = 0.1$ $s$, attached mass $m = 1$ $kg$*

Again its more interesting to look at the systems where the attached mass is $m = 0.0123$ kg giving a natural frequency of the systems of about 90 Hz. Figure 6.21 shows the shock spectrum, where (b) in the figure is a zoom in on the peak. These two systems have lower damping, the Kelvin system has $c = 0.8$ kg/s compared to $c = 1.81$ kg/s in the previous case. However the response of the SLS system is slightly smaller again which points towards the modulus effect discussed earlier. The difference is very small though. Again the most relevant interval of the pulse durations is

$$t_d = 0.5T_n = 5.6\,\text{ms} \qquad t_d = 1.5T_n = 16.7\,\text{ms}$$

which is close to the lower limit of the pulse duration times, 5 ms.

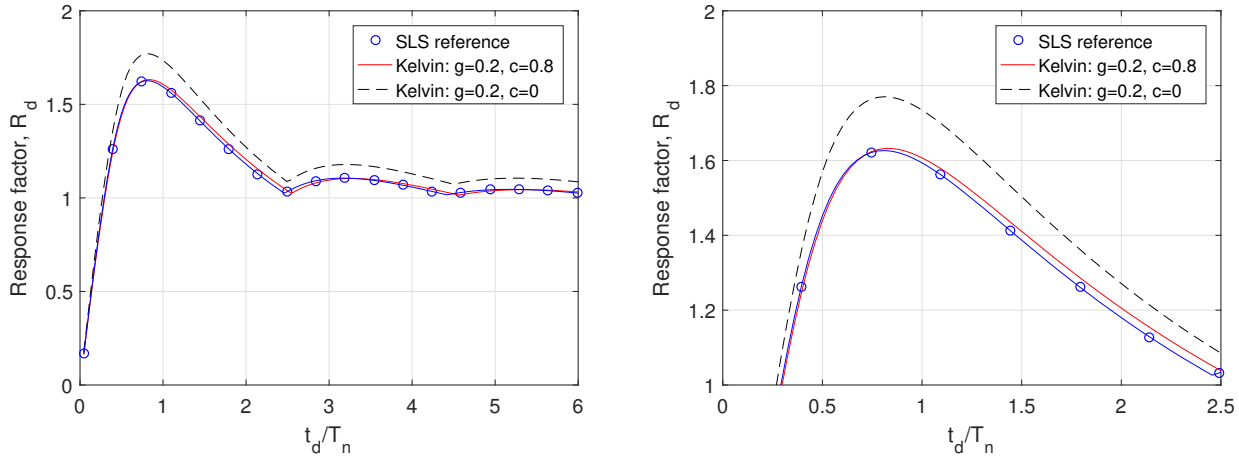


**(a)** **(b)** *Zoom in on the first peak*

**Figure 6.21:** *The Shock-spectrum of the three systems respectively. The SLS reference system ($g = 0.2$) is compared to both a damped ($c = 0.80kg/s$) and undamped ($c = 0kg/s$) Kelvin system. $T_n = 0.0111$ s, attached mass $m = 0.0123$ kg*

Figure 6.22 shows the response in time for the two systems. Here its obvious that these to systems have a more moderate damping than the systems showed in Figure 6.18, since the decay of the displacement is lower per cycle. Figure 6.22(a) roughly shows the maximum response of the system, which occur around $t_d = 0.8T_n = 9$ ms. Figure 6.22(b) shows the response to a pulse with $t_d = 2.5T_n = 28$ ms. Here two peaks have developed during the pulse.

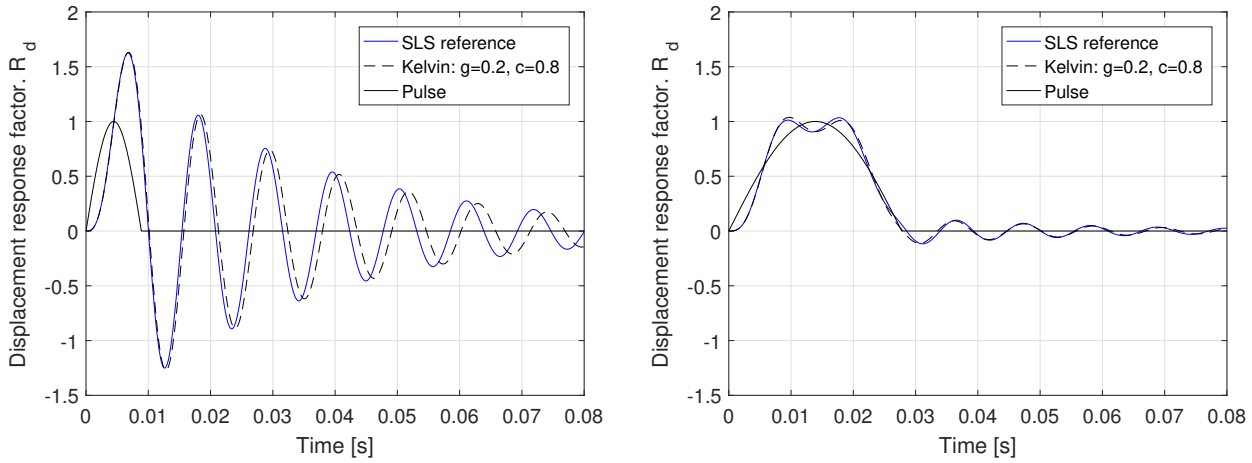


**(a)** $t_d = 0.8T_n = 0.0096$ s **(b)** $t_d = 2.5T_n = 0.0278$ s

**Figure 6.22:** *SLS parameters: $g = 0.2$, $t_r = 0.001$ s. Kelvin parameters: $k_\infty = 3948$ N/m, $c = 0.80$ kg/s. Period time: $T_n = 0.0111$ s, attached mass $m = 0.0123$ kg*

### 6.5.1 Response to pulse excitation: Summary

It seems to be no problem to use a fitted Kelvin system to approximate the response of a SLS system to a half sine pulse load. Pulse durations from 5 ms and upwards were studied.

The fit is based on measurements of the phase angle $\delta$ of the SLS material. Through a least-squares fit the Kelvin model approximately gets the same phase angle $\delta$ as the SLS material over the frequency range $[10, 90]$ Hz. This generates two material models with roughly the same damping, since the phase angle is closely connected to the damping of the material. The dynamic modulus $E_{dyn}$ is not taken into account.

Maybe a small modulus effect can be noticed for the SLS system with a natural period $T_n > 1/90 = 0.0111$ s, see Figure 6.17 and 6.21. From $t_d/T_n = 1$ the response of the SLS system is slightly smaller compared to the damped Kelvin system, perhaps this could be attributed to the extra stiffness connected to the modulus effect. In other words: the response seems to be controlled mainly by the spring stiffness $k_\infty$ which is the same for both systems and the damping, which is considerable for the systems with a short period time $T_n < 0.01$ ($f_n$: 90 Hz).

## 6.6 Concluding remarks

As we have seen in the previous sections it is possible to approximate the response of a SLS system to different dynamic events, e.g steady state vibrations and pulse excitation, with the use of a Kelvin system. The major concern prior to the analyses was that sudden changes in displacement, i.e high displacement rates $\dot{u}$, would yield an unphysical response of the Kelvin model. This was perhaps best visualized by applying a step-strain to the Kelvin material. As the strain rate $\dot{\varepsilon}$ was infinite during the step, the stress response became infinite. But what happens if this situation is simulated numerically. Of course the strain rate can not be infinite during a step-strain experiment, some time needs to pass as the step-strain is applied.

If 5-10 ms is the roughly estimated time needed to apply the sudden strain, then a strain-rate can be calculated and consequently also a "continuous" stress response even for the Kelvin model. This was tried for a Kelvin material and a reference SLS material with the following familiar material parameters.

| Material | $g$ | $E_\infty$ [MPa] | $t_r$ [s] | $\eta$ [Pa·s] |
|---|---|---|---|---|
| SLS reference | 0.5 | 3.948 | 0.0005 | - |
| Kelvin | - | 3.948 | - | 1810 |

It turned out that for the realistic strain application times (5-10 ms) the maximum stress-response of the Kelvin model did not deviate from the more physically correct response of the SLS model. Not even if the strain application time was lowered to 1 ms, a difference in maximum response occurred. Figure 6.23 shows the response of the two material models to a step-strain, where the strain was applied during a time interval of 1 ms. The time-step length in the calculations was $\Delta t = 0.1$ ms. (b) is a zoom in on the stress response peak.

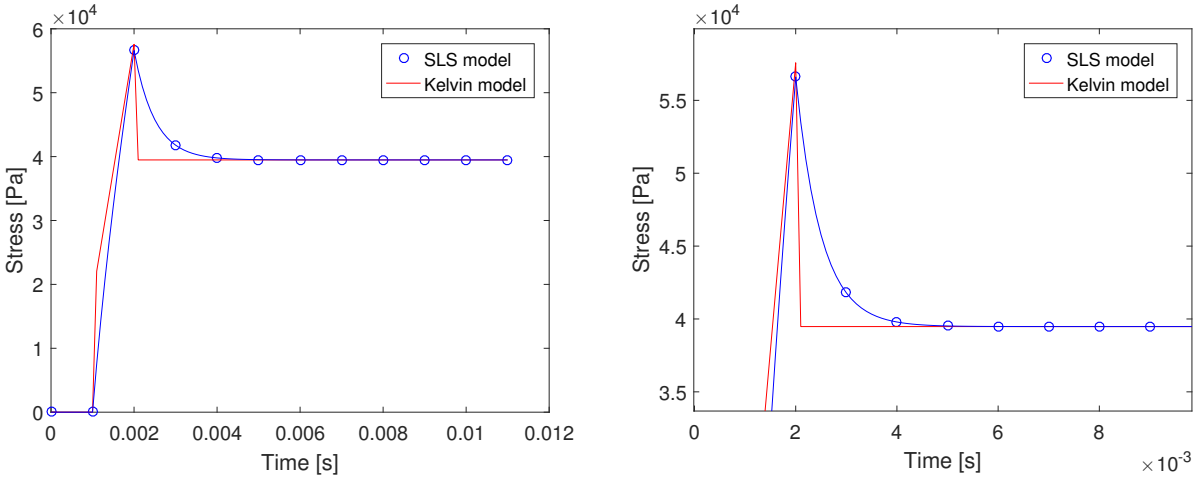


**Figure 6.23:** *The response to a step-strain. In (b) the peak of the response has been zoomed in.*

# Chapter 7

# Dynamics of SFS- and 5-parameter systems

This chapter contains an analysis of the *steady state* response of the dynamic SFS system. This material model is non-linear and as we will see this gives rise to a couple of phenomenas not visible in the study of the linear visco-elastic models. At the end a short section is devoted to the dynamic behavior of the *5-parameter model*, which combines the linear visco-elastic properties of the SLS model with the amplitude dependence of the SFS model.

## 7.1 Steady state analysis of the SFS-model

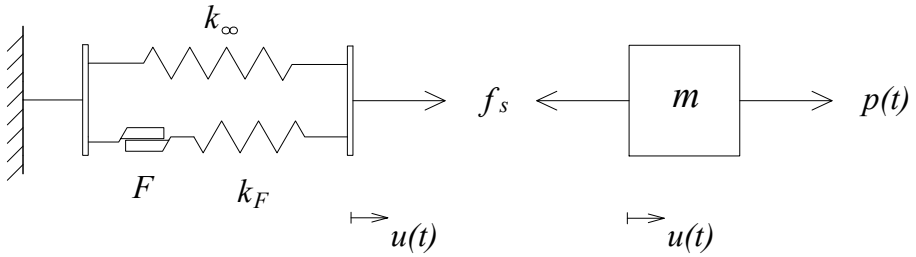


**Figure 7.1:** *The dynamic SFS system.*

The rate independent material model presented in Section 4.6 has now been turned into a dynamic system, see Figure 7.1. The material model consisted of a linear elastic spring coupled in parallel with an elastic perfectly plastic spring. The elasto-plastic spring was referred to as a friction element. The loading curve of the friction element is shown in Figure 7.2. Since the stress-response is bi-linear the stress in the friction element had to be evaluated through an algorithm. This will naturally be the case also for the dynamic system.

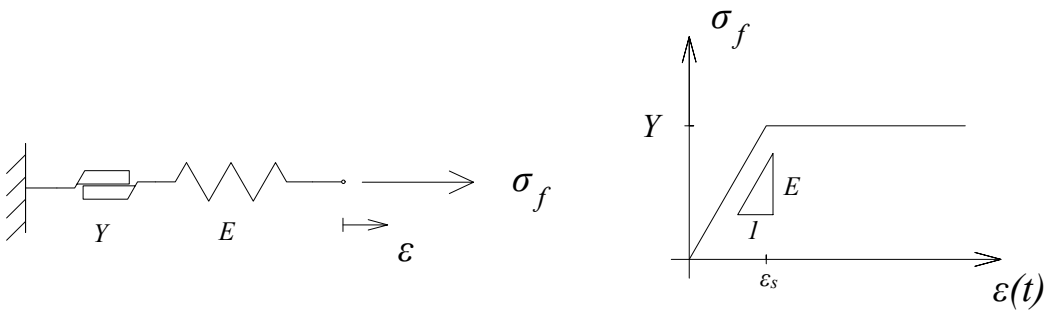


**Figure 7.2:** *Load-curve of the elastic perfectly plastic spring, referred to as the friction element*

The table below illustrates the transition from material to structure. This means that the same algorithm used to evaluate the stress in the friction element from the strains $\varepsilon$ can be used to evaluate the resisting force in the friction element from the displacements $u$ in the dynamic system, see Table 4.1.

| Material | | Structure |
|---|---|---|
| $E_\infty$ [Pa] | $\rightarrow$ | $k_\infty$ [N/m] |
| $E$ [Pa] | $\rightarrow$ | $k_F$ [N/m] |
| $Y$ [Pa] | $\rightarrow$ | $F$ [N] |

The dynamic system in Figure 7.1 is subjected to a sinusoidal load $p(t) = p_0 \sin(\omega t)$.

Two relations can be established that, as we will see, governs the response of the model to a sinusoidal load. These are

$$h = \frac{k_F}{k_\infty} \qquad \text{and} \qquad \frac{p_0}{F} \tag{7.1}$$

The $h$-parameter can be recognized from previous sections where it represented an equivalent quantity, namely $h = E/E_\infty$. Numerical testing shows that the quotient between the load amplitude and the yield-force $p_0/F$ represents the amplitude dependence of the model. It can be viewed as a normalized amplitude.

Most of the findings presented here was pointed at in the the article *Nonlinear dynamics of oscillators with bilinear hysteresis and sinusoidal excitation* [6], where the dynamic model with bilinear hysteresis was given a purely mathematical treatment.

The approach here is instead to use a time-stepping procedure, *the Central difference method*, to evaluate the response of the system to a sinusoidal load. The equation that is being solved numerically is the following

$$m\ddot{u} + f_s(u) = p(t) \tag{7.2}$$

where $f_s(u)$ has to be evaluated from increments of the displacement $\Delta u$. The material could either yield or not. If no yielding is present no energy is being dissipated from the system and the system is linear elastic with the stiffness $k = k_\infty + k_F$. So if the displacement amplitude is small, no yielding, the natural frequency of the system is

$$f_{n,2} = \frac{1}{2\pi}\sqrt{\frac{k_\infty + k_F}{m}} \tag{7.3}$$

### 7.1.1 Steady state SFS

Initially a result that is valid for a dynamic system with dry friction or Coulomb friction was tested numerically. Apparently, for dry friction the response to a sinusoidal load is unbounded at resonance if

$$p_o > \frac{4F}{\pi} = 1.273F \tag{7.4}$$

So for a sinusoidal load where the excitation frequency matches the natural frequency of the system ($f_{n,1} = \frac{1}{2\pi}\sqrt{\frac{k_\infty}{m}}$) the response is unbounded [1]. This result turned out to be valid also for the SFS model.

Now we move on to study the steady state response for values on the normalized amplitude which are below $p_0/F = 4/\pi$. The study is started at $p_0/F = 1.2$ and is continued down to values just above $p_0/F = 0.1$ The used system had the following stiffness parameters.

| | |
|---|---|
| $k_\infty$ | 3948 [N/m] |
| $k_F$ | 3948 [N/m] |
| $h$ | 1 |

The specific value of the yield limit $F$ is not of interest, the response is only dependent on the ratio between the force amplitude $p_0$ and the yield limit $F$. For this model, where $h = 1$, i.e $k_\infty = k_f$, and an attached mass of $m = 1$ kg the following two frequencies might be of interest

$$f_1 = \frac{1}{2\pi}\sqrt{\frac{k_\infty}{m}} = 10\text{ Hz} \qquad f_2 = \frac{1}{2\pi}\sqrt{\frac{k_\infty + k_F}{m}} = \frac{1}{2\pi}\sqrt{\frac{2k_\infty}{m}} = \sqrt{2}f_1 \tag{7.5}$$

With these relations, the frequency range of interest is

$$f = [10,\ \sqrt{2}\cdot 10]\text{ Hz}$$

The steady state response was calculated numerically. The response $u_0$ to a load $p(t) = p_0 \sin(2\pi f t)$ was recorded for $T_{tot} = 100$ s. The steady state response was taken as the maximum value of $u_0$ in the time interval $[0.9T_{tot}, T_{tot}]$. Initially it was made certain that steady

state was reached during this time-interval for all frequencies $f$ in the frequency interval. The steady state response $u_0$ was also normalized with regard to the quasi static response $u_{qs}$. The displacement response factor $R_d$ is defined as

$$R_d = \frac{u_0}{u_{qs}}$$

The quasi static displacement can be calculated with acceptable accuracy with the following algorithm, Table 7.1.

**Table 7.1:** *Calculation of quasi-static displacement $u_{qs}$*

| | |
|---|---|
| 1. If $u_{qs}$ is in linear elastic region: | $u_{qs} = \frac{p_0}{(k_\infty + k_F)}$ |
| 2. Calculate yield displacement: | $u_F = \frac{F}{k_F}$ |
| 3: Check: | $u_{qs} > u_F$ |
| 4: If yes: | $u_{qs} = \frac{p_0 - F}{k_\infty}$ |
| 5: If no: | $u_{qs} = \frac{p_0}{(k_\infty + k_F)}$ |

The tested frequency interval was normalized with regard to $f_n$, where $f_n$ is defined as

$$\text{Definition:} \qquad f_n = \frac{1}{2\pi}\sqrt{\frac{k_\infty}{m}}$$

With $h = 1$ this means that at around $f/f_n = 1.4$ we have the interesting value $\sqrt{2}f_n$.

In Figure 7.3 the steady state response as a function of frequency has been plotted. Different values of the normalized amplitude $p_0/F$ was tried. Looking at 7.3(a) it can be noted that the peaks increase in magnitude and creeps closer to $f/f_n = 1$ as the normalized amplitude is increased. This is consistent with the behavior of the dynamic modulus of the SFS model, see Figure 4.37. The stiffness approaches $k_\infty$ as the displacement amplitude is increased and consequently the resonance occur closer and closer to $f_n$. In (a) the curves are more or less horizontal until they take a steep turn upwards towards the peak, see low left corner of (a). When the curves are horizontal no energy is being dissipated.

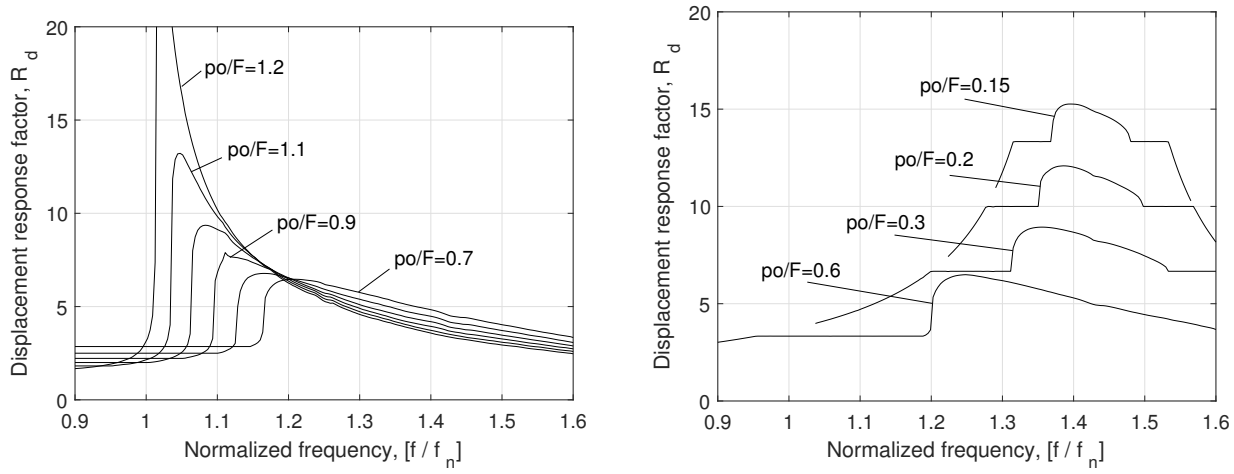


**(a)** **(b)**

**Figure 7.3:** *Steady-state response of the SFS system to different values of the normalized amplitude $p_0/F$. SFS-parameter: $h = 1$*

If the normalized amplitude $p_0/F$ is being decreased further strange things begin to happen. In Figure 7.3(b) it can be noted how the peaks move towards $\sqrt{2}f_n$ as the normalized amplitude is decreased, moreover the peaks of $R_d$ start to increase in magnitude.

How is this explained and will it be a problem for a structure?

At small displacements $u < u_F$ the response of the system is undamped and elastic with the natural frequency $\sqrt{2}f_n$ for $h = 1$. $u_F$ is the displacement where the system goes from elastic to plastic response and consequently the point at which energy is starting to dissipate in the system.

At another look at Figure 7.3(b) it can be seen that the peaks are surrounded by plateaus on both sides. At these plateaus and below, it could be checked that no energy was being dissipated. This means that the dynamic amplification $R_d$ times the quasi-static displacement $u_{qs}$ is roughly equal to $u_F = F/k_F$, i.e the displacement will reach the yield limit but not much further. At amplitudes below $p_0 < 4F/\pi$ the response is bounded at resonance.

However, with no energy being dissipated in the system other things can be observed. Take the curve where $p_0/F = 0.2$ as an example: Energy is only being dissipated on the curve-section where the peak is located, i.e from the plateau on the left side of the peak to the plateau on the right side of the peak, (approximately from $f/f_n = 1.35$ to $f/f_n = 1.5$).

At the plateaus where no energy is dissipated the forcing frequency $f$ coexists with the natural frequency of the system $\sqrt{2}f_n$, in the literature this is referred to as linear beating. See [8] for more information on the subject.

Two examples of this phenomena is included. Figure 7.4(a) shows the time signal of the response to a load with $p_0 = 0.2F$ and the frequency $f = 1.28f_n$. Doing a $FFT$ on the time signal reveals the frequency content. Figure 7.4(b) shows the response in the frequency domain, here it is clear that the response contains both the forcing frequency $1.28f_n$ and the natural frequency $\sqrt{2}f_n$ of the system.

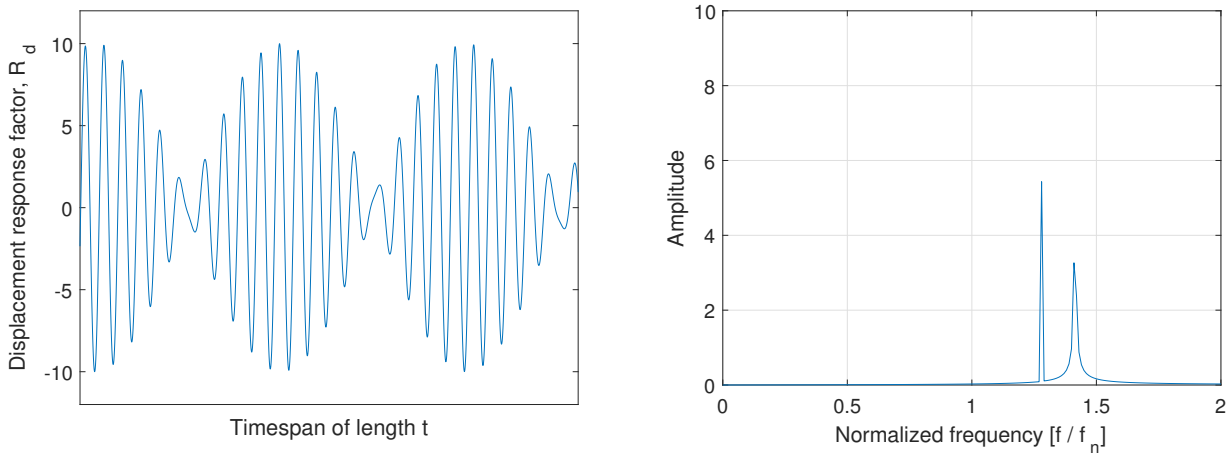


**(a)** *Time-signal* **(b)** *FFT of time-signal.*

**Figure 7.4:** *The steady state response to a sinusoidal load with the frequency $f = 1.28f_n$. The response contains both the forcing frequency $f = 1.28f_n$ and the undamped natural frequency of the system $\sqrt{2}f_n$.*

Figure 7.5 shows another example of linear beating but here the forcing frequency is changed to $1.33f_n$ which is closer to where the peak occurs. Figure 7.5(a) shows the time signal of the response and Figure 7.5(b) shows the frequency content. The signal obviously contains more of the forcing frequency $1.33f_n$ than of the natural frequency.

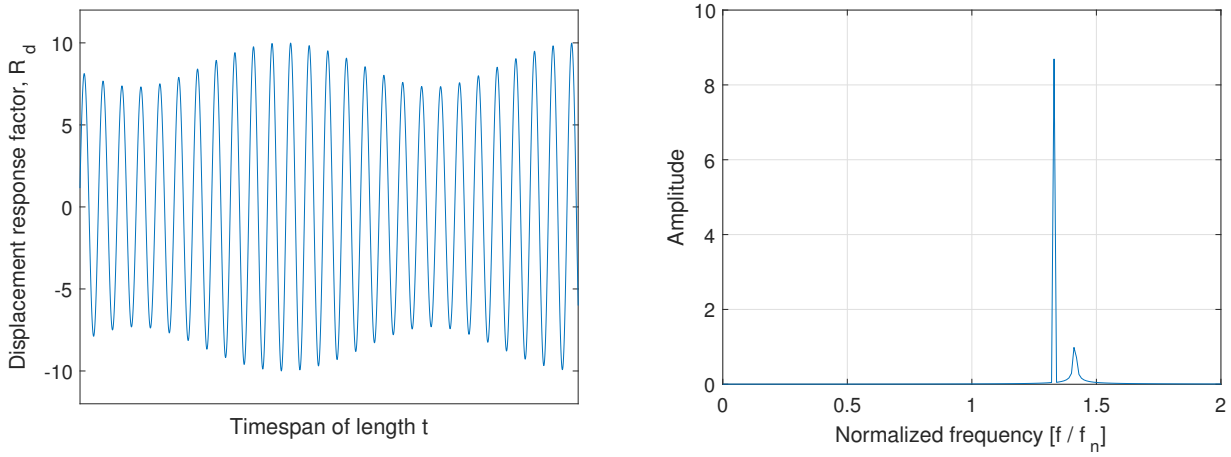


**(a)** *Time-signal* **(b)** *FFT of time-signal.*

**Figure 7.5:** *The steady state response to a sinusoidal load with the frequency $f = 1.33f_n$. The response contains both the forcing frequency $f = 1.33f_n$ and the undamped natural frequency of the system $\sqrt{2}f_n$.*

Looking back at Figure 7.3(a)-(b) it looks like energy is being dissipated for some values of the normalized amplitude $p_0/F$, but not at all frequencies. The relation between the normalized amplitude and the frequency seems to determine if energy is being dissipated or not. This relation was sought numerically and eventually it was possible to divide the frequency-amplitude plane into two parts, one part where no energy was being dissipated and one where energy was

being dissipated. Figure 7.6(a) shows this partition of the amplitude frequency plane for a SFS system with

$$m = 1\,\text{kg} \qquad h = 1 \qquad k_\infty = 3948\,\text{N/m} \qquad f_n = 10\,\text{Hz}$$

If the frequency/amplitude combination is in the ***shaded*** area of the plane there will be ***no*** hysteresis work done, i.e no dissipated energy. If the combination lands in the unshaded area of the plane energy will be dissipated.

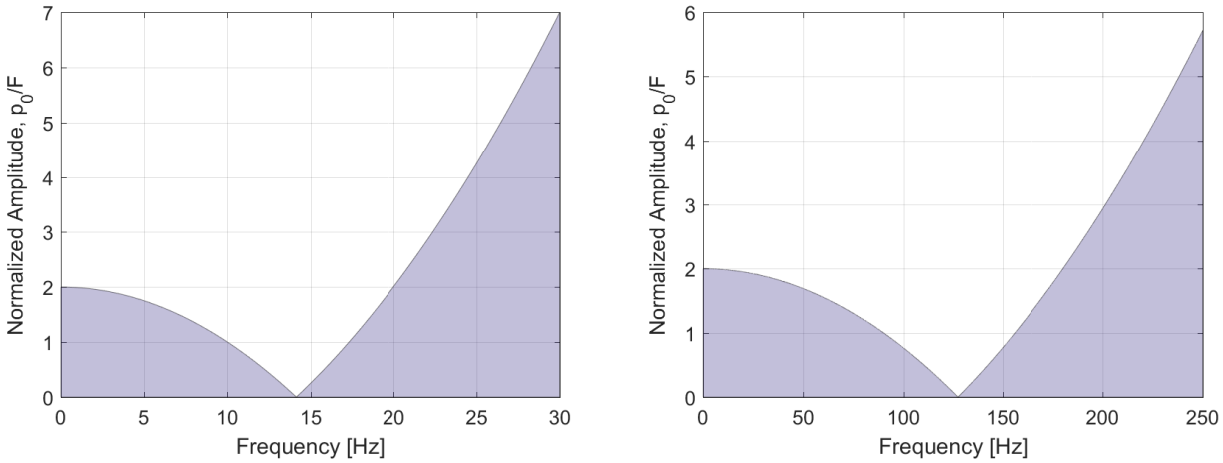


**(a)** $f_n = 10$ *Hz. Attached mass* $m = 1$ *kg* **(b)** $f_n = 90$ *Hz. Attached mass* $m = 0.0123$ *kg*

**Figure 7.6:** *Partition of the frequency-amplitude plane. In the* ***shaded*** *areas* ***no*** *energy is being dissipated in the system. SFS-parameter:* $h = 1$

Figure 7.6(b) shows a slightly different system. The system parameters are

$$m = 0.0123\,\text{kg} \qquad h = 1 \qquad k_\infty = 3948\,\text{N/m} \qquad f_n = 90\,\text{Hz}$$

The behavior of this model 7.6(b) is completely analogous to that of the system in 7.6(a). The frequency at which the normalized amplitude is zero but energy is still being dissipated is equal to $f = \sqrt{2} f_n$ in both systems, $f = \sqrt{2} \cdot 10$ Hz and $f = \sqrt{2} \cdot 90$ Hz respectively. This is of course due to the rate independent nature of the SFS material model.

Figure 7.7 shows the general behavior of a SFS system with $h = 1$. The partition is described by two curves. These are:

$$f < \sqrt{2} f_n \; : \qquad \frac{p_0}{F}(f) = 2\left(1 - \left(\frac{f}{\sqrt{2} f_n}\right)^2\right)$$

$$f > \sqrt{2} f_n \; : \qquad \frac{p_0}{F}(f) = 2\left(-1 + \left(\frac{f}{\sqrt{2} f_n}\right)^2\right)$$

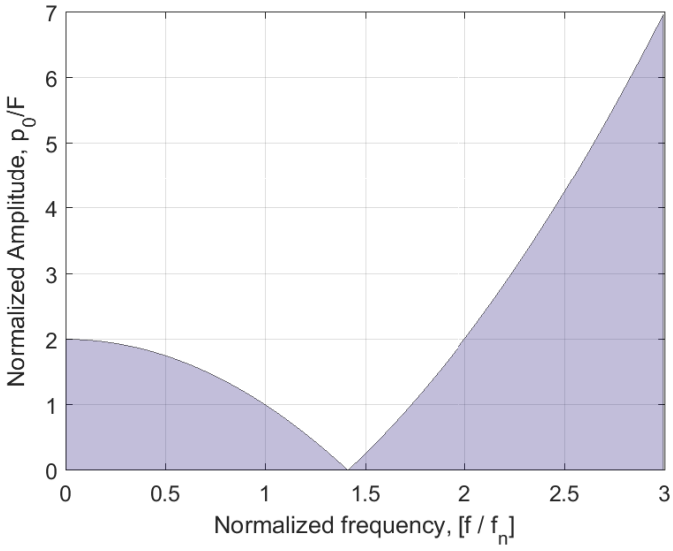


**Figure 7.7:** *Partition of the frequency-amplitude plane for $h = 1$ and normalized frequency $f/f_n$*

If a material with a different $h = k_F/k_\infty$-value is introduced the behavior of the coherent system will be slightly different. Figure 7.8 shows the behavior for $h = 2$ (a) and $h = 3$ (b). The curves describing the partition of the plane for $h = 2$ (a) could be approximated with

$$f < \sqrt{3} f_n \ : \qquad \frac{p_0}{F}(f) = 1.4 \left( 1 - \left( \frac{f}{\sqrt{3} f_n} \right)^2 \right)$$

$$f > \sqrt{3} f_n \ : \qquad \frac{p_0}{F}(f) = 1.4 \left( -1 + \left( \frac{f}{\sqrt{3} f_n} \right)^2 \right)$$

Why the starting value of the left curve is $\frac{p_0}{F}(0) = 1.4$ is not entirely clear, and a connection to $h$ can not be presented.

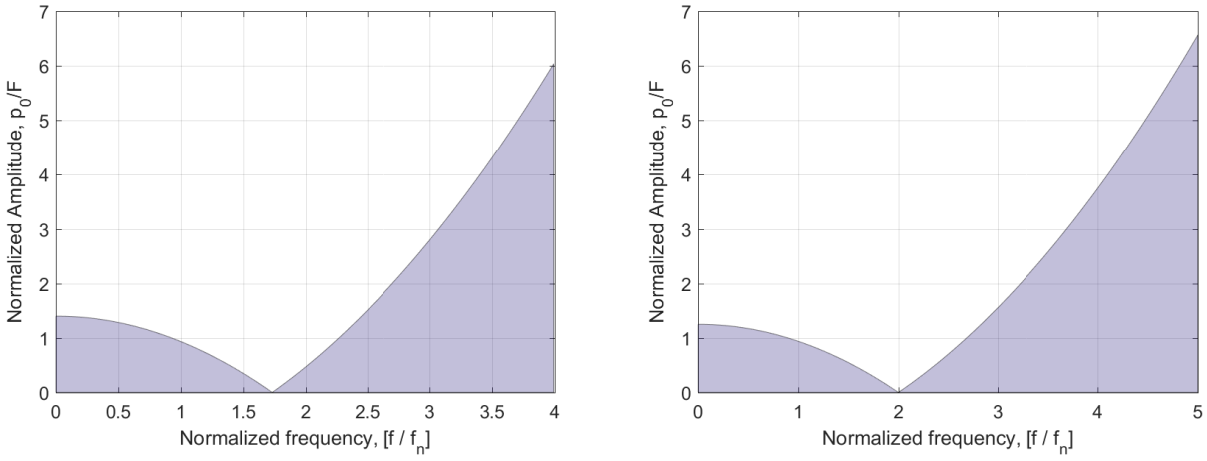


**(a)** $h = 2$ **(b)** $h = 3$

**Figure 7.8:** *Partition of the frequency-amplitude plane for $h = 2$ and $h = 3$, respectively. In the **shaded** areas **no** energy is being dissipated in the system.*

The curves describing the partition for $h = 3$ (b) has a similar approximation, namely

$$f < \sqrt{4}f_n \ : \qquad \frac{p_0}{F}(f) = 1.25\left(1 - \left(\frac{f}{\sqrt{4}f_n}\right)^2\right)$$

$$f > \sqrt{4}f_n \ : \qquad \frac{p_0}{F}(f) = 1.25\left(-1 + \left(\frac{f}{\sqrt{4}f_n}\right)^2\right)$$

Here the starting point of the left curve in (b) has been moved down even further. The amplitude value where the frequency is $f = 0$ is now $\frac{p_0}{F}(0) = 1.25$. Maybe a connection to the increased $h$-value is to be found.

A more general observation is that the part of the amplitude-frequency plane where hysteresis do occur seems to get bigger as the $h$-value increases, and perhaps in the next analysis it will be clear why.

The next objective is to study the influence of the $h$-value on the steady state response. Numerically the steady state analysis was carried out in the same manner as the previous steady state analysis of the SFS system, which was described earlier in this section. Figure 7.9 shows the response in terms of the displacement response factor $R_d$ as the $h$-value is being altered. The amplitude was kept fixed at $p_0 = F$

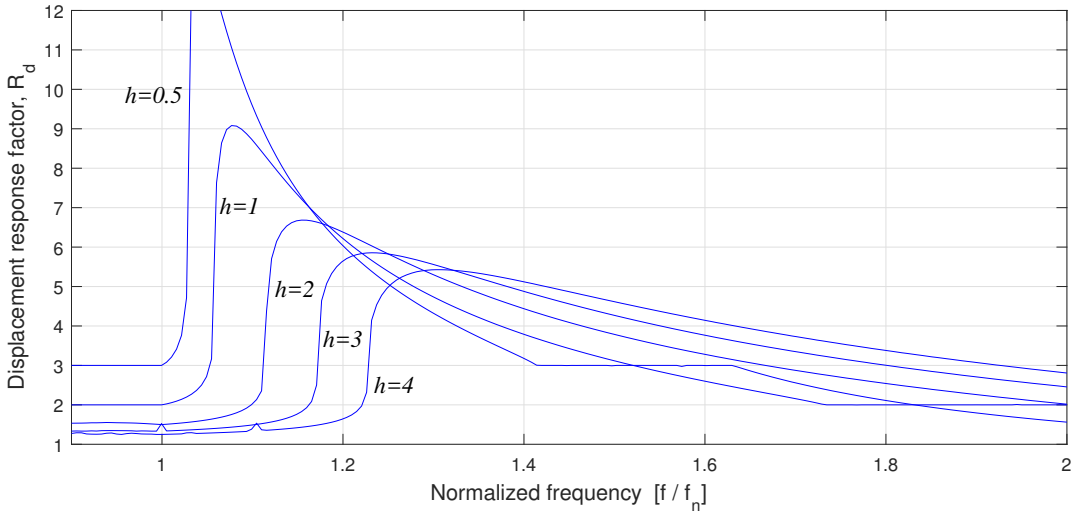


**Figure 7.9:** *The variation of the steady-state response of the SFS-system to different h-values.*

Evaluating the damping at the peaks, in terms of an equivalent phase angle $d$, will explain the overall behavior. With $\alpha = (k_F u_0)/F$ the equivalent phase angle can be calculated through

$$d = \frac{4(\alpha - 1)}{\pi(1 + k_\infty \alpha / k_F)\alpha}$$

see, Equation (4.52) and Figure 4.39 for more details. The following table, 7.2, shows how the equivalent phase angle, i.e the damping $d$ is varying with $h$.

**Table 7.2:** *Variation of the damping, d, with the normalized stiffness h*

| $h$-parameter | Equivalent phase angle, $d$ |
|---|---|
| 0.5 | 0.097789 |
| 1 | 0.17919 |
| 2 | 0.30592 |
| 3 | 0.39908 |
| 4 | 0.46992 |

The reason the damping $d$ grows with $h$ can be explained by the following equation which describes the energy that is being dissipated in one vibration cycle. The energy is described in terms of the material.

$$U_c = 4Y(\varepsilon_0 - \varepsilon_s)\ [\mathrm{J/m^3}] \qquad \text{where} \qquad \varepsilon_s = \frac{Y}{E}$$

An increase of the $h$-factor can be interpreted as an increase in the $k_F$ stiffness which is the stiffness of the elasto-plastic spring (the friction element). In terms of the material this quantity

is referred to as $E$. How an increase of the stiffness in the friction element is affecting the hysteresis work is illustrated in Figure 7.10. In (a) the material has a stiffness $E_1$ which is bigger than the stiffness in (b) which is $E_2$. The displacement $\varepsilon_0$ is the same. It is clear that an increase in stiffness generates a bigger enclosed area, which means a larger hysteresis work. So with

$$E_1 > E_2 \qquad \Rightarrow \qquad U_{c,1} > U_{c,2}$$

under the assumption that the displacement $\varepsilon_0$ is the same.

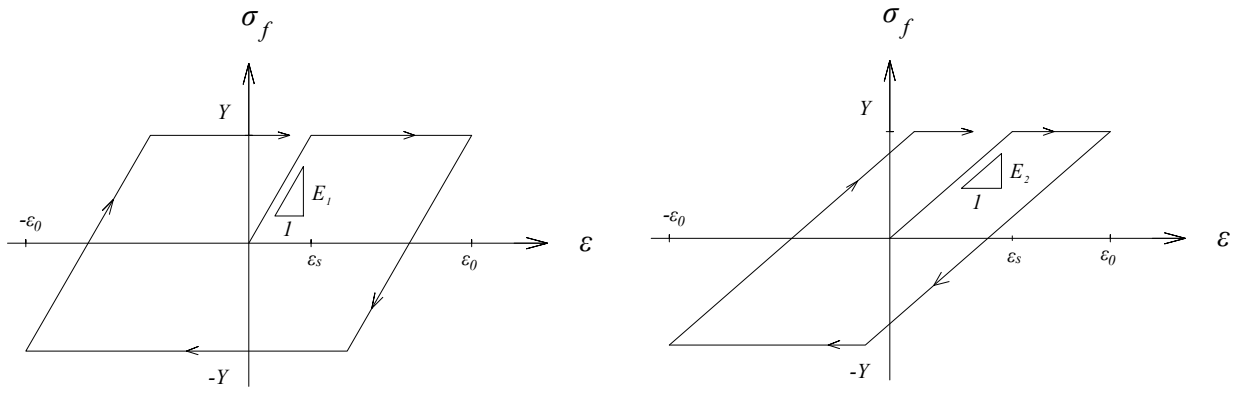


**(a)** $E_1$ **(b)** $E_2$

**Figure 7.10:** *The hysteresis work is dependent on the stiffness E of the friction element. Here $E_1 > E_2$, which yields $U_{c,1} > U_{c,2}$, where $U_c$ is the area enclosed by the loop.*

### 7.1.2 Response to a swept sine-wave

A final topic to be examined is the response of the SFS system to a load $p(t) = p_0 \sin(\omega t)$ with a increasing/decresing frequency in time. This is known as a sine-sweep where the freuquency of the sine-wave is being increased or decreased as time goes on. The sine-sweep used here is a linear frequency-sweep starting at a frequency $f_0$ and stopping at a frequency $f_1$. It is possible to change the direction of the sweep from low $\rightarrow$ high frequencies, to high $\rightarrow$ low frequencies. The built in Matlab function `chirp(t, f0, t(end), f1)` was used to generate the load vector $p(t)$, where [`t, t(end)`] marks the starting and end point of a time-vector.

The system studied had the following stiffness parameters and mass. Different values of the normalized amplitude $p_0/F$ was being used to examine the effect of this choice. The natural frequency $f_n$ according to previous definition.

**Table 7.3:** *System parameters*

| | |
|---|---|
| $k_\infty$ | 3948 [N/m] |
| $k_F$ | 3948 [N/m] |
| $h$ | 1 |
| $m$ | 1 [kg] |
| $f_n$ | 10 [Hz] |

The frequency range was set to [7, 21] Hz and the total sweep-time was 100 seconds, giving 7.14 [s/frequency]. Time step length: $5 \cdot 10^{-4}$ seconds.

At an early stage it was discovered that the response in terms of the displacement response factor $R_d$ was dependent on the direction of the sweep, i.e if the sweep was from a low to a high frequency or vice versa. Figure 7.11 shows this for a normalized amplitude $p_0/F$ of 1.0. In 7.11(a) the sweep was from 7 to 21 Hz and in 7.11(b) from 21 to 7 Hz. The peaks have roughly the same magnitude but the occur at slightly different frequencies. When sweeping from 21 to 7 Hz the peak moves closer to $f_n$ and the appearance of the peak in 7.11(b) is less pointy, compared to 7.11(a). The frequency axis has been normalized.

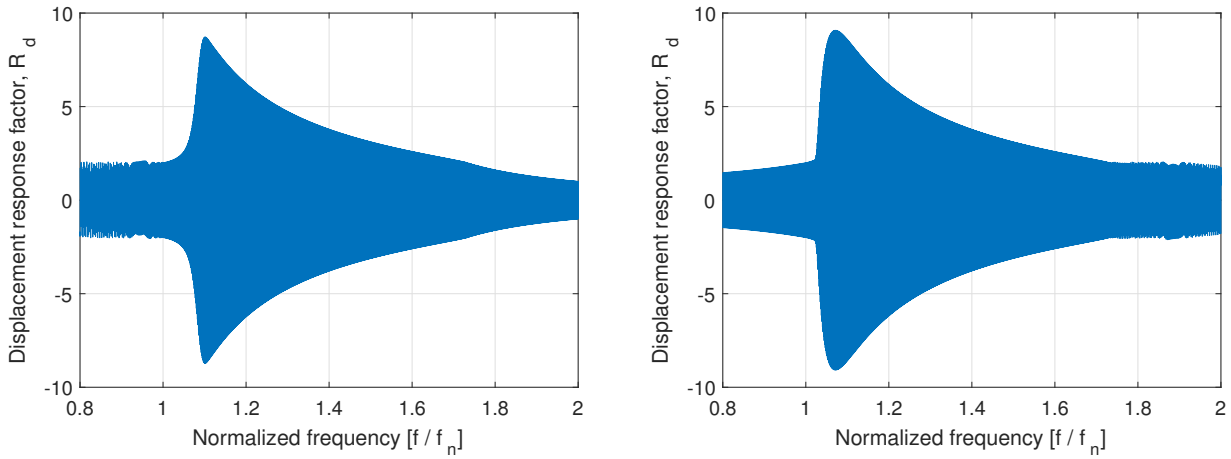


**(a)** *Sweep from 7 to 21 Hz during 100 seconds.* **(b)** *Sweep from 21 to 7 Hz during 100 seconds.*

**Figure 7.11:** *The influence of sweep-direction. Amplitude:* $p_0 = 1.0F$.

In Figure 7.12 the amplitude was increased to $p_0 = 1.1F$. The difference in response caused by the sweep direction is now increasing. In 7.12(a) the magnitude of the peak is smaller and the peak occurs further away from $f_n$ than in 7.12(b).

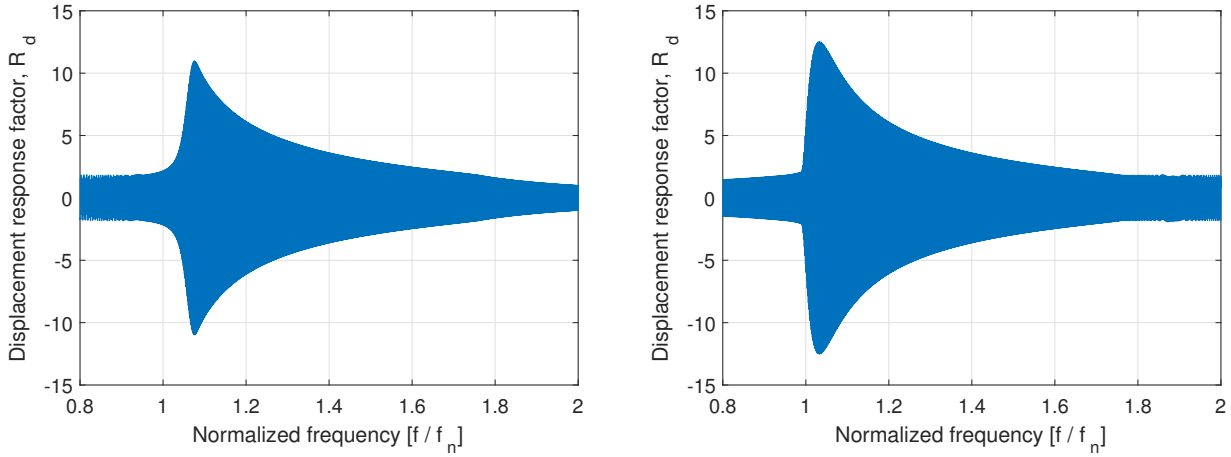


**(a)** *Sweep from 7 to 21 Hz during 100 seconds.* **(b)** *Sweep from 21 to 7 Hz during 100 seconds.*

**Figure 7.12:** *The influence of sweep-direction. Amplitude:* $p_0 = 1.1F$.

A further increase of the amplitude generates the same pattern. In Figure 7.13 the amplitude was increased to $p_0 = 1.2F$. Now $R_d \approx 15$ in 7.13(a) compared to $R_d \approx 20$ in 7.13(b). The frequency at which the peaks occur is also quite different, now the peak in 7.13(b) occur very close to $f_n$.

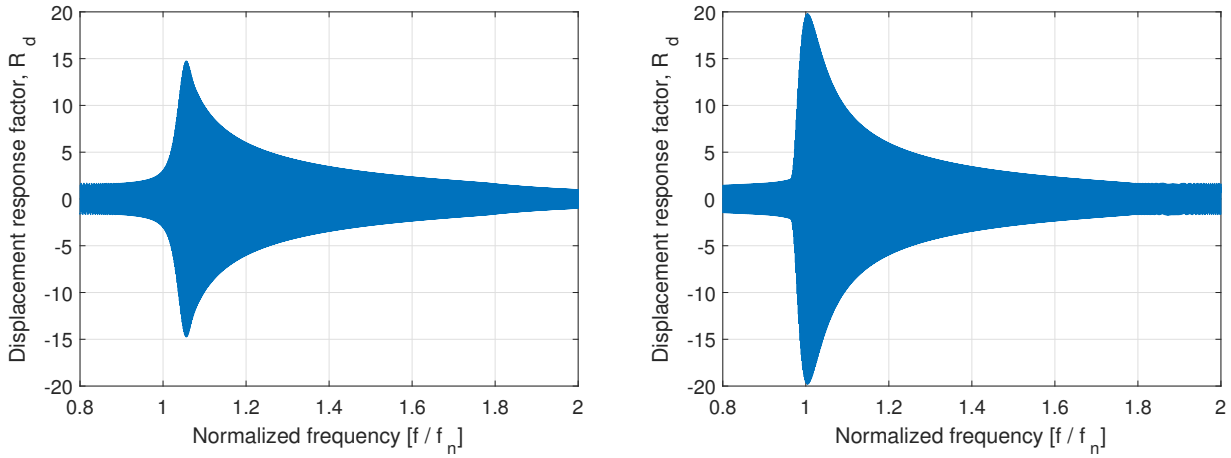


**(a)** *Sweep from 7 to 21 Hz during 100 seconds.* **(b)** *Sweep from 21 to 7 Hz during 100 seconds.*

**Figure 7.13:** *The influence of sweep-direction. Amplitude:* $p_0 = 1.2F$.

This behavior of the SFS system to a swept sine-load might be useful knowledge in real-world situations. Since the linear visco-elastic systems are independent of the sweep-direction it might be an idea to try both sweep-directions when a real dynamic system is being tested. If the response is independent of sweep-direction the system could be modeled as linear. If it is not independent of the sweep-direction the response is in part non-linear. So in order to investigate if damping in the form of friction is present in a dynamic system it could be an idea to try both sweep-directions.

If the amplitude is increased even further another peculiarity of the SFS system is revealed.

For an amplitude slightly smaller than $p_0 = 2F$ resonances well below $f_n$ occur in the system. Kalmar-Nagy and Shekhawat [6] refer to these as sub-harmonic resonances. Figure 7.14 shows this. In Figure 7.14(a) the system has a mass $m = 1$ kg, with the same stiffness parameters as in Table 7.3, this gives the natural frequency $f_n = 10$ Hz.

In Figure 7.14(b) the mass of the system has been changed to $m = 0.0123$ kg and with the same stiffness parameters this results in a natural frequency of $f_n = 90$ Hz

Consequently the highest peak of the sub-harmonic resonances occur at roughly $0.4f_n$. Figure 7.15 shows the general case with normalized frequency.

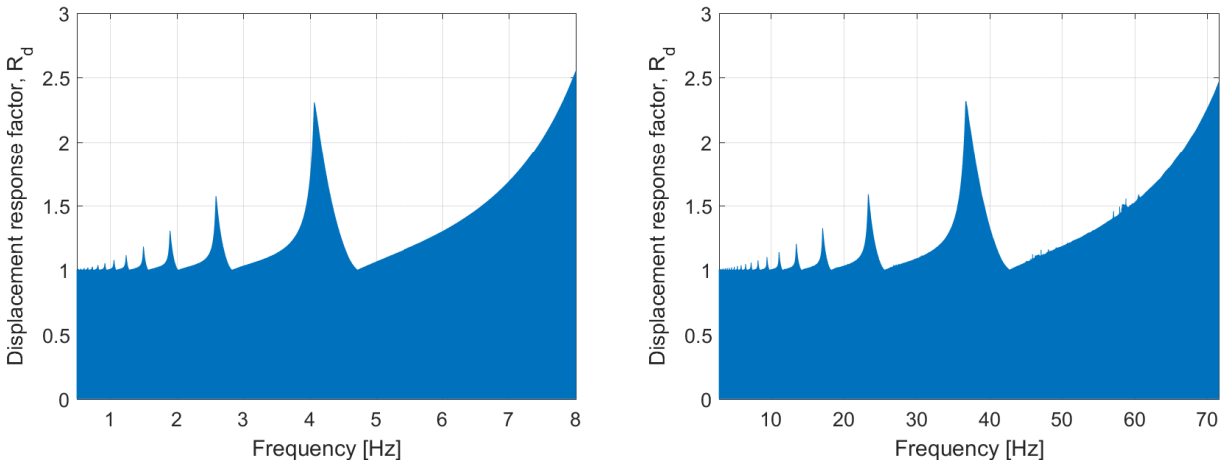


**(a)** $m = 1$ *kg*, $f_n = 10$ *Hz* **(b)** $m = 0.0123$ *kg*, $f_n = 90$ *Hz*

**Figure 7.14:** *Sub-harmonic resonances. System parameters:* $h = 1$, $p_0 = 2F$

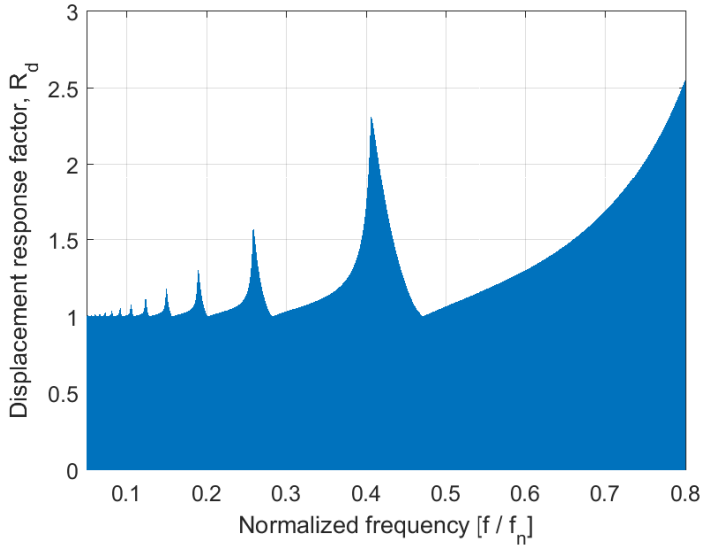


**Figure 7.15:** *Sub-harmonic resonances occurring from* $f = 0.4f_n$ *and down for* $h = 1$ *and* $p_0 = 2F$.

One thing that might be in connection to the sub-harmonic resonances was the response to

a sine-wave with forcing frequency $f = 3$ Hz. At all other frequencies $f$ that *was tried*, both lower and higher, the Fourier spectrum only contained odd harmonics of the forcing frequency, i.e $3f, 5f, 7f...$ etc. But for $f = 3$ Hz the signal contained a whole range of frequencies, Figure 7.16 shows this, where 7.16(b) is a zoom in of 7.16(a). The main peaks occur at $f = 3, 9, 15$ Hz then there are several frequencies in between. The peak occurring slightly to the left of $f = 3$ Hz, see 7.16(b), seems to coincide with one of the sub-harmonic resonances that can be found at a frequency close to $f = 2$ Hz, see Figure 7.15. I was unable however to determine if this observed behavior at $f = 3$ Hz held any significance to the occurrence of the sub-harmonic resonances.

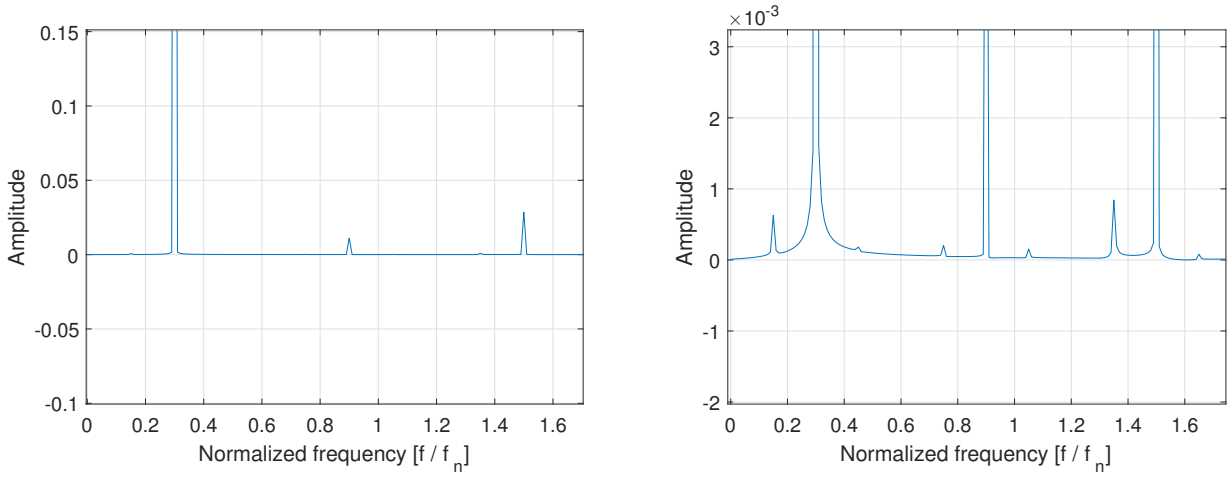


**(a)** **(b)** *Zoom in*

**Figure 7.16:** *Frequency content of the response to a load with the frequency $f = 3$ Hz. System parameters: $m = 1$ kg, $f_n = 10$ Hz*

## 7.2 Summary and concluding remarks

Some of the things that could be concluded in this section, concerning the dynamic SFS system, is summarized in the following bullet list.

- The system can be characterized to some extent by the following quantities

  Normalized amplitude: $p_0/F$

  Normalized stiffness: $h = k_F/k_\infty$

- If the amplitude/yield limit relation exceeds

$$p_0 > \frac{4}{\pi}F$$

  the response at resonance will be unbounded

- The resonances occur in a frequency interval that is determined by $h$. Ex. with $h = 2$ the interval becomes

$$[f_n,\ \sqrt{3}f_n]$$

- The combination of loading frequency $f$ and normalized amplitude $p_0/F$ determines if energy is being dissipated in the system. It was possible to make a partition of the amplitude-frequency plane to establish this relation
- An increased $h$-value resulted in increased damping in the system leading to a smaller response at resonance.
- If the load $p(t)$ is a swept sine wave the response of the system is dependent on sweep-direction, i.e from low to high frequency or vice versa. The sensitivity to sweep-direction increases with increased amplitude.
- Sub-harmonic resonances occur at $0.4f_n$ and downwards if the amplitude is roughly $p_o = 2F$ or higher.

## 7.3 5-parameter dynamic system

In this short section some attention will be directed towards the concern involving amplitude-dependence of natural frequencies. When the SFS model was studied it was concluded that the resonance frequency would occur in a frequency interval dependent on the ratio of the stiffness parameters of the system.

For $h = 1$ the frequency interval would be $[f_n,\ \sqrt{2}f_n]$ etc. If the normalized amplitude $p_0/F$ was big the resonance occurred close to $f_n$ and if $p_0/F$ was small the resonance occurred at $\sqrt{2}f_n$.

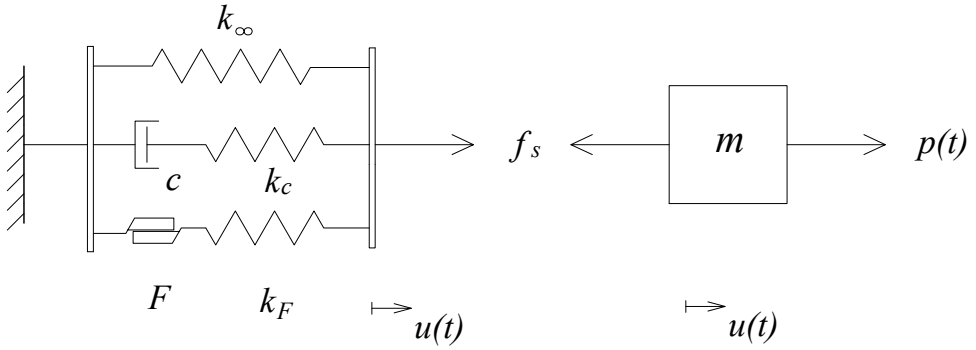


**Figure 7.17:** *5 parameter system*

Now if it is assumed that the damping in a structure is of both a viscous and frictional nature the *5-parameter model* could be used to build up the dynamic system, Figure 7.17 shows the dynamic model.

The question is: will the viscous part of the damping to some extent soften the effects of the load-amplitude on the resonance frequency.

In order to investigate this a sine-sweep was used. Table 7.4 shows the parameters of the first system that was examined.

**Table 7.4:** *System parameters*

| | |
|---|---|
| $k_\infty$ | 3948 [N/m] |
| $k_c$ | 3948 [N/m] |
| $k_F$ | 3948 [N/m] |
| $m$ | 1 [kg] |
| $f_n$ | 10 [Hz] |

In Figure 7.18(a) the load amplitude $p_0$ was 5 times higher than the friction factor $F$. This yields a displacement response $u(t)$ which to its shape and resonance frequency is similar to that of a viscous system. Lowering the amplitude however the resonance frequency will again appear at a higher frequency, roughly $f = \sqrt{2}f_n$. This is shown in Figure 7.18(b) for an amplitude of $p_0 = 0.1F$. The peak has the flat top which indicates that this is the only place where friction is the cause of the damping. From a previous discussion, see Figure 7.3(b), it is possible to conclude that

$$\text{For} \qquad p_0 = 0.1F \qquad R_d u_{qs} \approx u_F$$

This means that the maximum displacement of the system at this load amplitude is roughly $u_F$ which is the yield limit.

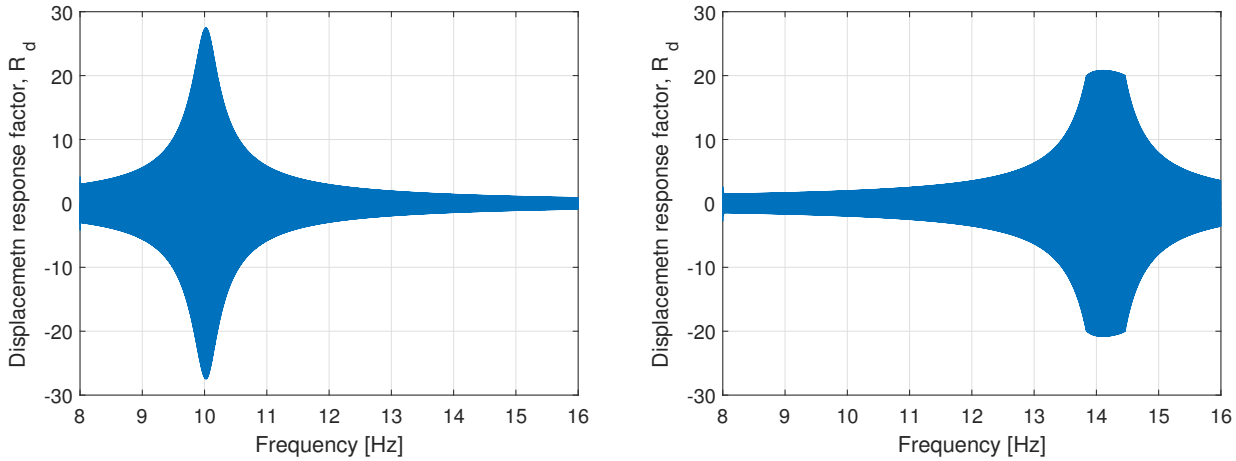


**(a)** $p_0 = 5F$ **(b)** $p_0 = 0.1F$

**Figure 7.18:** *5-parameter system. Sine sweep. Attached massm = 1 kg*

Another system was tried where the mass was exchanged for a lighter one which increased the natural frequency of the system. Table 7.5 shows the used parameters.

**Table 7.5:** *System parameters*

| | |
|---|---|
| $k_\infty$ | 3948 [N/m] |
| $k_c$ | 3948 [N/m] |
| $k_F$ | 3948 [N/m] |
| $m$ | 0.0123 [kg] |
| $f_n$ | 90 [Hz] |

In Figure 7.19(a) the amplitude is $p_0 = 5F$. At these higher frequencies the viscous damping effects are more accentuated than in the previous system.

In figure 7.19(b) the amplitude is $p_0 = 0.1F$. The amplitude dependence of the resonance frequency seems to remain also for this system. In this case no energy is being dissipated in the friction block, not even at resonance. The damping in the system is purely viscous.

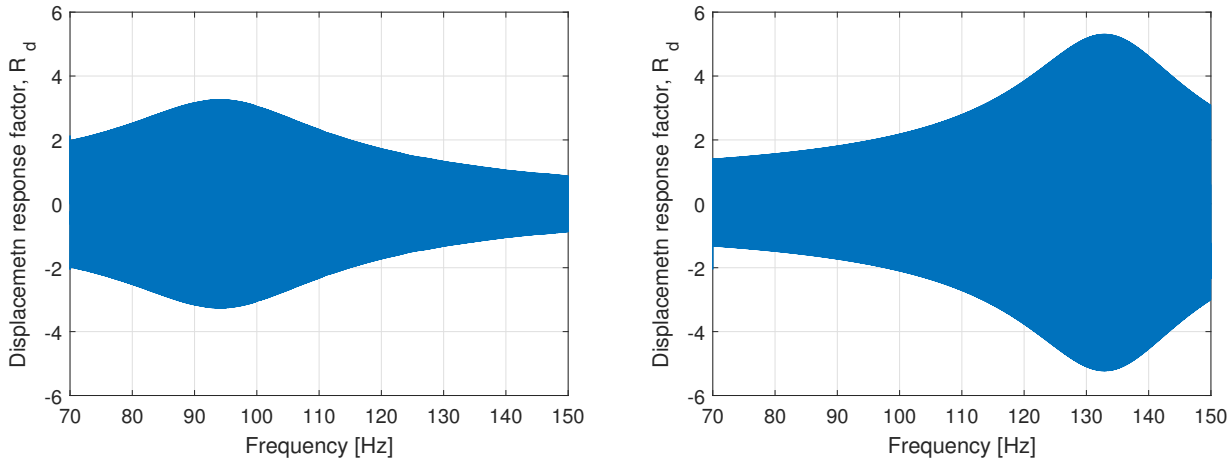


**(a)** $p_0 = 5F$ **(b)** $p_0 = 0.1F$

**Figure 7.19:** *5-parameter system. Sine sweep. Attached* $m = 0.0123$ *kg*

This section was included in order to illustrate the amplitude dependence of resonance frequencies in systems with partly bilinear hysteresis. The effect of the rate-independent bilinear hysteresis is greater at low frequencies due to the rate-dependent nature of the viscous element. At high amplitudes the viscous part of the damping introduces a boundary on the displacement response $u$, something that was lacking in the purely frictional model.

When the *5-parameter model* was used no apparent influence of sweep direction could be observed, which is in contrast to SFS system.

# Chapter 8

# Discussion

In this thesis the dynamic response of different material models has been investigated in the frequency interval [10, 90] Hz. Periodic sine shaped loads and half-sine shaped pulses has been applied to the different dynamic systems.

## 8.1 A comparison between Kelvin- and SLS systems

The first aim of this thesis was to investigate if more complex visco-elastic solid models are needed to properly represent the behavior of solid materials in dynamic events, or if the Kelvin model, despite its weaknesses, is sufficient in the studied frequency interval.

It could be concluded that if the phase angle of the Kelvin model was fitted to the phase angle of an SLS model in a satisfactory way over the frequency interval [10, 90] Hz, the maximum dynamic steady state response of the fitted Kelvin system and a SLS system would be similar. Especially in terms of damping.

If the normalized frequency range $[0, \omega t_r]$ was short a satisfactory fit between the phase angles of the respective models were easier to obtain. 90 Hz is the maximum frequency in the frequency interval, consequently the maximum of the normalized frequency range is dependent on the relaxation time of the SLS model. Maximum of $\omega t_r$ is equal to $2\pi 90 t_r$.

By doing parallel calculations of the *equivalent viscous damping ratio* $\zeta_{eq}$ an even more successful way of approximating the damping of the SLS system was found. The relationship found was

$$\delta = 2\zeta \tag{8.1}$$

where the phase angle $\delta$ of the SLS model could be calculated for different frequencies in the interval. The steady state response of a dynamic SLS system at resonance could then be approximated by a Kelvin system with the damping ratio $\zeta = \delta/2$. This was shown in Section 6.3.

The main difference in the dynamic steady state response of the Kelvin and SLS system could

be traced to the modulus effect. A Kelvin model is build up of only one spring with stiffness $k_\infty$, this means that the undamped natural frequency of the system is always $\omega_n = \sqrt{k_\infty/m}$.

The SLS model however contains two springs $k_\infty$ and $k_c$ which can contribute to the stiffness of the system depending on the frequency. At high natural frequencies, in this thesis obtained by lowering the mass $m$, the natural frequency of the SLS system is deviating from the Kelvin system. This was shown in Section 6.4

Both methods presents an opportunity to estimate the damping, in terms of the damping ratio $\zeta$, of a material purely based on measurements of the phase angle $\delta$. This is a short-cut compared to the widely used concept of equivalent viscous damping, where dynamic measurements are needed.

As a summary it can be said that a Kelvin system can be used in order to approximate the damping of a SLS system, but if a modulus effect is desired the Kelvin model will not be able to deliver this. However a suggestion on how to mimic a modulus effect of the Kelvin system is included in Section 6.3.

Numerically the force in the SLS system is calculated from increments of displacement. This force increment $\Delta f_M$ is dependent on the time-step length $\Delta t$ since approximations of integrals, by the trapezoidal rule, is used in the evaluation of the increment. Perhaps the SLS system could be more sensitive to the choice of time-step lengths due to this?

## 8.2 Dynamic SFS systems

The behavior of dynamic systems with bilinear hysteresis is obviously a lot different compared to the response of visco-elastic solids.

If amplitude dependent hysteresis is present in a system it is perhaps necessary to take this into account. Here are two suggestions on how to investigate this.

If dynamic experiments are possible a sine sweep can be used. If the response of the system is dependent on sweep-direction, from low to high etc., this could be a sign of non-linear response and perhaps a Kelvin model will not be a good choice of material model.

Periodic quasi static displacement controlled loading is a material-test in order to determine if damping is present in the material even at really low frequencies. If energy is being dissipated at low frequencies it is probably not a good idea to use a model which only covers viscous damping.

The inclusion of bilinear hysteresis in the computational models comes with a computational cost since the stresses is updated with use of an algorithm. A check is required to see if the stress is purely alastic or both elastic and plastic.

# Chapter 9

# Bibliography


[1] A. K. Chopra, *Dynamics of structures*, vol. 3. Prentice Hall New Jersey, 1995.

[2] S. Spanne, *Lineära system*, vol. 3. Matematiska institutionen Lunds tekniska högskola, 1995.

[3] N. S. Ottosen and M. Ristinmaa, *The mechanics of constitutive modeling*. Elsevier, 2005.

[4] S. Thelandersson, *Notes on linear viscoelasticity*. Structural Mechanics, Lund University, 1987.

[5] C. Dyrbye, *Bygningsdynamik*, vol. 2. Afdelingen for Baerende Konstruktioner, D.t.H, 1977.

[6] T. Kalmar-Nagy and A. Shekhawat, "Nonlinear dynamics of oscillators with bilinear hysteresis and sinusoidal excitation," *Physica D: Nonlinear Phenomena*, vol. 238, no. 17, pp. 1768–1786, 2009.

[7] P. E. Austrell, "Modeling of elasticity and damping for filled elastomers," *Report TVSM*, vol. 1009, 1997.

[8] A. Persson and L.-C. Böiers, *Analys i en variabel*. Studentlitteratur AB, 2010.

# Chapter 10

# Appendix A

## SLS system: Equivalent viscous damping approach

The following is a description of how the equivalent viscous damping is calculated for a SLS system. The equivalent viscous damping is defined as

$$\zeta_{eq} = \frac{1}{2\pi}\frac{1}{\omega/\omega_n}\frac{E_D}{ku_0^2}$$

In the above equation $k$ is equal to the quasi-static stiffness $k_\infty$. The dissipated energy $E_D$ in a SLS material during one cycle is

$$E_D = \pi p_0 u_0 \sin\delta$$

In forced vibration the maximum amplitude $u_0$ occur when the phase angle is approximately $\delta = 90°$ (At the natural frequency the phase angle $\delta = 90°$). If the natural frequency of the SLS model is roughly

$$f_n = \sqrt{\frac{k_\infty}{m}}$$

and the maximum amplitude occur at the frequency $f$, an equivalent viscous damping parameter could be determined through

$$\zeta_{eq} = \frac{1}{2\pi}\frac{1}{(f/f_n)}\frac{\pi p_0 u_0}{k_\infty u_0^2}$$

where $\sin\delta \approx 1$ has been used, and the above expression simplifies to

$$\zeta_{eq} = \frac{1}{2}\frac{1}{(f/f_n)}\frac{p_0}{k_\infty u_0}$$